HORIZONTAL SHEAR TRANSFER FOR FULL-DEPTH PRECAST CONCRETE BRIDGE DECK PANELS

by

Joseph A. Wallenfelsz

Thesis submitted to the faculty of the
Virginia Polytechnic Institute and State University
in partial fulfillment of the requirements for the degree of

MASTER OF SCIENCE
IN
CIVIL ENGINEERING

APPROVED:

_____
Dr. Carin L. Roberts-Wollmann, Chairperson
Department of Civil and Environmental Engineering

_____
Dr. Thomas E. Cousins
Department of Civil and Environmental Engineering

_____
Dr. Rodney T. Davis
Virginia Transportation Research Council

April 25th, 2006
Blacksburg, Virginia

Keywords: Precast Panels, Horizontal Shear, Shear Connectors, Shear Friction

HORIZONTAL SHEAR TRANSFER FOR FULL-DEPTH PRECAST BRIDGE DECK PANELS

by

Joseph A. Wallenfelsz

ABSTRACT

Full-depth precast deck panels are a promising alternative to the conventional cast-in-place concrete deck. They afford reduced construction time and fewer burdens on the motoring public. In order to provide designers guidance on the design of full-depth precast slab systems with their full composite strength, the horizontal shear resistance provided at the slab-to-beam interface must be quantified through further investigation. Currently, all design equations, both in the AASHTO Specifications and the ACI code, are based upon research for cast-in-place slabs. The introduction of a grouted interface between the slab and beam can result in different shear resistances than those predicted by current equations.

A total of 29 push off tests were performed to quantify peak and post-peak shear stresses at the failure interface. The different series of tests investigated the surface treatment of the bottom of the slab, the type and amount of shear connector and a viable alternative pocket detail.

Based on the research performed changes to the principles of the shear friction theory as presented in the AASHTO LRFD specifications are proposed. The proposal is to break the current equation into two equation that separate coulomb friction and cohesion. Along with these changes, values for the coefficient of friction and cohesion for the precast deck panel system are proposed.

ACKNOWLEDGEMENTS

This research was funded by the Virginia Department of Transportation. The findings, conclusions and opinions presented herein are those of the author and do not necessarily represent those of the sponsoring agency.

I would first and foremost like to thank Dr. Carin-Roberts Wollmann for her guidance, support and patience throughout this research. Without her direction this research would not have been possible. I would also like to thank Dr. Cousins for his input into this project and care for his students as a professor. I would also like to thank Dr. Rodney Davis and the Virginia Transportation Research Council for sponsoring this project. I also thank Dr. Rodney Davis for his input and serving on my committee. Thanks also to the Nelson Stud Welding Group for providing shear stud materials.

I also owe my family a huge amount of gratitude for their support and for believing in my dreams. I thank them for being there when I needed them and I hope I can continue to make them proud.

Last but not least I must thank all of my coworkers out at the lab. These guys have not just been coworkers but they have also been true friends. Brett Farmer, Dennis Huffman and Clark Brown have taught me more than I ever imagined and when I leave here I will be missing three great friends. Also I must thank my friends Kirsten Baldwin-Metzger, Anthony Barret, Dave Martin, Onur Avici, Greg Williamson, Sean Sullivan, Buck Berardy, Chuck Newhouse and Chris Carroll. Thanks also to the rest of the graduate students and faculty here whom I worked with.

TABLE OF CONTENTS

ABSTRACT ii
ACKNOWLEDGEMENTS iii
TABLE OF CONTENTS iv
LIST OF FIGURES vi
LIST OF TABLES iii
CHAPTER 1: INTRODUCTION 1
1.1 Full-Depth Concrete Bridge Deck Panels 1
1.2 Research Objective and Scope 2
1.3 Thesis Organization 2
CHAPTER 2: BACKGROUND AND LITERATURE REVIEW 4
2.1 Precast Concrete Bridge Deck Panel System Background 4
2.2 Horizontal Shear Stress in Composite Members 5
2.3 Shear Friction Model 8
2.4 Horizontal Shear Strength Research for Cast-In-Place Decks 10
2.4.1 Hanson 10
2.4.2 Mast 11
2.4.3 Saemann and Washa 11
2.4.4 Birkeland 12
2.4.5 Shaikh 12
2.4.6 Loov 13
2.4.7 Walraven 13
2.4.8 Mattock 14
2.4.9 Mau and Hsu 14
2.4.10 Loov and Patnaik 14
2.5 Horizontal Shear Strength Research For Precast Deck Systems 15
2.5.1 Menkulasi 15
2.5.2 Scholz 16
2.6 Headed Stud Connectors for Composite Action 17
2.7 AASHTO Standard Specification Provisions 18
2.8 AASHTO LRFD Bridge Design Specifications for Horizontal Shear 19
2.9 Summary of Literature Review 20
CHAPTER 3: DESCRIPTION OF TESTS 22
3.1 Overview 22
3.2 Material Properties 22
3.2.1 Concrete & Grout Material Properties 22
3.2.2 Reinforcing Steel and Headed Shear Studs 24
3.3 Push-Off Test 24
3.3.1 Specimen Fabrication 25
3.3.2 Headed Stud Shear Connectors 27
3.3.3 Haunch and Pocket Grouting 29
3.3.4 Hidden Pocket Detail 31

3.3.5 Push-Off Test Setup 32
3.3.5.1 Description 32
3.3.5.2 Instrumentation 33
3.3.5.3 Testing Procedure 34
3.3.6 Test Parameters and Series Details 36
CHAPTER 4: PRESENTATION OF RESULTS & ANALYSIS 38
4.1 Push-Off Tests 38
4.2 Tests with No Shear Connectors 44
4.3 Tests with Shear Connectors 45
4.3.1 Reinforcing Bar Stirrups 46
4.3.2 Headed Shear Studs 48
4.4 Surface Treatment 50
4.5 Hidden Pocket Detail 51
4.6 Yield in Shear Connectors 51
4.7 Coefficient of Friction 53
4.8 Comparison with Current Code Equations 55
CHAPTER 5: SUMMARY, RECOMENDATIONS AND CONCLUSIONS 56
5.1 Summary 56
5.2 Conclusions 57
5.3 Design Recommendations 58
5.4 Construction Recommendations 61
REFERENCES 63
APPENDIX A 67
APPENDIX B 110

LIST OF FIGURES

Figure 2.1: Free Body Diagram from (AASHTO Figure C5.8.4.1-1)....6
Figure 2.2: Aggregate Interlock....9
Figure 2.3: Previous Research Results....21
Figure 3.1: a) 4 in.x 8 in. Concrete Cylinder b) 2 in. mortar cube....23
Figure 3.2: Typical Push Off Test....25
Figure 3.3: Beam Side Specimen....26
Figure 3.4: Slab Side Specimen....27
Figure 3.5: Headed Studs....28
Figure 3.6: Headed Shear Stud Specimen....29
Figure 3.7: Specimen formed for grouting....30
Figure 3.8: Full Depth Pre-cast Bridge Deck Panel Schematic....31
Figure 3.9: Hidden Pocket Detail....32
Figure 3.10: Test Setup....33
Figure 3.11: Strain Gage Placement....34
Figure 3.12: Typical Load versus Slip Plot....35
Figure 4.1: Typical Load vs. Slip Plots....39
Figure 4.2: Specimen Grouting....41
Figure 4.3: Push-Off Specimen after failure....41
Figure 4.4: Typical Load vs. Slip Plot for a Specimen with no Shear Connectors....44
Figure 4.5: Plate to be embedded in top of beam side specimen....46
Figure 4.6: Average Peak Shear Stress (10% Error Bars)....47
Figure 4.7: Load versus Slip for Exposed Aggregate Tests....48
Figure 4.8: Average Peak Shear Stresses for Headed Shear Stud Tests....49
Figure 4.9: Load versus Slip for Headed Shear Stud Tests....50
Figure 4.10: Normal Pocket versus Hidden Pocket Average Peak Shear Stress....51
Figure 4.11: Percent of Yield Stress in Shear Connectors....52
Figure 4.12: Reinforcing Bar Stirrups and No Connectors at Sustained Load....54
Figure 4.13: Headed Shear Stud at Sustained Load....54
Figure 4.14: Peak Shear Stress vs. Clamping Stress....55
Figure 5.1: Peak Shear Stress Results with Proposed Equations....60
Figure 5.2: Post Peak Results with Proposed Equations....60

LIST OF TABLES

Table 3.1: Concrete Mix Design per yd^3 23
Table 3.2: Mixing Quantities per 50 lb bag 30
Table 3.3: Test Summary 37
Table 4.1: Push-off Test Combined Results 43

CHAPTER 1: INTRODUCTION

1.1 Full-Depth Concrete Bridge Deck Panels

With the ever increasing traffic volume and urban sprawl throughout the country, transportation projects are producing an immense burden on the motoring public. These congested work zones cause significantly increased commute times and degradation of safety. To alleviate some of the inconveniences associated with the construction, maintenance and rehabilitation of bridges, transportation agencies throughout the country are seeking solutions to reduce the complexity and time involved in the construction of their transportation structures. The predominant concept is of a deck made almost entirely of precast pieces such as the full-depth precast bridge deck system. The system affords a very rapid and uncomplicated construction process.

The benefits of the precast system are numerous. All concrete can be cast in the controlled environment of a precasting yard before construction ever begins. There are no large amounts of concrete to be placed and cured at the site, improving construction speed and the quality of concrete. The amount of formwork is significantly reduced compared to the labor intensive forming of a conventional cast-in-place deck. Rehabilitation may only require replacement of a few panels on an individual basis thus complete closure of the bridge can be avoided. All of these factors offer a product of higher quality with decreased traffic interruptions.

The system is constructed by first positioning the girders atop their supports. The precast panels are then laid on the girders along the length of the bridge. These panels are typically 7 to 10 in. thick, 10 ft long and of varying widths depending on the project

geometry. The panels are adjusted into place with leveling devices to match the final grade profile and then the haunch formwork is placed. Once the panels are laid upon the girders the transverse joints are grouted or filled with epoxy then post-tensioned longitudinally to close and tighten the joint. To connect the deck panels to the girders shear connectors extend from the girder into pockets already formed into the deck. These pockets as well as the haunch are then filled with a high strength non-shrink grout. These grouts typically obtain sufficient strength in a matter of days or even hours allowing early opening of the bridge. After grouting of the bridge any barrier rails and wearing surfaces are added.

1.2 Research Objective and Scope

The objective of this research is to better understand the horizontal shear behavior at the beam-to-deck interface for precast concrete deck slab systems, and provide recommendations for the design of the beam-to-deck interface and connection. This research also focuses on constructability aspects of the system with recommendations to facilitate simplified construction of the system. Performance of the system requires that the slip between the girders and slab be minimal so that the full composite strength of the girder-slab system can be developed. To achieve these objectives 29 push-off tests were performed that investigated different parameters involved in the horizontal shear transfer between the precast deck and girders.

1.3 Thesis Organization

Chapter 2 presents background information and design equations used in the past for horizontal shear transfer. Most of the previous research presented was done for cast-in-place deck system. Chapter 3 outlines the testing parameters and testing procedures

performed throughout this research. Chapter 4 presents results and analysis of the tests performed. Chapter 5 presents results and conclusions of this research. Recommendations and proposed design equations are also presented.

CHAPTER 2: BACKGROUND AND LITERATURE REVIEW

2.1 Precast Concrete Bridge Deck Panel System Background

Precast bridge deck panels have been used for quite some time, however, an increase in the number of bridges undergoing reconstruction and rehabilitation has focused attention on the use of the fully precast system. A fully precast system can ensure quality and minimize hardship on the motoring public by minimizing construction related delays.

The construction of the bridge deck is the last component of bridge construction that requires refinement to achieve a fully functional totally pre-fabricated bridge system. Full-depth bridge deck panels have been developed and used extensively in the United States in the past decade. Virginia currently has at least four bridges that utilize a full-depth precast bridge deck panel system. These bridges include the Route 7 Bridges over Route 50 in Fairfax, the Route 229 Bridge over Big Indian Run in Culpepper, the Route 235 Bridge over Dogue Creek in Fairfax and the Woodrow Wilson Bridge over the Potomac River in Arlington. The Woodrow Wilson Bridge is currently being replaced with an entirely new structure.

Issa et. al (1995) performed a survey of the different construction and detailing techniques that various transportation agencies in the United States and Canada use to implement precast bridge deck panels. They sent a detailed questionnaire which solicited information pertaining to the types of details currently used and comments on the performance of different components of a precast bridge deck panel system. From the

questionnaire, conclusions were drawn on construction sequencing, grouting material, transverse prestressing, longitudinal prestressing, joint types and shear connector types.

Issa et. al (1995) then followed up the previous studies with field inspections to evaluate the field performance of the precast concrete bridge deck panels. The visual field inspections took place over an 18 month period. They concluded that precast bridge deck panels are an efficient and economical means for replacing a degraded bridge deck. In most cases the performance of the system was found to be excellent. In those cases where performance of the bridge was poor, it was most often attributed to the horizontal shear connection, joint configuration between adjacent panels, lack of longitudinal post-tensioning or the materials used. In order to keep the deck in good repair a waterproofing membrane was essential. The study also found that fewer problems were encountered when the supporting girders were made of precast concrete rather than steel.

In 1998 following the two original papers presented by Issa et. al (1995) a third paper presented by Issa et. al (1998) was presented describing analysis of a precast bridge deck system. Two bridges were modeled in the finite element package ALGOR. One of the bridges was the Route 229 Bridge over Big Indian Run in Culpepper, Virginia. The research presented suggested post-tensioning stress levels necessary to secure the longitudinal joints. A stress level of 200 psi was recommended to secure the longitudinal joints for simply supported bridges while a stress level of 450 psi was needed at an interior support of continuous bridges.

2.2 Horizontal Shear Stress in Composite Members

Composite construction allows the designer to utilize the strength of the deck coupled with the girder to provide a more efficient and economical design. In order to

account for this, the designer must accurately predict the horizontal shear developed at the interface between the slab and girder and provide adequate connectivity between the two to develop the full composite action. A free body diagram of the forces developed in a composite deck-girder system is seen in Figure 2.1 where V_u, V_{uh}, M_u, C_u and T_u are the vertical shear, horizontal shear, moment, resultant compression and resultant tension respectively at end one or two. The term dV is the incremental change of shear across the incremental length $d\ell$.

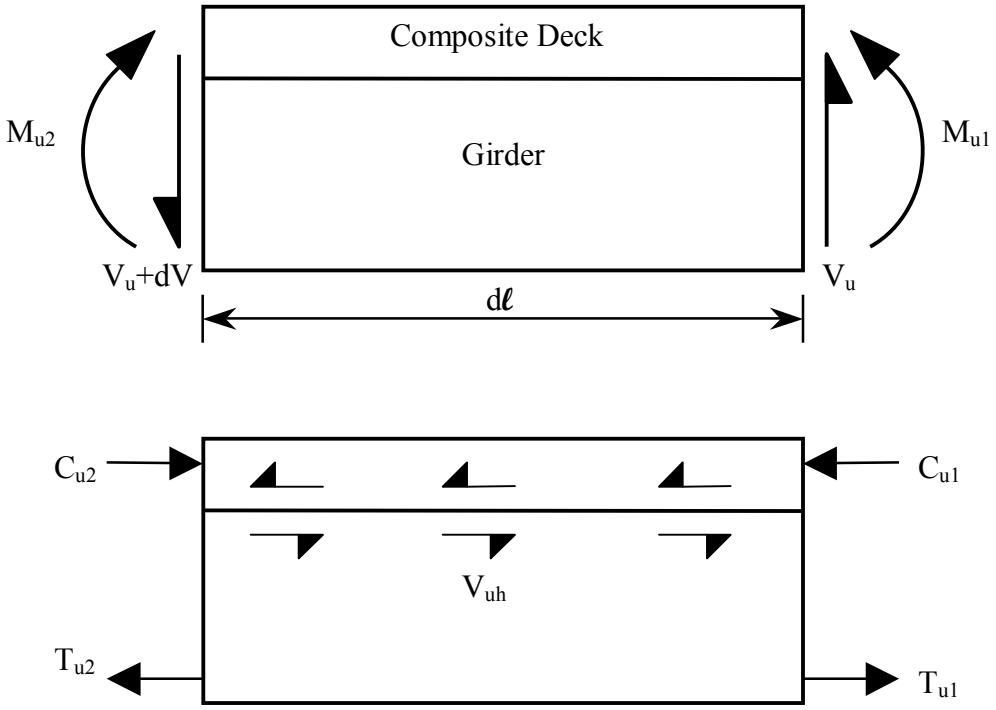

Figure 2.1: Free Body Diagram from (AASHTO Figure C5.8.4.1-1)

The calculation of the horizontal shear between the girder and slab is complicated by several factors. Theoretically, the horizontal shear stress can be calculated by equation 2.1, however, this equation applies only for a linearly elastic section. The assumption that the section is linear elastic is only valid for service loads.

$$v_h = \frac{VQ}{Ib} \tag{2.1}$$

where

v_h = horizontal shear stress

V = vertical shear force at section

I = moment of inertia

b = interface width

Q = first moment of the area above (or below) the fiber being considered

In reality the composite section of the precast girder, precast slab and haunch are not linear elastic at ultimate conditions. In addition, the cross section consists of different concretes. The slab is normally made of a lower strength concrete than the girder and the haunch consists of a grout mortar. These complexities are also present for a cast-in-place slab.

Loov and Patnik (1994) have shown that for the cast-in-place slab the theoretical equation should yield reasonable results under the condition that the cracked section moment of inertia and area moment of a transformed composite section are used. The slab is transformed into the same material as the beam using the modular ratio as is typically done in flexural design. For the precast slab system the haunch would have to be transformed as well.

An alternate to the theoretical equation was proposed by Kamel (1996) using equilibrium forces. See Figure 2.1 for a free body diagram. This method provides the best approximation of the horizontal shear stress and is the method recommended by the PCI Bridge Design Manual (1997).

$$v_h = \frac{V}{(jd)b_v} \tag{2.2}$$

where

V = factored vertical shear at the section

d = effective member depth

jd = distance between the tension and compression resultant forces

b_v = interface width

A third method is presented as an alternative in the ACI 318-05 (2005) commentary and allows the designer to take the horizontal shear as the actual change in compressive or tensile force at the interface. This is also the method that is currently used for steel design and is presented in the AISC specifications (1999).

$$v_h = \frac{F}{b_v l_v} \tag{2.3}$$

where

F = total compressive or tensile force

b_v = interface width

l_v = interface length

2.3 Shear Friction Model

Shear friction models have proved to accurately describe the actual physical behavior of the horizontal shear interface strength. The models can be broken down into two components; Coulomb friction due to surface roughness and cohesion between the two surfaces.

The first component, coulomb friction can be broken down even further. For a rough surface if there is a failure surface such as the crack at the slab beam interface there is aggregate interlock according to Walraven (1987). As the angular pieces of aggregate bind against one another, they provide aggregate interlock.

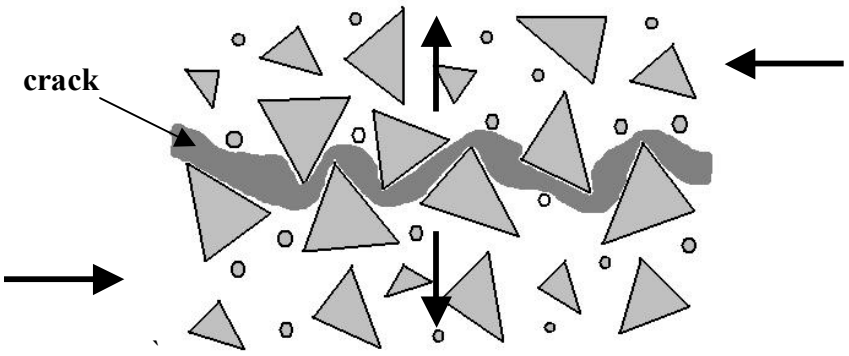

Figure 2.2: Aggregate Interlock

In order to overcome this interlock one of two things must happen. The aggregate pieces must ride over one another thus opening the crack or the sharp edges of the aggregate must crush. Usually the failure is a combination of the two. As the larger pieces of aggregate ride over one another and open the crack, the reinforcing steel is strained. All current models assume that the crack separates enough to fully yield the reinforcing steel. This force transferred into the reinforcing steel can then in turn be treated as a normal force.

The CEB-FIP Model Code 90 (1990) includes another variable. It accounts for dowel action of the reinforcing bars. Dowel action is the ability for rebar crossing a concrete interface to transfer shear. Depending on the geometrical conditions, however, dowel action may be neglected. In order for dowel action to provide horizontal resistance the dowel must be mobilized. Mobilization refers to the fact that the dowels do not begin

to take load until after the concrete has displaced sufficiently to engage the steel into sheer. Concrete easily splits at small shear displacements therefore preventing complete mobilization of the dowel bar before peak resistance is obtained in most cases. ACI 318-02 (2002) addresses this issue in the commentary by recommending an artificially low coefficient of friction for situations that dictate accounting for dowel action.

2.4 Horizontal Shear Strength Research for Cast-In-Place Decks

In 1963 the ACI Building Code Requirement for Reinforced Concrete (1963) presented provisions for the design of the steel crossing the interface between a precast girder and cast-in-place slab. The design provisions then presented were based on the ACI-ASCE 333 report (1960) which included the research of Hanson (1960). The shear friction approach was not introduced in the ACI code until 1970. The provisions for the shear friction approach were based on push-off tests performed by Birkeland (1966), Mast (1968), Kriz and Raths (1965) and Hofbeck et al. (1969).

2.4.1 Hanson

The original design provisions presented in the ACI Building Code Requirement for Reinforced Concrete (1963) were based on much of the work done by Hanson (1960). Hanson determined that push-off tests were representative of beam tests by comparing shear-slip plots. Hanson also found that peak shear resistance was obtained when a slip of 0.005 in. occurred. Research by Saeman and Washa (1964) would later incorporate this slip limit. However, setting a slip limit was not widely accepted and others suggested that no slip limit should be set.

Hanson's tests indicated that for a precast girder with a cast-in-place slab the ultimate shear capacity at a smooth interface was 300 psi and for a roughened interface

was 500 psi. Also Hanson found that ultimate shear capacity could be increased by 175 psi for each percent of reinforcement crossing the interface.

2.4.2 Mast

Mast (1968) was the first to introduce a linear shear friction equation. Further refinement of the equation was done by Birkeland and Anderson (1960). The equation as introduced by Mast is as follows:

$$v_n = \rho_v f_y \mu \tag{2.4}$$

where

v_n = ultimate horizontal shear strength

$\rho_v f_y$ = clamping stress

μ = empirical coefficient of friction

The equation was designer friendly but not extremely accurate. For low clamping stress the equation was too conservative and for high clamping stresses it was un-conservative.

2.4.3 Saemann and Washa

Saemann and Washa (1965) recognized that the ACI-ASCE 333 (1960) recommendations and test results indicated that modifications to design provisions could provide increased economy due to overly conservative design values. Their test program included 42 T-beams with 36 combinations of variables. The variables tested were surface roughness, interface position relative to composite section neutral axis, percent of steel crossing interface and concrete compressive strength.

The results of the research provided the following equation. The equation takes into account steel crossing the interface and the ratio of the shear span to effective depth.

Surface roughness is ignored since it has a diminishing effect as the amount of steel crossing the interface is increased.

$$Y = \frac{2700}{X+5} + 300P\left(\frac{33-X}{X^2+6X+5}\right) \quad \text{(psi)}$$

(2.5)

where

Y = ultimate shear stress capacity (psi)

X = effective depth (in.)

P = percent of steel crossing interface (%)

2.4.4 Birkeland

Birkeland (1966) was the first to introduce a non-linear function for the ultimate shear capacity of the interface. The equation introduced was as follows:

$$v_n = 33.5\sqrt{\rho_v f_y} \qquad \text{(psi)} \qquad (2.6)$$

2.4.5 Shaikh

Shaikh (1978) proposed a modification to the shear-friction provisions of ACI. These modifications were incorporated in 1970 in the ACI code. The equation Shaikh proposed can be simplified to the following:

$$v_u = \phi\rho_v f_y \mu_e \qquad (2.7)$$

where

$$\mu_e = \frac{1000\lambda^2}{v_u} \text{(psi)} \qquad (2.8)$$

In this simplified equation 1.0λ has been substituted for μ and the concrete density is accounted for by λ. Below are the values used for different densities of concrete.

$\lambda = 1.0$ for normal weight concrete

$\lambda = 0.85$ for sand-lightweight concrete

$\lambda = 0.75$ for all-lightweight concrete

The strength reduction factor for shear was $\phi = 0.85$

If equation (2.7) and (2.8) are combined a parabolic equation for v_u as a function of clamping force is obtained (2.9).

$$v_u = \lambda\sqrt{1000\phi\rho_v f_y} \le 0.25f'_c\,\lambda^2 \text{ and } 1000\lambda^2 \qquad (2.9)$$

2.4.6 Loov

Loov (1978) was the first to introduce the influence of concrete strength into the horizontal shear strength equation. Below is the equation presented by Loov:

$$v_n = k\sqrt{\rho_v f_y f'_c} \quad \text{(psi)} \qquad (2.10)$$

where

k = constant (0.5 was suggested for an initially un-cracked interface)

When the concrete strength is equal to 4480 psi this equation is the same as the one presented by Birkeland.

2.4.7 Walraven

Walraven (1988) performed a statistical analysis on 88 push-off tests. From that statistical analysis Walraven suggested the following equation for a pre-cracked interface.

$$v_n = C_1(0.007\rho_v f_y)^{C_2}\,\text{(psi)} \qquad (2.11)$$

when f'_c is assumed equal to 0.85 of the compressive strength of 6 in. cubes:

$$C_1 = 0.167 \cdot f'^{0.303}_c$$

$$C_2 = 0.0371 \cdot f'^{0.303}_c$$

2.4.8 Mattock

Mattock (1974) has over the years refined his equations used to determine the horizontal shear capacity. One of the early equations Mattock proposed was a modification to previous work to include the effects of concrete strength. The equation he proposed was:

$$v_n = 4.5 f'^{0.545}_c + 0.8(\rho_v f_y + \sigma_n) \leq 0.3 f'_c \text{ (psi)} \qquad (2.12)$$

Later Mattock (1975) proposed the following equation for an interface that has already been cracked:

$$v_n = 400 + 0.8\rho f_y \text{ (psi)} \qquad (2.13)$$

Mattock (1976) also investigated horizontal shear strength for members constructed of lightweight concrete. This research is reflected in the proposed revision by Shaikh (1978).

2.4.9 Mau and Hsu

Mau and Hsu (1987) suggested an equation similar to Loov's (1978) equation. However, they suggested using a k of 0.66 and assumed this to be valid for both un-cracked and initially cracked interfaces.

2.4.10 Loov and Patnaik

In 1994, Loov and Patnaik (1994) investigated horizontal shear strength further. They tested 16 composite beams while varying the clamping stress with a fixed concrete strength and then they varied concrete strength with a fixed clamping stress. In this study

Loov and Patnaik observed that slip was not significant nor were the shear connectors stressed until the horizontal shear stress reached 220 to 290 psi. The shear connectors became mostly engaged once the horizontal shear stress reached 430 psi.

From the study Loov and Patnaik developed an equation to estimate the horizontal shear strength of composite beams without shear connectors. The equation is as follows:

$$v_{no} = 0.6\sqrt{15f'_c} \quad \text{(psi)} \tag{2.14}$$

To provide a continuous curve they suggested a general equation for horizontal shear strength by combing (2.14) with the equation Loov presented in 1978 (2.10).

$$v_n = k\lambda\sqrt{(15 + \rho_v f_y)f'_c} \le 0.25f'_c \quad \text{(psi)} \tag{2.15}$$

where k = 0.6 provided a good lower fit for the data.

2.5 Horizontal Shear Strength Research For Precast Deck Systems

2.5.1 Menkulasi

Very little research has been done in the past to investigate horizontal shear strength of full-depth precast slab systems. Menkulasi (2002) performed 36 push off tests varying the parameters of haunch heights, grout types, amount of steel crossing the interface and the type of shear connector.

Based on the test data Menkulasi recommended the following lower bound equations for an uncracked and cracked interface. The uncracked equation (2.16) is to be used in situations where the cohesive bond at the interface has not been broken. Once the cohesive bond at the interface has been broken and the interface becomes cracked equation (2.17) must be used to predict the horizontal shear resistance.

$$v_{nh} = 0.05 + 0.65\frac{(A_{vh}f_y + P_n)}{b_v s} \quad \text{(ksi)} \qquad \text{(uncracked)} \tag{2.16}$$

$$v_{nh} = 0.69\frac{(A_{vh}f_y + P_n)}{b_v s} \qquad \text{(ksi)} \qquad \text{(cracked)} \qquad (2.17)$$

where

A_{vh} = area of steel crossing interface (in^2)

f_y = steel yield stress (ksi)

P_n = permanent net compressive force (kips)

b_v = interface width (in.)

s = shear connector spacing (in.)

Menkulasi found that the pre-crack shear strength was not affected by varying haunch heights. Haunch heights of 1 in., 2 in. and 3 in. were tested. In order to prevent a pry-out type failure, a development length of the shear connector into the slab of at least 5 in. was recommended. It was also shown that the introduction of a shear key on the beam side may significantly increase the horizontal shear strength.

After making a comparison of the results of the study with current code provisions, the researchers concluded that ACI 318-02 (2002), AASHTO Standard Specifications for Bridge Design, 17th Edition (2003) and AASHTO LRFD Bridge Design Specifications, 3rd Edition (2004) result in unconservative predictions of strength. AASHTO LRFD provided the best correlation with the data.

2.5.2 Scholz

Scholz (2004) investigated the performance of grouts in full-depth precast deck systems. In addition, Scholz performed a series of 8 push-off tests and a series of slant cylinder tests. Based on criteria such as compressive strength, tensile strength, shrinkage, flow, workability and bond strength two brands of commercially available grouts were suggested, and performance specifications were developed. The grouts were Five Star®

Highway Patch and Set® 45 Hot Weather. The grouts also performed well with aggregate extensions. Scholz was unable to find any correlation between slant shear cylinder tests and the push-off tests.

2.6 Headed Stud Connectors for Composite Action

The use of the welded headed shear stud has been widely used to develop composite action between a steel girder and concrete slab. Significant research has been devoted to developing design provisions for welded headed shear studs and significant changes have been incorporated in the 2005 AISC Specifications for Structural Steel Buildings (2005). The shear strength of the stud has been found to be a function of the concrete properties and stud cross sectional area. The equation for stud strength as presented in the AISC Specifications is as follows:

$$Q_n = 0.5A_{sc}\sqrt{f'_c E_c} \le A_{sc}F_u \qquad \text{(kips)} \qquad (2.18)$$

Topkaya (2004) has investigated the effects of composite shear stud strength for early concrete ages. A total of 24 push-out tests were performed. A equation similar to the one presented in the Specifications for Structural Steel Buildings was proposed and is applicable for concretes at early ages. The equation is as follows:

$$Q_n = 2.5A_{sc}\left(f'_c E_c\right)^{0.3} \qquad \text{(kips)} \qquad (2.19)$$

Lam (2005) identified three different types of failure modes for a push-out specimen. The first type of failure mode was a concrete cone failure where the stud does not fail. Before the stud yielded the concrete around the stud failed in compression. The second failure mode identified involved complete yielding of the stud without a concrete failure around the stud. The third failure mode was yielding of the stud as well as concrete failure. All three failure modes were seen in Lam's research.

2.7 AASHTO Standard Specification Provisions

AASHTO Standard Specifications for Bridge Design, 17th Edition (2003) do not dictate the location of the critical section in horizontal shear design, but standard practice is to design at the same section as the critical section for vertical shear. It is also necessary to check the entire length of the span when the stirrups will extend from the beam into the slab to provide for the horizontal shear since the spacing of vertical reinforcement likely will vary along the length of the span.

To quantify the horizontal shear capacity, the Standard Specifications bases its requirements on empirical data from research by Birkeland and Birkeland (1966), Mast (1968), Kriz and Raths (1965) and Hofbeck, et al (1969). This research, however, was performed for cast-in-place slab systems and very well may not be valid for the precast slab system. The Standard Specifications approach is as follows:

$$V_u \leq \phi V_{nh}$$

where

V_u = factored vertical shear

V_{nh} = nominal horizontal shear strength

ϕ = strength reduction factor = 0.90

When contact surfaces are intentionally roughened, nominal shear capacity is obtained from one of the following three conditions. An intentionally roughened surface is one of exposed aggregate raked to an amplitude of ¼ in.

a) when no reinforcement is provided:

$$V_{nh} = 80 b_v d$$

b) when minimum vertical ties are provided:

$$V_{nh} = 350 b_v d$$

c) when required area of ties, A_{vh}, exceeds the minimum area:

$$V_{nh} = 350 b_v d + 0.40 \frac{A_{vh} f_y d}{s}$$

The minimum area of ties is:

$$A_{vh} = 50 \frac{b_v s}{f_y}$$

where

b_v = interface width

d = distance from extreme compression fiber to centroid of the prestressing force (need not be taken less than 0.80h)

$s = \min \begin{vmatrix} 4(b_w) \\ 24\text{in.} \end{vmatrix}$ where b_w is the least web width

2.8 AASHTO LRFD Bridge Design Specifications for Horizontal Shear

The provisions of the AASHTO LRFD Bridge Design Specifications, 3rd Edition present a different approach based on the well-established shear friction theory. To calculate the design horizontal shear however the LRFD specifications gives no guidance. The designer can choose between one of the methods presented previously in this thesis in Section 2.1: Horizontal Shear in Composite Members. The PCI Bridge Design Manual (1997) recommends the method of equilibrium forces be used to calculate the design horizontal shear load.

The basic design equation for the LRFD method is:

$$v_{uh} A_{cv} \leq \phi V_n$$

To compute the horizontal shear resistance the shear friction model is:

$$V_n = cA_{cv} + \mu[A_{vf} f_y + P_c] \leq \min \begin{vmatrix} 0.2f'_c A_{cv} \\ 0.8A_{cv} \end{vmatrix} \quad (in^2)$$

where

c = cohesion factor = 100 psi for concrete cast on a roughened surface

75 psi for concrete cast against a smooth surface

25 psi for concrete cast against a steel surface

μ = friction factor = 1.0 for concrete cast on a roughened surface

0.6 for concrete cast against a smooth surface

0.7 for concrete cast against a steel surface

A_{cv} = interface area of concrete engaged in shear transfer (in^2)

P_c = permanent net compressive force normal to the shear plane (lbs) (may conservatively be neglected)

f_y = yield strength of the shear reinforcement (psi)

The minimum area of steel is:

$$A_{vf} = \frac{0.05 b_v s}{f_y} \quad (in^2)$$

It is important to note that the equation used to calculate the horizontal shear resistance assumes that as a crack is formed at the interface and separates it yields the steel that crosses the interface. In reality the steel crossing the interface may not have reached the yield stress.

2.9 Summary of Literature Review

This chapter has presented the theories and evolution of shear friction. Through the years numerous equations and revisions to the design codes have occurred. Unfortunately, most of this research has focused on cast-in-place construction and may

not be valid for precast deck panel systems. Menkulasi as well as Scholtz have recently performed push-off tests for precast deck panel systems. The research performed by Menkulasi, however, may not accurately model an actual precast deck panel system as a result of the grouting orientation of the push-off specimens in that research. Figure 2.3 below depicts the results of the research that has been previously discussed. In this figure the horizontal shear resistance is plotted against the clamping stress.

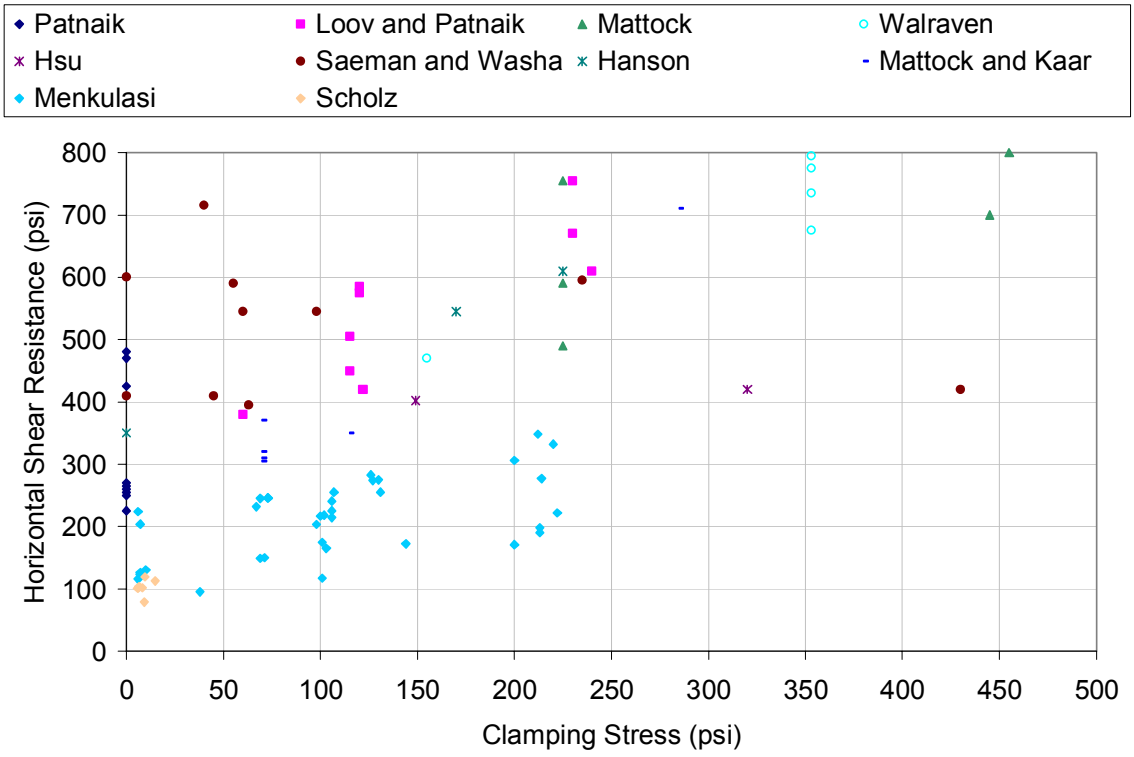

Figure 2.3: Previous Research Results

CHAPTER 3: DESCRIPTION OF TESTS

3.1 Overview

To examine the horizontal shear strength of a precast full-depth bridge deck panel system on precast girders 29 push-off tests were conducted. This chapter describes the dimensions and procedures used to fabricate, instrument and test each specimen. Material properties for the grout and concrete used to construct the specimens were taken from compressive tests. Haunch height was not one of the parameters investigated. Menkulasi (2002) found that varying the haunch height does not pose any significant changes in the peak shear stresses obtained. Listed below are the various properties examined in this research.

- Shear connector type
- Cross-sectional area of shear connector
- Grout Type
- Surface Treatment
- Pocket Type

3.2 Material Properties

3.2.1 Concrete & Grout Material Properties

The compressive strength of the grout and concrete was taken each day of testing. The grout strength was measured in accordance with ASTM C109 (2002): Standard Test Method for Compressive Strength of Hydraulic Cement Mortars Using 2-in. Cube Specimens (modified). The compressive strength of the concrete was measured using 4 in. by 8 in. cylindrical specimens in accordance with ASTM C39 (2001): Standard Test Method for Compressive Strength of Cylindrical Concrete Specimens (See Figure 3.1).

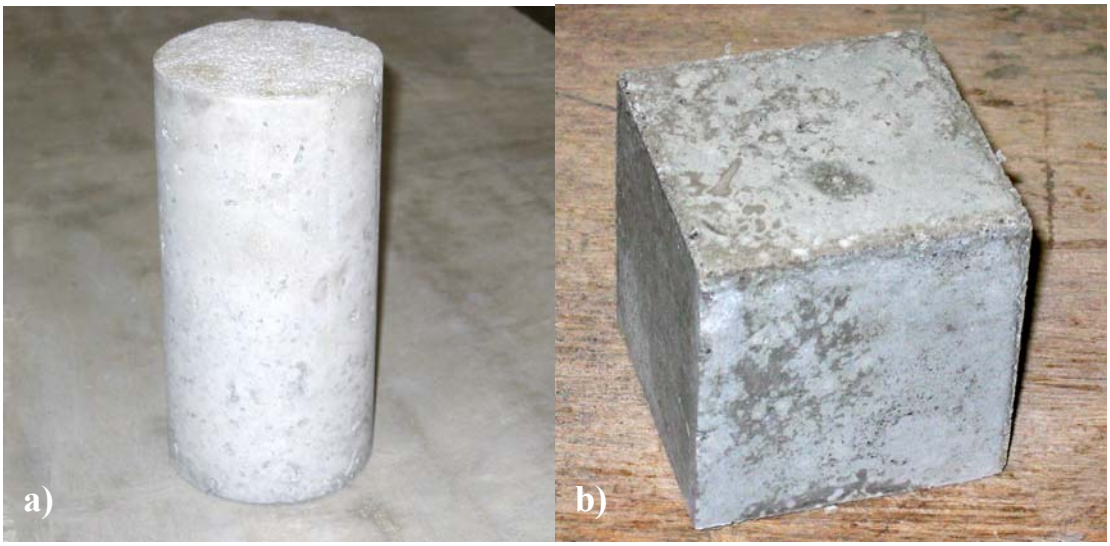

Figure 3.1: a) 4 in.x 8 in. Concrete Cylinder b) 2 in. mortar cube

The concrete used to form the beam and slab side specimens for the 29 push-off tests was VDOT class A4 modified concrete. This type of concrete mix design is a standard Virginia bridge deck mix. The concrete was supplied by CONROCK ready mix of Blacksburg, Virginia. The mix design for the concrete is presented in Table 3.1. This mix results in a slump of 2-4 in. and an air content of 6-½ % $\pm$ 1½ %. The grouts used in this research were Five Star® Highway Patch and Set® 45 Hot Weather.

Table 3.1: Concrete Mix Design per yd^3

Material	Quantity	Source	Location
Type I/II Cement	501 lbs	Titan (Roanoke)	Troutville, VA
Pozzolans	167 lbs	Boral-Belews Creek	Walnut Cove, NC
Sand	1203 lbs	ACCO	Blacksburg, VA
No. 57 Stone	1773 lbs	ACCO	Blacksburg, VA
Water	291 lbs	Town of Blacksburg	Blacksburg, VA
Admixture	varies	Sika Corporation	Trenton, NJ
Retarder	varies	Sika Corporation	Trenton, NJ
Water reducer	varies	Sika Corporation	Trenton, NJ

3.2.2 Reinforcing Steel and Headed Shear Studs

Six tensile tests were performed on samples of the reinforcing bars to determine the actual yield stress of the material used. The reinforcing bars used were made of grade 60 steel. Tensile test results can be found in Appendix B. No tensile tests were performed on the headed stud shear connectors and the yield stress of the connectors specified by the manufacturer of 49 ksi was used for all calculations. The Young's Modulus for both materials was 29,000 ksi.

3.3 Push-Off Test

Push-off tests were used to investigate the horizontal shear resistance of a precast concrete deck panel system on precast concrete girders. A schematic of this test is presented in Figure 3.2. This representative test evaluates the performance of the bond at the interface between the grout and concrete as well as the contribution of the shear connector. Various combinations of surface treatment, shear connector, and pocket type were tested. These tests have been used extensively in the past by other researchers for cast-in-place decks and have been shown to correlate well with data taken from full scale beam tests. However, few push-off tests have investigated the horizontal shear capacity of precast deck panel systems.

To represent a precast deck panel system the shear connector pocket and haunch are added to the push-off test specimen. Instead of casting the deck specimen onto the beam specimen as has been done in the past, the two were cast separately and connected with grout. Menkulasi (2002) performed such tests, however, the orientation of the specimens during grouting was with the specimens on their side. A more appropriate way, which is more representative of field grouting operations, is with the orientation as

shown in Figure 3.2 with the grout poured down the pocket. More recently, Sholtz (2004) performed a small series of tests grouted in this manner without shear connectors.

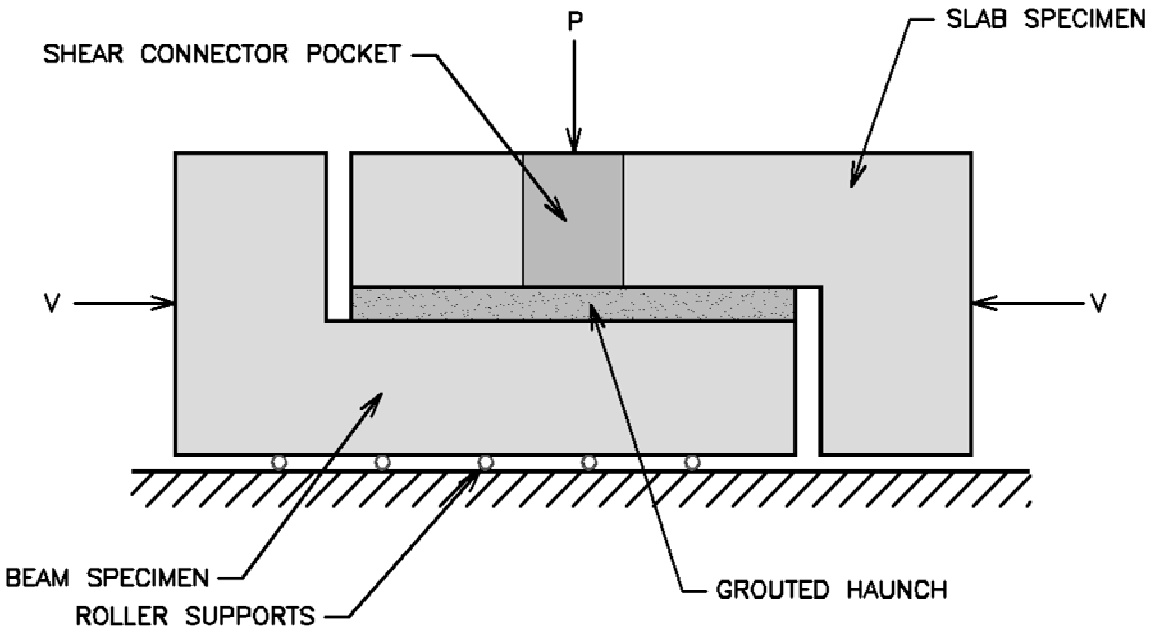

Figure 3.2: Typical Push Off Test

3.3.1 Specimen Fabrication

Two L-shaped blocks of VDOT standard A-4 concrete were formed for each test. The bottom section represented the beam and the top section represented the slab. The dimensions of the beam side specimen and the slab side specimen are seen in Figure 3.3 and 3.4, respectively. The top surface of the beam specimen was given a raked surface treatment with amplitude of ¼ in. The bottom of the slab section had either a smooth surface or an exposed aggregate surface depending on the particular test variable. Menkulasi's specimens and many in this research program had reinforcing bar stirrups extending from the beam side specimens into the shear pocket to serve as the shear connector.

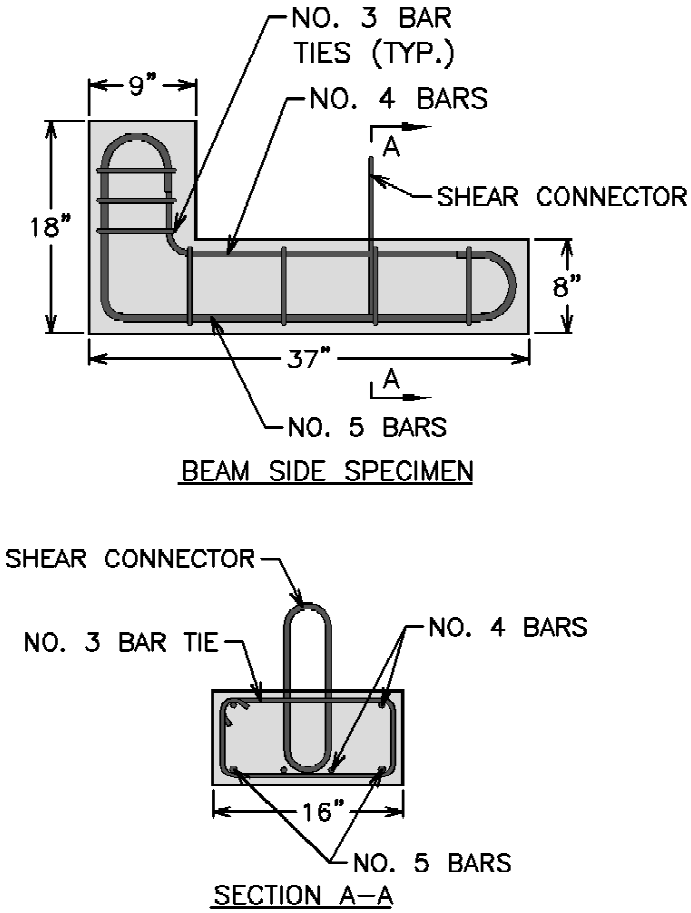

Figure 3.3: Beam Side Specimen

To represent actual slab casting practices, the smooth surface was the side of the slab against formwork, therefore this was not a hand finished surface. For the tests requiring an exposed aggregate surface, the formwork was coated with a surface retarder. The retarder was generously painted on the formwork an hour before the concrete was placed. The next day the formwork was stripped and the surface requiring an exposed aggregate finish was brushed and hosed with water. The water removed the unhardened paste and sand while large aggregate remained protruding producing an exposed aggregate surface.

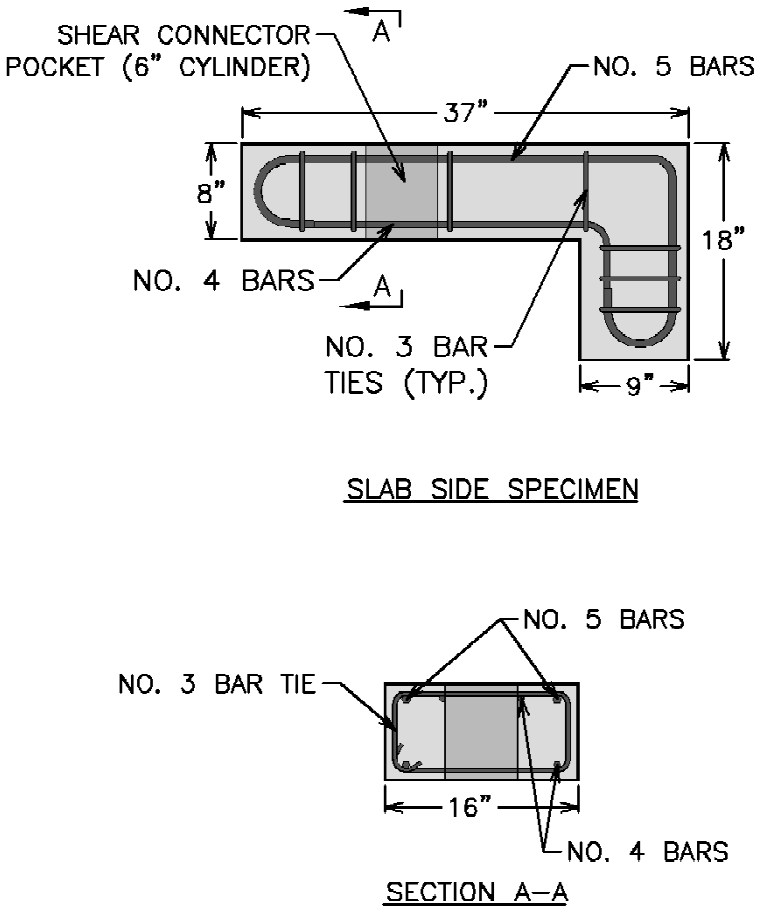

Figure 3.4: Slab Side Specimen

3.3.2 Headed Stud Shear Connectors

A new detail was developed that has potential to ease construction difficulties. This detail entailed the use of Headed Studs (Figure 3.5) with a precast girder. The problem that can arise during construction is that when precast girders and precast slabs are used the pockets and stirrups are in a fixed position. If there are any alignment problems and the two do not line up properly major problems can result during erection.

Figure 3.5: Headed Studs

The benefit of the welded stud system is that the slabs can be placed on top of the girders, they can be aligned and leveled then the welded studs can be shot onto the girder via the pockets. This not only eliminates problem associated with fabrication errors and misalignments, but the slabs are also much easier to place without having to guide the pockets over the studs.

In order to use welded studs on pre-cast concrete girders a steel plate must be attached to the surface of the concrete. This can be seen in Figure 3.6. Headed studs were welded to the bottom of a ¼ in. plate then embedded into the concrete as the concrete was cast. The ¾ in. headed studs to be used as shear connectors were then welded to the top of the beam specimen. The AISC Specifications for Structural Steel Buildings (1999) states that the stud diameter shall not exceed 2.5 time the flange thickness. For the test specimen, the plate thickness requirement was slightly violated (0.3 in. required and 0.25 in. provided). To ensure failure occurred in the haunch and

pocket, the studs on the bottom of the plate embedded in the precast concrete outnumbered the studs used as shear connectors.

Figure 3.6: Headed Shear Stud Specimen

3.3.3 Haunch and Pocket Grouting

To connect the two specimens and fill the haunch and area around the shear connectors, two brands of non-shrink grout were used. The first brand of grout used was Five Star Highway Patch. The second brand used was Set-45 Hot Weather. The Set-45 Hot Weather was also used in extended form by adding clean pea gravel. Grout mixing information is presented in Table 3.2. Before grouting, formwork was placed along the sides of the haunch and sealed using silicon sealant and weather stripping. It was critical that the haunch be formed well to ensure that the grout did not leak. When the grout is mixed properly it is able to flow very well and can present problems by deforming the forms and leaking if extra care is not given to the formwork. Figure 3.7 shows a

specimen with formwork in place, ready to be grouted. The strain gage lead wires can be seen exiting the side of the beam side specimen.

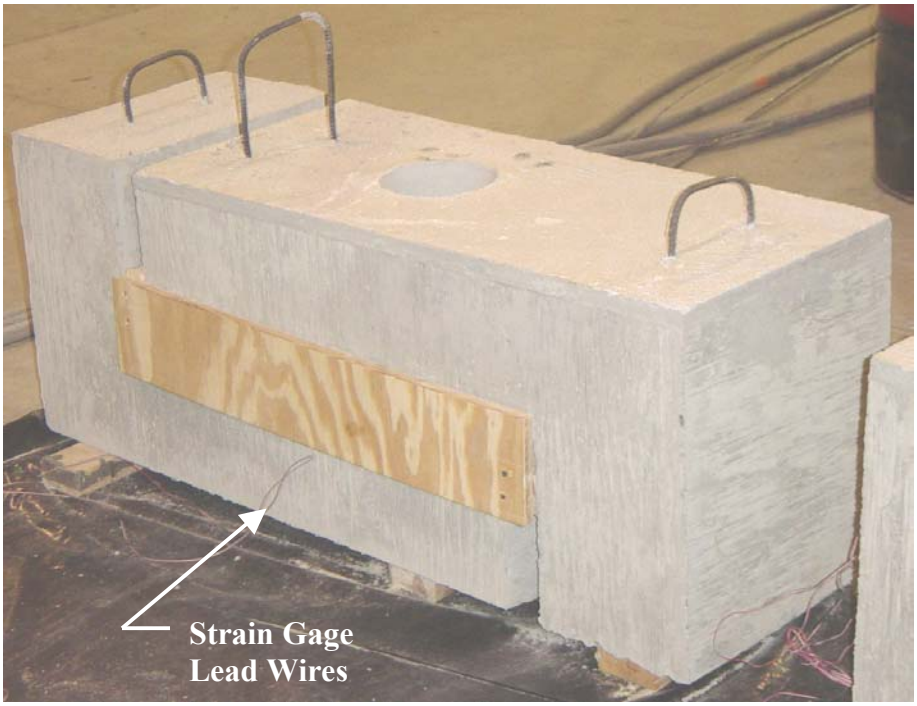

Figure 3.7: Specimen formed for grouting

The grout was mixed according to the manufacture's specifications in a small mortar mixer. Due to the size of the mixer each specimen required approximately three batches of grout. Table 3.2 shows the maximum amounts of water and yield volume per bag of grout. It is important to not exceed the max water amount so that the grout will gain its full strength, but it is also necessary to maintain the proper amount of flow.

Table 3.2: Mixing Quantities per 50 lb bag

Grout Type	Max water, pints	Aggregate, lbs	Yield volume, ft^3
Five Star® Highway Patch	6 pints	0	0.4
Set® 45 Hot Weather	3.75 pints	0	0.39
Set® 45 Hot Weather Extended	3.75 pints	30	0.58

3.3.4 Hidden Pocket Detail

One problem with the precast bridge deck panel system is that the pockets, which extend through the deck to the riding surface, can be unattractive. This can be seen in Figure 3.8 in which the riding surface has a patchy appearance. One solution to this problem is the hidden pocket detail, which provides a more uniform and aesthetically pleasing bridge deck. Another option is to provide an overlay to the bridge deck.

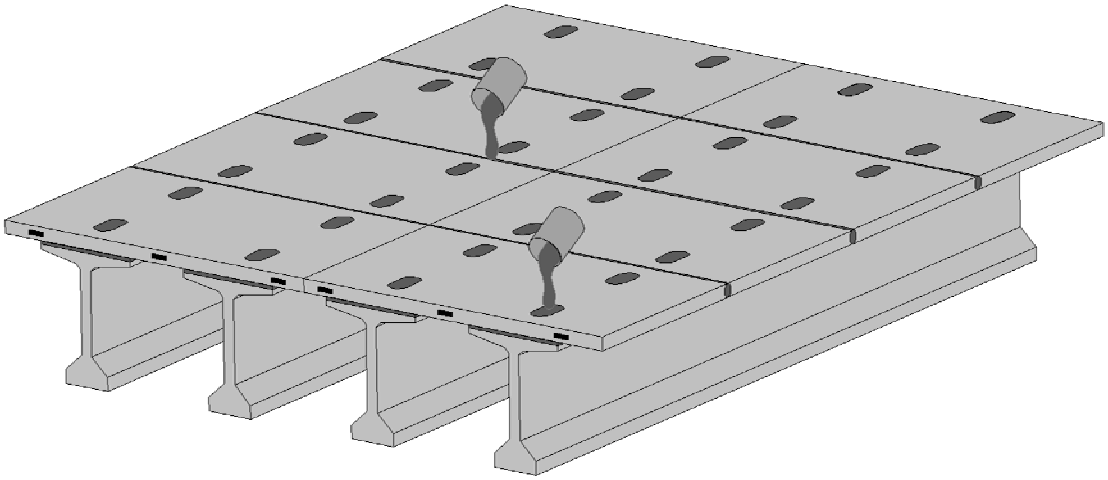

Figure 3.8: Full Depth Pre-cast Bridge Deck Panel Schematic

The trial detail in this investigation was an inverted cone type detail as shown in Figure 3.9. Since the top of the pocket was 2 in. below the riding surface the only access to the pocket by grout is through the haunch. Once the haunch was formed grout was pumped through the side port of the haunch. An important requirement of this detail is that grout vents be placed in the top of the pocket so that any air may escape. These

grout vents exit at the top of the bridge deck and are small enough in diameter to not disturb the aesthetics of the bridge deck.

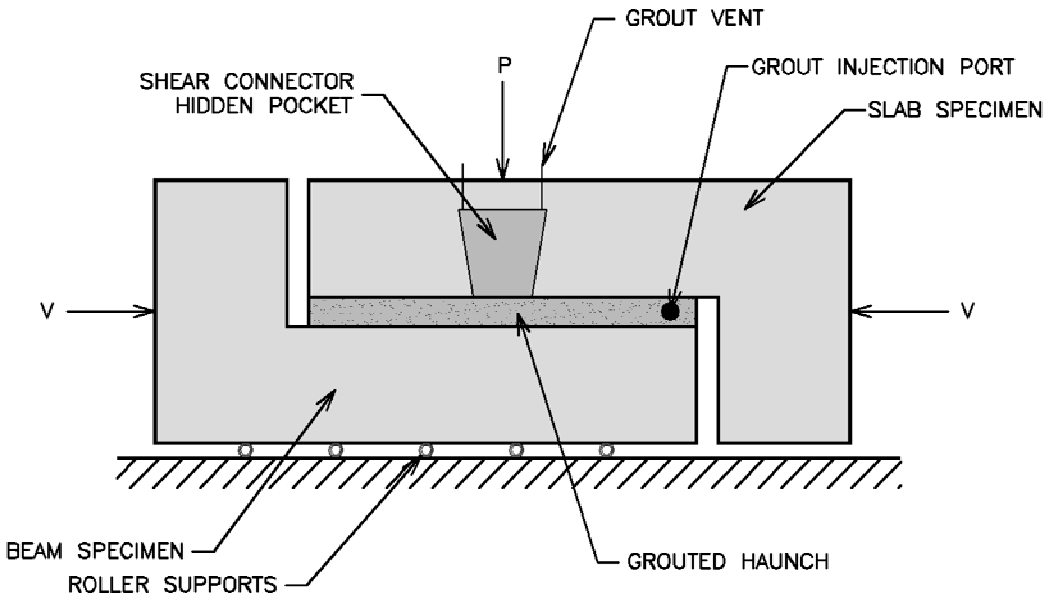

Figure 3.9: Hidden Pocket Detail

3.3.5 Push-Off Test Setup

3.3.5.1 Description

For each test, the grouted specimens were placed on steel tubing which allowed the beam side portion of the specimen to slide freely. The entire test frame can be seen in Figure 3.10. The slab side of the specimen was fixed in place with an abutment. To minimize eccentricity of the applied load relative to the haunch, a ½ in. steel plate 4 in. wide was placed between the abutment and the specimen at the height of the haunch.

A 50 ton vertical ram was used to exert a normal force of 2.5 kips on the specimens. This normal force was to simulate dead load present due to the slab, wearing surface and barrier rails. A 60 ton ram placed horizontally against another abutment was

used to impose the shearing force. Another ½ in. thick steel plate at the height of the haunch on the live end was used so that the shearing force was distributed across the width of the specimen and without eccentricity relative to the haunch.

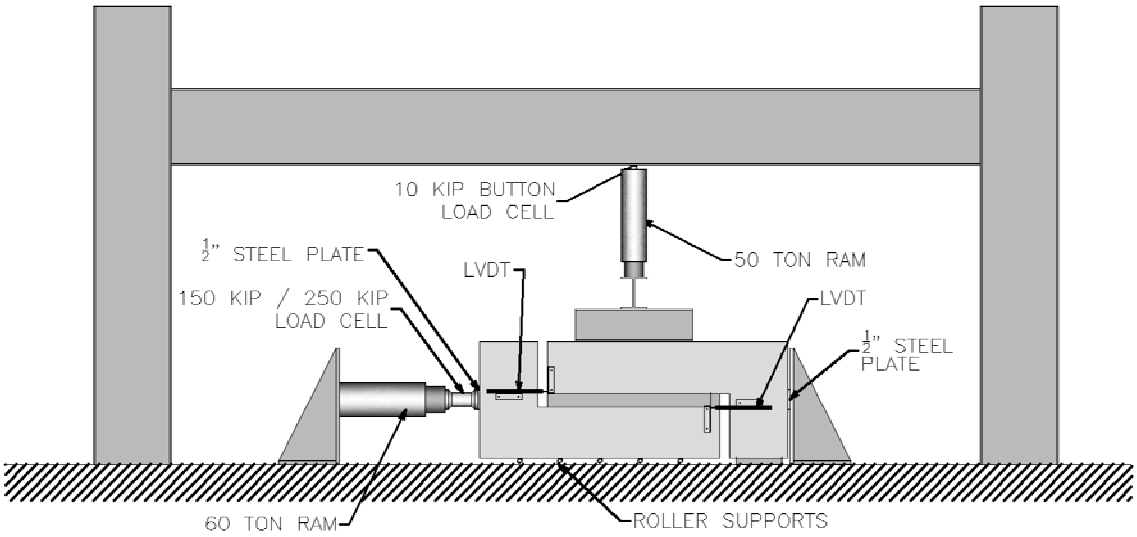

Figure 3.10: Test Setup

3.3.5.2 Instrumentation

Each specimen was equipped with two load cells, two LVDTs and two strain gages if shear connectors were used for the specimen. A 10 kip button load cell was used above the vertical ram. The horizontal ram used a 150 kip load cell or a 250 kip load cell depending on the test. The LVDTs were used to measure slip of the beam side and slab side specimens relative to one another. One LVDT was attached to the slab side and the other was attached to the beam side specimen. The LVDTs were attached to the specimens using a small section of angle attached to the specimens with concrete anchor screws. Another angle was placed perpendicular to the LVDT for the plunger to push against. The strain gages were placed on the shear connectors before grouting. One gage was placed on the front side of one leg of the connector the other was placed on the other

side of the opposite connector. The strain gages were placed such that they were at the mid-height of the haunch. The placement of the strain gages can be seen in Figure 3.11. The strain gage lead wires then exited the haunch either through the beam side specimen or through the bottom of the haunch. Due to the location and sensitivity of the strain gages some were damaged during grouting and others were damaged early in the test.

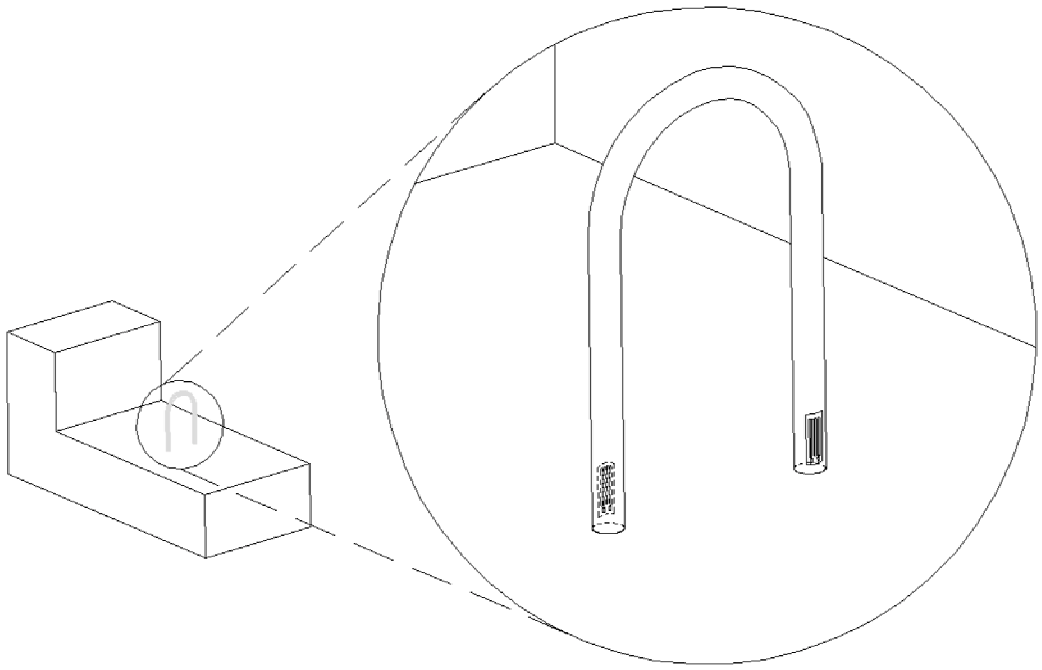

Figure 3.11: Strain Gage Placement

3.3.5.3 Testing Procedure

All testing occurred 24 hours after grouting operations had taken place. Additional time could have been given to allow the grout to cure but it was desired to represent worst case scenario in the field. The emphasis of this project is rapid bridge construction therefore this represented the extreme scenario of opening the bridge up to traffic the day after grouting operations.

All instrumentation was hooked into a System 5000 scanner and data was recorded using the Micro Measurements Group data acquisition software Strain Smart. Readings were taken continuously throughout the test. To begin the test an initial vertical load of 2.5 kips was applied. This load simulated the weight of the additional slab that would be outside the girder along with any wearing surface and barrier system. Then the shear load was applied slowly until a peak load occurred. The peak load occurred at the time that a crack appeared or sometime soon after and the crack progressed across the interface and the two sides of the specimen began slipping relative to one another. Due to separation of the specimens which occurs as the crack surfaces ride over one another the normal load increased. This was permitted to occur and the normal load was not reduced. The horizontal displacement was increased until the gap between the two specimens closed. This required approximately 1.5 in. of slip. Following this all load was removed and data acquisition ceased. A typical load versus slip behavior is seen in Figure 3.12.

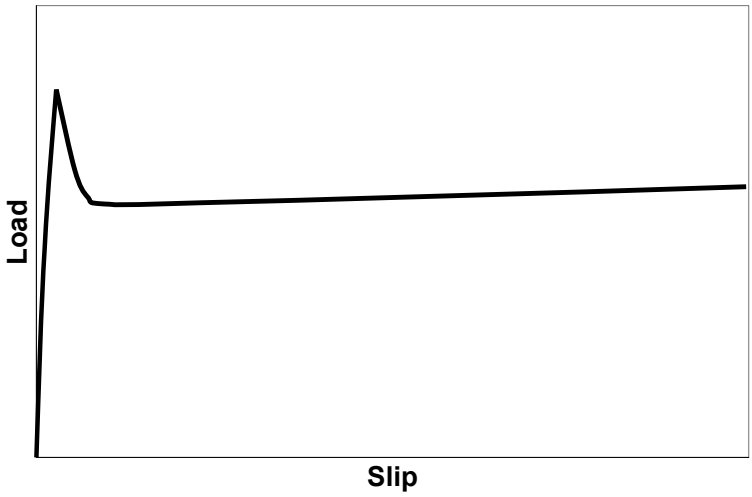

Figure 3.12: Typical Load versus Slip Plot

3.3.6 Test Parameters and Series Details

Within each series, different parameters were varied. A summary of the test series is presented in Table 3.3. A minimum of two repetitions was performed for each detail. The parameters that were varied included the grout type, the type of connectors, the slab bottom surface treatment and the pocket type. The types of grout used were Five Star® Highway Patch, Set® 45 Hot Weather, and Set® 45 Hot Weather extended with pea gravel. The slab surface treatments were smooth and exposed aggregate.

The connectors used were either double legs stirrups or headed shear studs. The double leg stirrups were either No. 4 bars or No. 5 bars. Arrangements of two, three and four headed shear studs were used. The studs were ¾ in. diameter and 7 in. in length. The headed shear studs were attached to a plate embedded in the beam side specimen. The bottom of the plate had studs attached to properly anchor the plate in the concrete.

Also a variation of the pocket was tried. The typical pocket was a cylinder of 6 in. diameter extending through the slab side specimen. The variation on the pocket consisted of an upside down conical shaped hidden pocket. This detail is presented in Fig. 3.9.

Table 3.3 presents the variables examined in each test series. The individual results from within each series can be found in Appendix A.

Table 3.3: Test Summary

Series	Shear Connector	Grout Type	Surface Treatment	Repetitions	Pocket
1	2 No. 4 Bars	Five Star Highway	Exposed Aggregate	2	6" Cylinder
2	2 No. 4 Bars	Set 45 Extended	Exposed Aggregate	2	6" Cylinder
3	2 No. 4 Bars	Set 45 Neat	Exposed Aggregate	3	6" Cylinder
4	2 No. 5 Bars	Set 45 Extended	Exposed Aggregate	2	6" Cylinder
5	2 No. 5 Bars	Five Star Highway	Exposed Aggregate	2	6" Cylinder
6	2 No. 5 Bars	Set 45 Neat	Exposed Aggregate	3	6" Cylinder
7	2 No. 4 Bars	Five Star Highway	Smooth	2	6" Cylinder
8	2 No. 5 Bars	Five Star Highway	Smooth	3	6" Cylinder
9	No Shear Studs	Five Star Highway	Smooth	2	6" Cylinder
10	2 Nelson Studs	Five Star Highway	Smooth	2	6" Cylinder
11	4 Nelson Studs	Five Star Highway	Smooth	2	6" Cylinder
12	3 Nelson Studs	Five Star Highway	Smooth	2	6" Cylinder
13	2 No. 4 Bars	Five Star Highway	Exposed Aggregate	2	Hidden Pocket

CHAPTER 4: PRESENTATION OF RESULTS & ANALYSIS

4.1 Push-Off Tests

In order to investigate the horizontal shear capacity of the precast deck panel system, push-off tests were performed. From the data collected during push off tests, plots of horizontal load versus relative slip were produced. The plots can be broken down into three categories. A typical push off test load versus slip plot of each category can be seen in Figure 4.1. As the un-cracked specimen is loaded horizontally, the load increases with little slip until a crack is formed. This crack was typically found at the top interface between the slab and the haunch rather than the bottom interface between the beam and the haunch. This can be seen in Figure 4.3. However, this was not true of the headed shear Stud specimens.

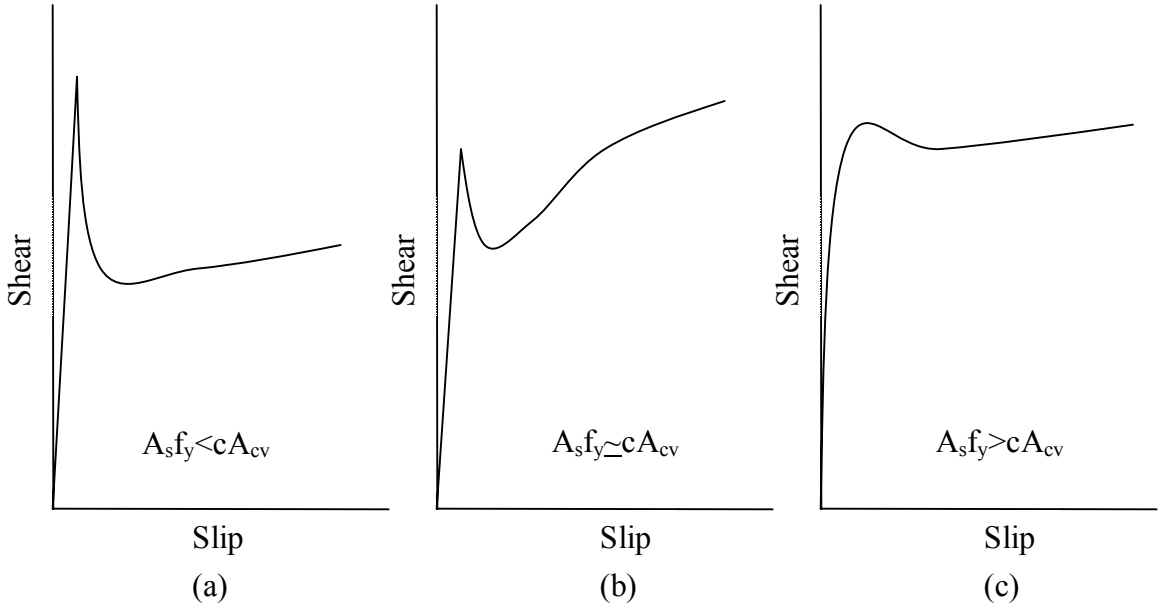

Figure 4.1: Typical Load vs. Slip Plots

As seen in Figure 4.1(a) when the horizontal shear resistance of the shear connectors is less than the resistance due to cohesion the load has a sharp drop following cracking of the interface. Then, an approximately constant load is maintained. When the horizontal shear resistance of the connectors is approximately equal to the cohesion a small sudden drop is seen as the crack is formed then the sustained load is about equal to the peak load. This can be seen in Figure 4.1(b). If the horizontal shear resistance of the shear connectors is greater than the cohesion, a different behavior can be seen as in Figure 4.1(c). As in the other cases the load is increased as the relative slip remains low then as a crack at the interface forms load is transferred from cohesion to the shear connectors. This can be seen where the slope changes. Then a peak load is reached where the connectors begin to yield. Beyond that point the sustained load is slightly lower than the peak load.

Most previous research that investigated push-off tests and horizontal shear strength was for cast-in-place slab systems. When these specimens were created, concrete was cast on concrete. For this research there is a haunch that is grouted and the tests have shown that the casting orientation is significant. Menkulasi performed push off tests that included a haunch, but grouted them while they lay on their side. A more accurate method, which is more representative of the way precast panels are grouted is with the beam side on the bottom and slab side on the top. The grout is then poured down through the shear pocket. Grouting the haunch with the specimens on their sides causes the cohesion and friction to be larger than would be after field grouting operations. This reduced cohesion and friction is a result of air trapped at the top interface between the haunch and slab, as shown in Figure 4.2.

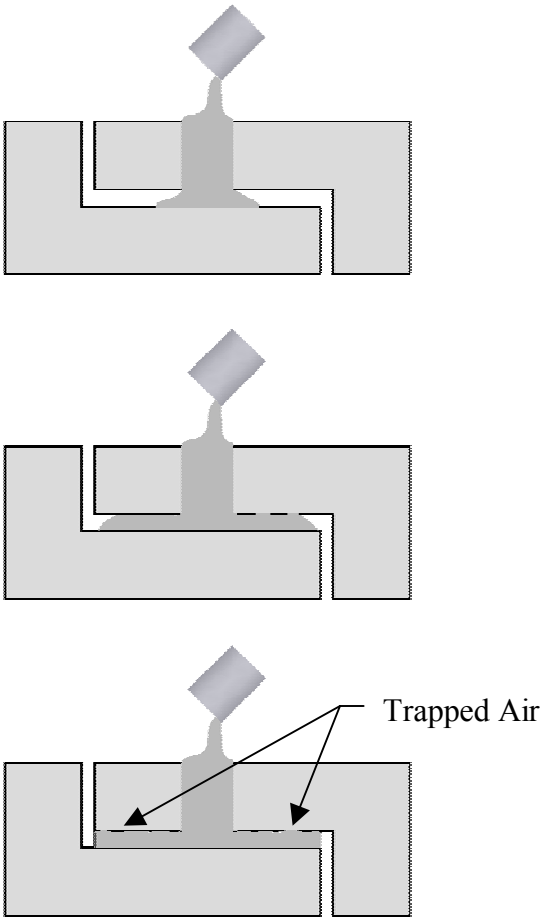

Figure 4.2: Specimen Grouting

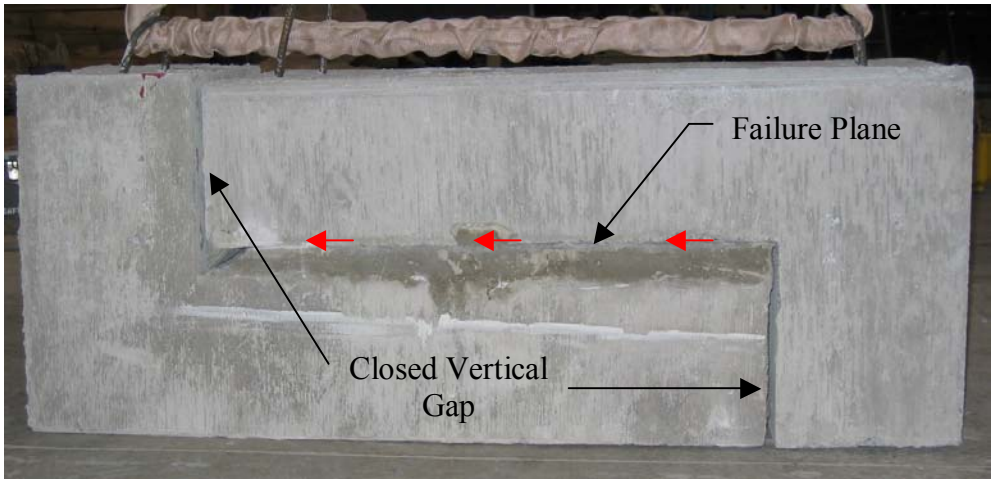

Figure 4.3: Push-Off Specimen after failure

Table 4.1 below shows the combined results from all of the tests. Below is a key to decipher the test designation.

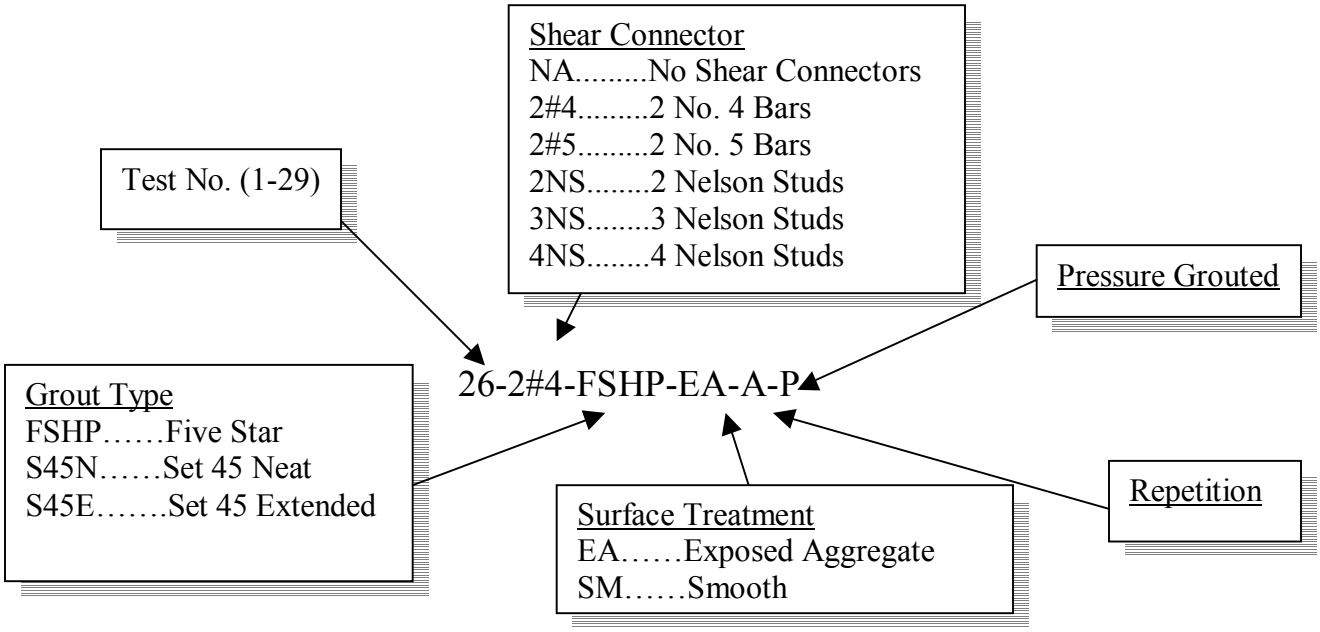

A_{cv} = Interface area

A_v = Shear connector cross sectional area

V_{peak} = Peak shear load

$V_{sustained}$ = Sustained shear load

P_n = Applied normal force

Slip = Average of both LVDT's measured slip at peak load

$\%F_y$ = Percentage of the yield stress based on measured strain

Failure plane = Haunch interface where crack first formed

F_c' concrete = Concrete compressive strength

F_c' grout = Grout compressive strength

Table 4.1: Push-off Test Combined Results

Test Designation	A_{cv}, (in^2)	A_v, (in^2)	V_{peak}, (Kips)	$V_{sustained}$, (Kips)	P_n, (Kips)	Slip, in.	% Fy (60 ksi)	Failure Plane	f'c, Grout (psi)	f'c, Concrete (psi)	Clamping Stress at Peak Load (psi)	Post Peak Clamping Stress (psi)	Peak Shear Stress (psi)	Sustained Shear Stress (psi)	Sustained Load region (in.)
1-2#4-FSHP-EA-A	424	0.40	45.6	29.4	3.4	0.018	20	Top	4500	5900	21.7	76.8	107.5	69.3	0.15-0.30
27-2#4-FSHP-EA-B	424	0.40	39.3	34.6	5.6	0.005	4	Top	3400	4600	16.0	82.1	92.7	81.6	0.08-0.15
2-2#4-S45E-EA-A	424	0.40	40.6	27.6	4.0	0.023	21	Top	4750	5900	23.9	78.3	95.6	65.1	0.15-0.30
3-2#4-S45E-EA-B	424	0.40	28.2	28.8	3.2	0.010	18	Top	4750	5900	20.0	76.5	66.5	67.9	0.08-0.15
4-2#4-S45N-EA-A	424	0.40	45.9	25.5	6.0	0.020	20	Top	2500	6000	28.0	83.1	108.3	60.1	0.15-0.30
5-2#4-S45N-EA-B	424	0.40	47.4	36.7	5.8	0.030	20	Top	2500	6000	27.5	82.6	111.8	86.6	0.15-0.30
24-2#4-S45N-EA-C	424	0.40	52.3	33.4	6.7	0.038	20 *	Top	6200	4600	29.6	84.7	123.3	78.8	0.15-0.30
6-2#5-S45E-EA-A	424	0.62	49.1	45.3	5.6	0.039	20	Top	3600	4300	34.5	119.9	115.9	106.8	0.15-0.30
7-2#5-S45E-EA-A	424	0.62	48.7	46.1	5.1	0.072	55	Top	3600	4300	70.6	118.7	115.0	108.7	0.15-0.30
8-2#5-FSHP-EA-A	424	0.62	42.1	38.8	5.6	0.034	30	Top	3250	4300	45.3	120.0	99.2	91.5	0.08-0.15
9-2#5-FSHP-EA-B	424	0.62	50.1	37.3	6.9	0.092	31	Top	2350	4300	49.4	123.1	118.2	88.0	0.15-0.30
10-2#5-S45N-EA-A	424	0.62	66.2	53.8	3.7	0.028	36	Top	2700	4300	47.1	115.4	156.0	126.9	0.15-0.30
11-2#5-S45N-EA-B	424	0.62	42.4	43.1	4.1	0.015	68 *	Top	2700	4300	81.7	116.4	100.1	101.7	0.06-0.10
29-2#5-S45N-EA-C	424	0.62	52.0	42.9	5.8	0.036	99	Top	6200	4600	119	120	123	101	0.15-0.30
12-2#4-FSHP-SM-A	424	0.40	47.1	38.0	2.8	0.033	72	Top	3200	5000	56.2	75.4	111.1	89.6	0.15-0.30
13-2#4-FSHP-SM-B	424	0.40	50.7	40.1	2.7	0.030	57	Top	3200	5000	45.5	75.1	119.6	94.6	0.15-0.30
14-2#5-FSHP-SM-A	424	0.62	59.5	43.5	28.8	0.030	76	Top	3200	5000	149.1	174.7	140.2	102.6	0.15-0.30
16-2#5-FSHP-SM-B	424	0.62	47.1	37.8	5.3	0.038	80	Top	3500	5000	97.9	119.2	111.0	89.2	0.15-0.30
28-2#5-FSHP-SM-C	424	0.62	56.3	49.7	6.9	0.037	78 *	Top	3400	4600	99.5	123.0	132.8	117.2	0.08-0.15
15-NA-FSHP-SM-A	424	0.00	34.7	38.5	27.9	0.024		Top	3500	5000	65.8	65.8	81.7	90.8	0.15-0.30
17-NA-FSHP-SM-B	424	0.00	29.3	8.4	5.3	0.003		Top	3500	5000	12.6	12.6	69.2	19.8	0.15-0.30
18-2NS-FSHP-SM-A	424	0.88	43.7	28.0	5.0	0.116	58	Bottom	3100	5400	71.1	114.0	103.0	66.0	0.75-1.00
20-2NS-FSHP-SM-B	424	0.88	30.6	23.0	4.7	0.019	7.5	Bottom	3100	5300	18.7	113.2	72.1	54.2	0.75-1.25
19-4NS-FSHP-SM-A	424	1.77	72.4	51.7	7.1	0.129	60	Bottom	3100	5400	139.2	220.8	170.8	121.9	0.75-1.00
21-4NS-FSHP-SM-B	424	1.77	70.8	63.3	11.0	0.132	88	Bottom	2900	5300	205.6	230.1	167.0	149.3	0.25-1.00
22-3NS-FSHP-SM-A	424	1.33	57.9	41.0	6.8	0.107	56	Bottom	2900	5300	101.7	169.1	136.6	96.7	0.50-1.00
23-3NS-FSHP-SM-B	424	1.33	54.5	47.7	6.0	0.116	92	Bottom	2900	5300	155.1	167.4	128.5	112.5	0.20-0.70
25-2#4-FSHP-EA-A-P	424	0.40	42.3	36.0	4.7	0.030	100	Top	3400	4400	80.0	80.0	99.8	84.9	0.13-0.80
26-2#4-FSHP-EA-B-P	424	0.40	48.5	35.6	4.2	0.012	100	Top	3400	4400	78.8	78.8	114.4	84.0	0.10-0.30

* Percentage of yield estimated because strain gage failed prior to peak load

4.2 Tests with No Shear Connectors

Two push-off tests were done without any reinforcement crossing the interface. Scholz (2004) performed six push-off tests without reinforcement crossing the interface. The only difference between the tests was that in this research the slab side specimens were not prepared with an exposed aggregate treatment as Scholz's specimens were. Since there are no dowels crossing the interface, these tests can be expected to be a representation of shear friction theory. A normal force is first applied to the test specimen. Then a shearing load is applied until the cohesive bond and static friction are overcome. Once this load is reached the specimen is no longer capable of carrying a load of that magnitude. Beyond the peak load a reduced but constant load is maintained as the specimen continues to slip. A typical load versus slip plot for a push-off test with no shear connectors is seen in Figure 4.4.

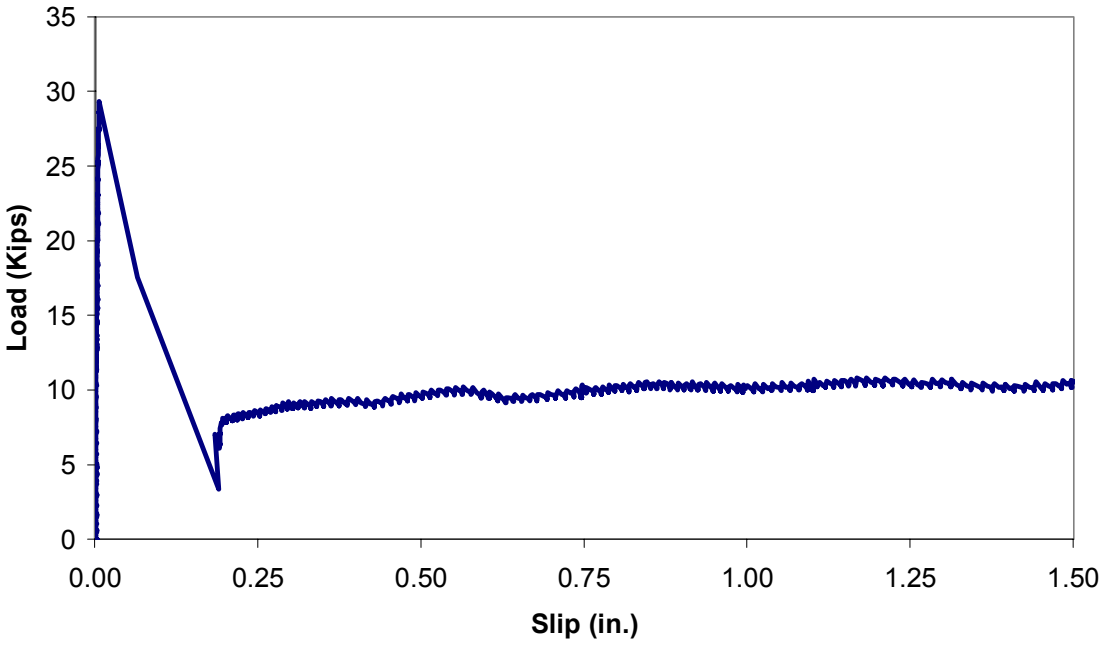

Figure 4.4: Typical Load vs. Slip Plot for a Specimen with no Shear Connectors

The average peak shear stress of the six tests performed by Scholz which had no reinforcing bar connectors was 103 psi and the tests ranged from 79 psi to 119 psi. The average of the two tests performed in this research was 75 psi suggesting that some additional cohesion may be obtained with an exposed aggregate slab. However, further tests are necessary to confirm this.

4.3 Tests with Shear Connectors

Two different types of shear connectors were tested in this research. The first type of connector tested was the typical reinforcing bar stirrup extending from the beam side specimen. For precast concrete beams this is the most common way of connecting the beam to the slab for composite action. Typically, the stirrups used for vertical shear are extended into the slab for horizontal shear. For these specific tests double leg stirrups of either No. 4 bars or No. 5 bars of Grade 60 steel were tested. From tensile tests the actual yield stress of the reinforcing bars was 73 ksi. The second type of connector was a headed stud. Headed studs are typically used on steel girders and have a yield stress of 49 ksi. They are generally made of mild steel and have a Young's Modulus of 29,000 ksi. A special type of welding gun is used to attach the studs in the field to the top flange of a steel girder. As typical in bridge applications ¾ in. headed shear studs were used. Since this research focused on precast girders a detail allowing studs to be welded to a plate embedded in concrete was used. Figure 4.5 shows the plate that was embedded into the top of the beam side specimen when the concrete was poured.

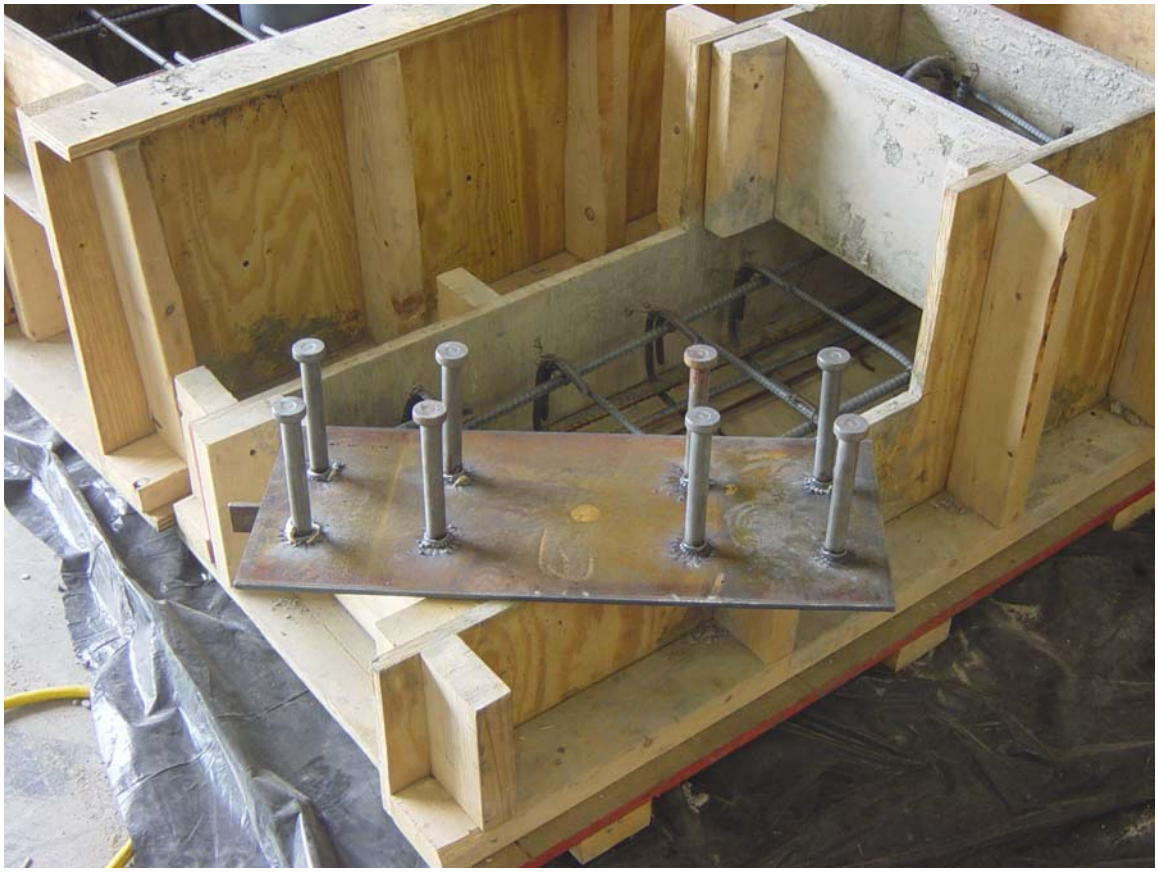

Figure 4.5: Plate to be embedded in top of beam side specimen

4.3.1 Reinforcing Bar Stirrups

Currently the most common way to provide connectivity between a concrete slab and concrete beam is by extending the stirrups used for vertical shear into the slab. Various tests using two legs of No. 4 bars or using two legs of No. 5 bars were carried out. As seen in Figure 4.6, a bar chart of the results shows that as the size of connectors was increased the average horizontal peak shear capacity was only increased slightly. As expected the specimens containing no shear connectors had the lowest shear capacity. However, there was only a small increase in the peak shear stress of the test with No. 5 bars compared to the tests with the No. 4 bars. Ten percent error bars suggest there is no difference in the peak shear stresses. Figure 4.7 demonstrates that while the peak shear

stresses are nearly the same, the tests with larger amounts of steel crossing the interface are capable of maintaining a higher post crack load.

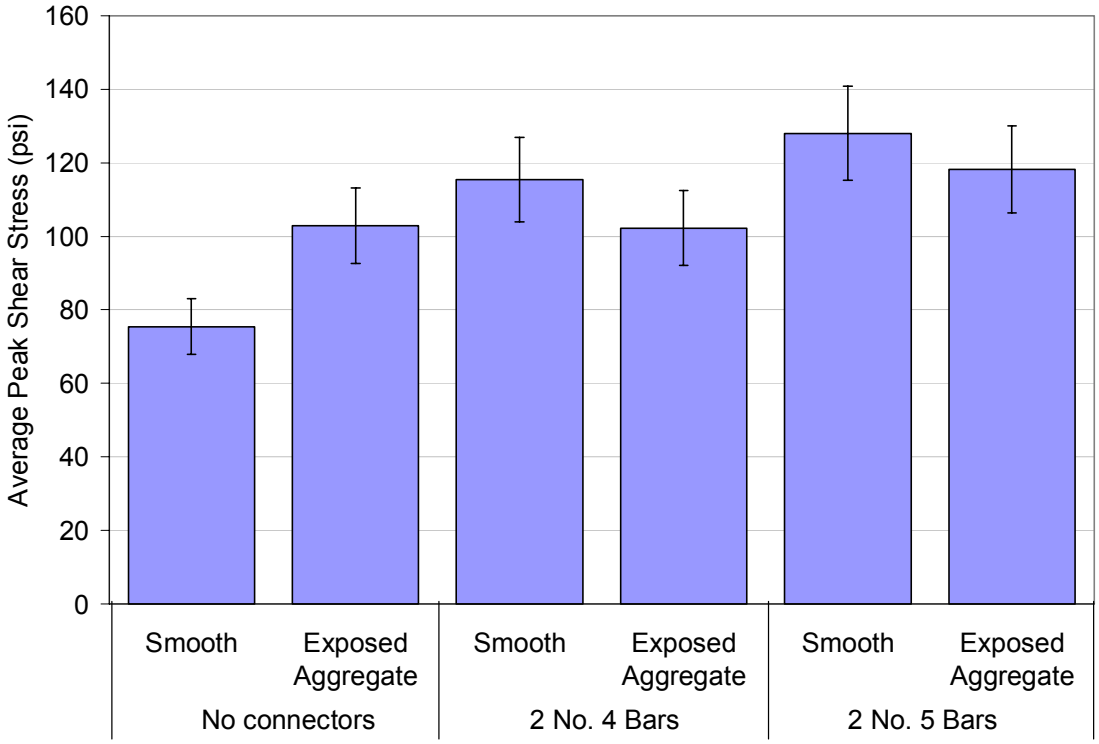

Figure 4.6: Average Peak Shear Stress (10% Error Bars)

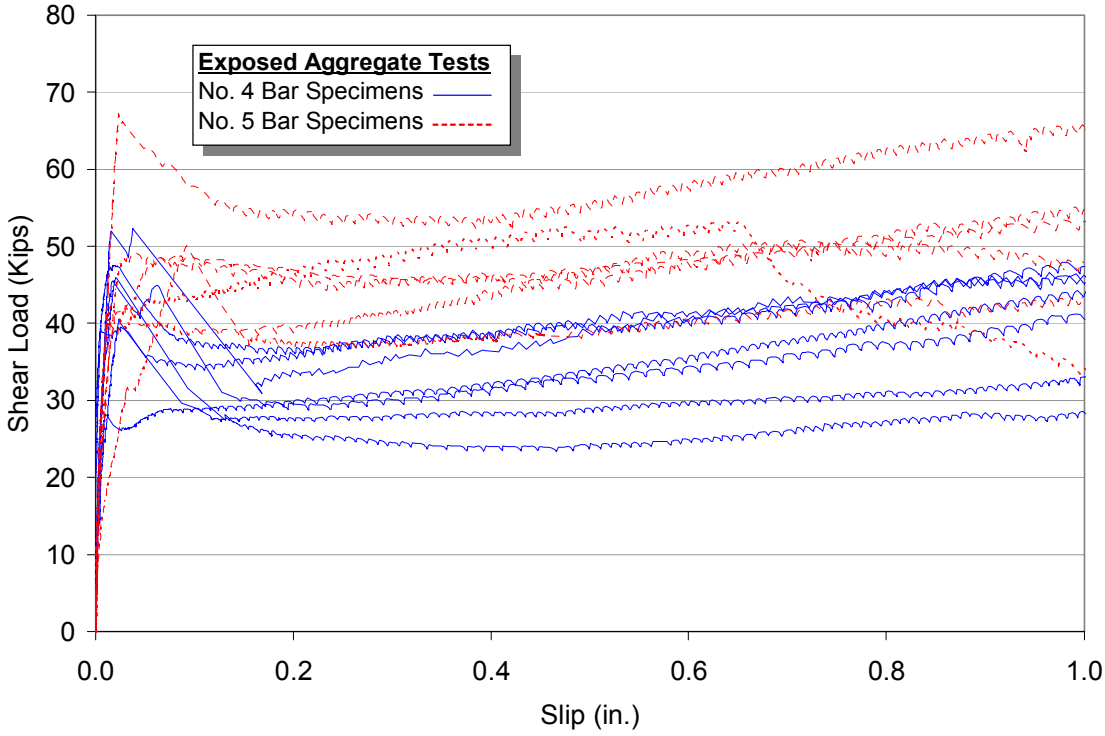

Figure 4.7: Load versus Slip for Exposed Aggregate Tests

4.3.2 Headed Shear Studs

Headed shear studs are typically used when precast slabs are supported on steel girders. Headed shear studs are advantageous since they can be welded to the girder after the panels have been placed. This eliminates problems associated with maneuvering the shear pockets over the studs as the panels are being lowered onto the girders as well as preventing fabrication errors. This series of tests consisted of specimens with groups of two, three and four ¾ in. studs. The respective amounts of steel crossing the interface are 0.88 in^2, 1.33 in^2 and 1.77 in^2. Figure 4.8 demonstrates with ten percent error bars that increasing the number of studs has an impact on the peak shearing stress.

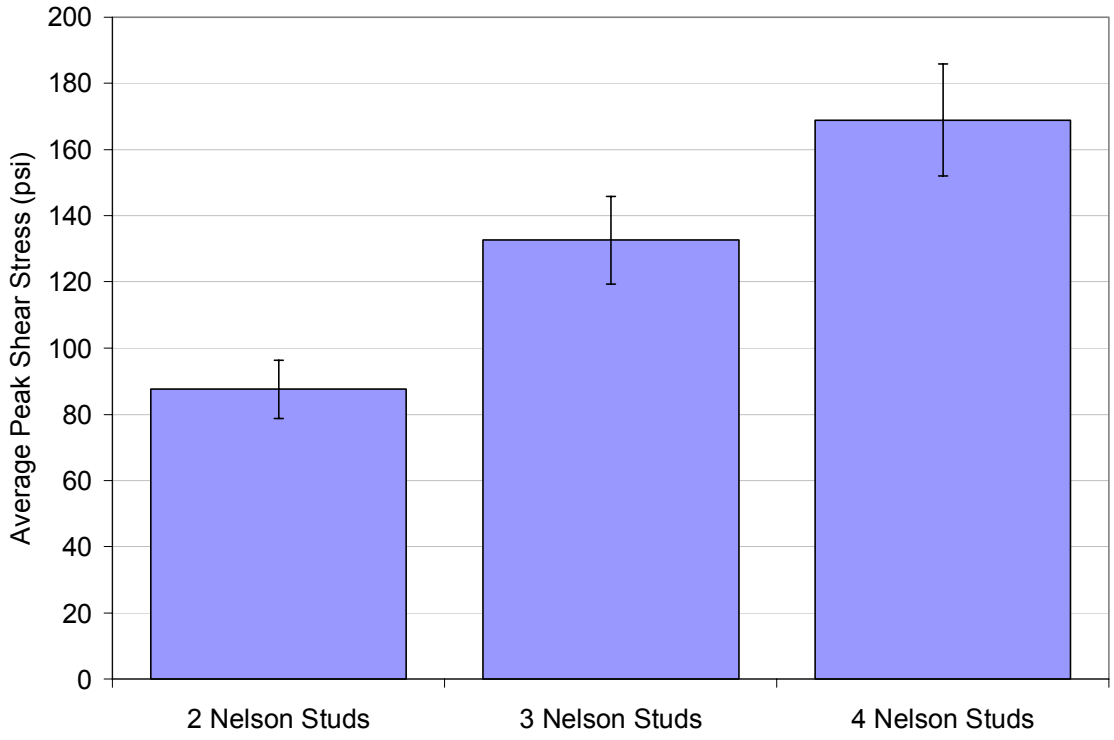

Figure 4.8: Average Peak Shear Stresses for Headed Shear Stud Tests (10 % Error Bars)

This significant increase was not seen in the tests with reinforcing bar stirrups. This is likely due to the fact that there is significantly more steel crossing the interface in these tests. As the amount of steel crossing the interface is increased so is the shear resistance that the shear connectors can provide. Once the shear resistance of the shear connectors exceeds the cohesive capacity the peak load can be carried by the shear connectors. For the tests with No. 4 bar and No. 5 bar stirrups the shear resistance capacity of the stirrups was lower than the cohesive capacity and the peak load was greater than the shear resistance of the connector. This explains why the peak loads of those tests were approximately the same.

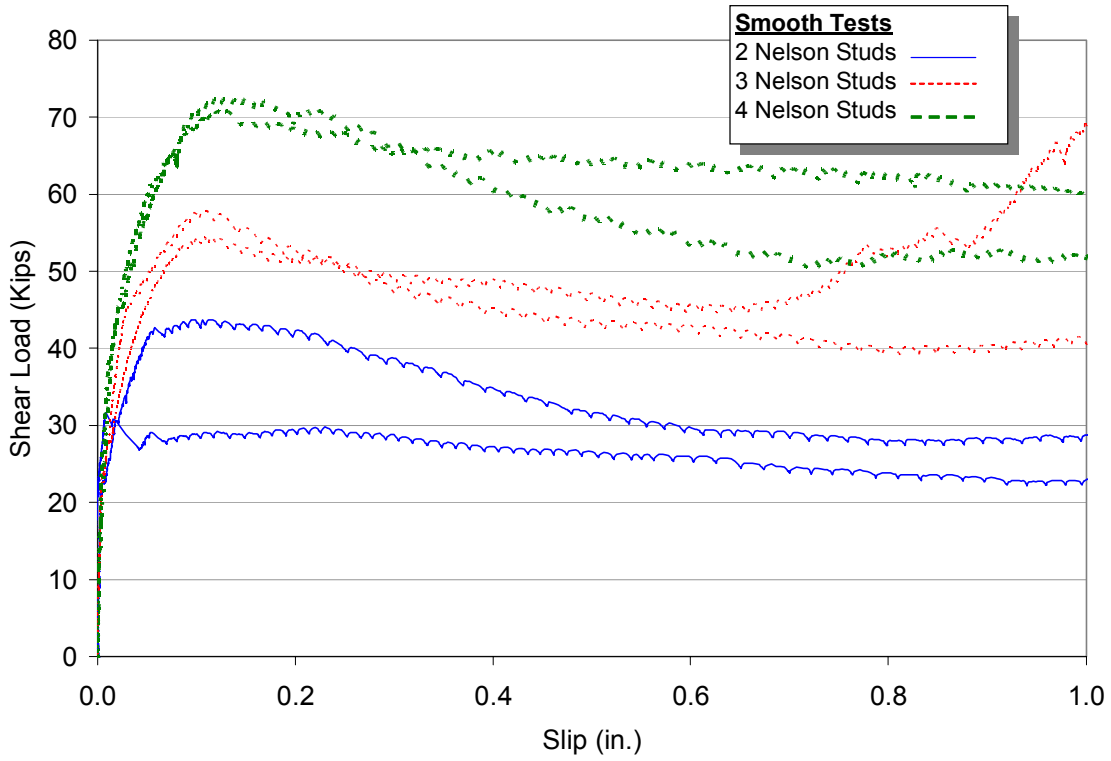

Figure 4.9: Load versus Slip for Headed Shear Stud Tests

4.4 Surface Treatment

To investigate an exposed aggregate surface treatment on the bottom of the slab versus a smooth finish on the bottom of the slab this parameter was varied for the double leg stirrup tests. As was seen in Figure 4.6 with ten percent error bars the surface treatment of the slab had little effect on the peak shear stress obtained. This is likely attributed to the casting orientation. One might expect the exposed aggregate slab to perform better. However, the casting orientation makes it easy for the exposed aggregate slab to collect pockets of air at the bottom of the slab (see Figure 4.2). This results both in a reduced coefficient of friction and reduced cohesion.

4.5 Hidden Pocket Detail

A trial detail of a hidden pocket was conducted. The hidden pocket was the shape of an inverted cone and had two grout vents at the top to allow air to escape. One benefit of the hidden pocket is that the riding surface of the bridge has a much cleaner and uniform appearance. The two trial tests of this detail however did not show any noticeable improvement or decrease in shear strength. Figure 4.10 shows the normal 6 in. cylindrical pocket detail strength compared with the hidden pocket detail strength with ten percent error bars.

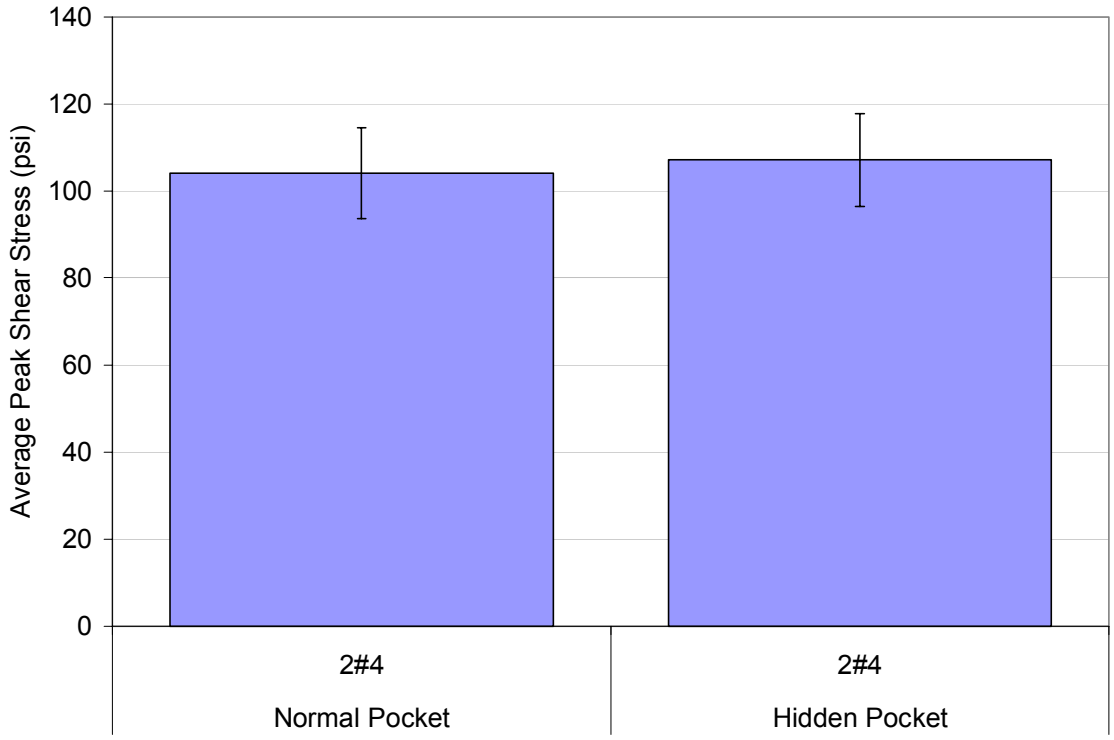

Figure 4.10: Normal Pocket versus Hidden Pocket Average Peak Shear Stress

4.6 Yield in Shear Connectors

Part of the theory in shear friction models is that the steel crossing the interface provides a clamping force. This clamping force is provided as a crack is opened. As the

crack continues to dilate the reinforcing steel restrains the opening of that crack providing a clamping force in addition to any normal force applied to the slab. However, there is some speculation about whether the reinforcing bars are actually fully yielded before the peak load is obtained. In most equations the stress in the reinforcing bars is taken to be the yield stress. In order to measure the axial stress in the reinforcing bars strain gages were applied to the shear connectors at the level of the haunch. Unfortunately strain gages are extremely sensitive and are easily damaged. Several of the strain gages were damaged by the grout and concrete around them before the peak load was reached. Figure 4.11 shows the average percent of yield for the various connector arrangements. It appears that as the cross sectional area of the connectors increases the connectors are closer to yield.

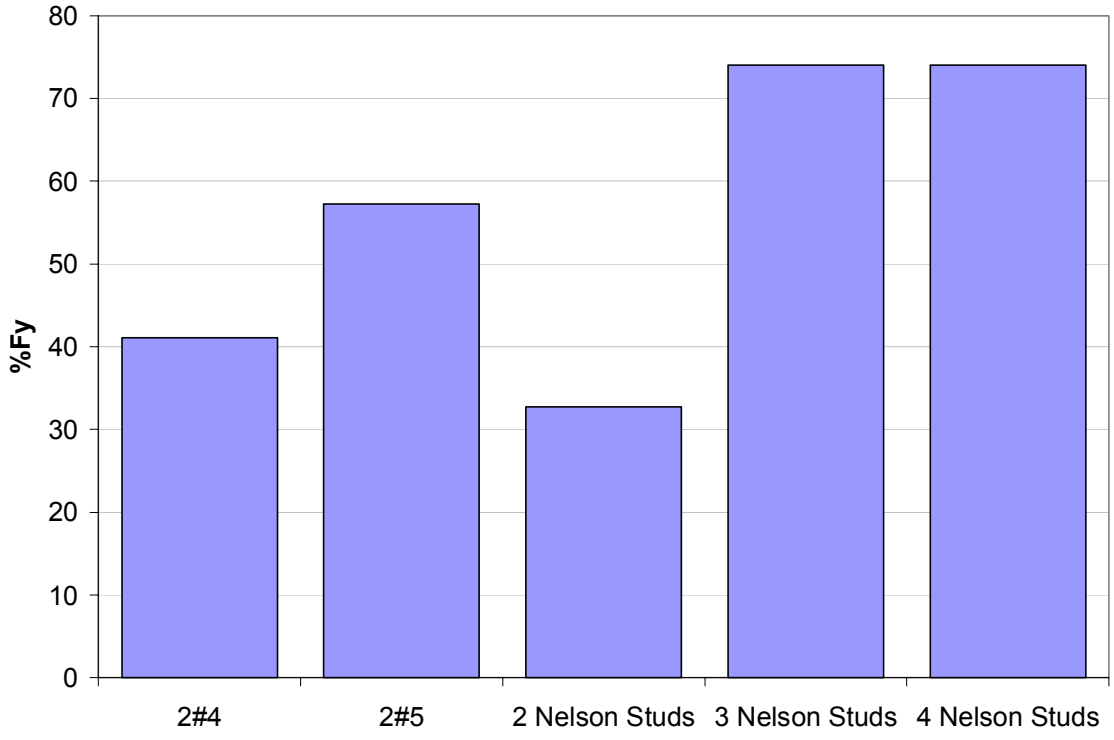

Figure 4.11: Percent of Yield Stress in Shear Connectors

In general if the horizontal shear resistance of the shear connectors is greater than the shear resistance from cohesion then the reinforcement will be yielded at the peak load. If the connectors crossing the interface have less resistance than the resistance provided by cohesion the yielding of the connectors occurs sometime after the peak load. This happens after a slip in the range of 0.15 in. to 0.30 in. has occurred.

4.7 Coefficient of Friction

If the clamping stress versus shear stress is plotted for the sustainable load which occurs just past peak one can measure a coefficient of friction. The coefficient of friction can be taken as the slope of the line passing through zero. This is not a true coefficient of friction as in the coulomb friction equation. Since there are shear connectors present this coefficient of friction also accounts for the shear resistance provided by the shear connectors. Since these are post peak loads the stress in the steel is taken to be at yield. From tension tests the actual average yield stress of the reinforcing bar stirrups used in this research was 73 ksi. Figure 4.12 shows the coefficient of friction for the reinforcing bars stirrup test as $\mu = 0.9$ and Figure 4.13 shows the coefficient of friction for the headed shear stud test as $\mu = 0.6$. As expected the tests with headed shear studs exhibited a lower friction coefficient. These tests cracked at the interface between the beam and haunch rather than on the slab side. This was expected since this surface consisted of grout against the steel plate embedded in the concrete, a much smoother surface with less cohesion.

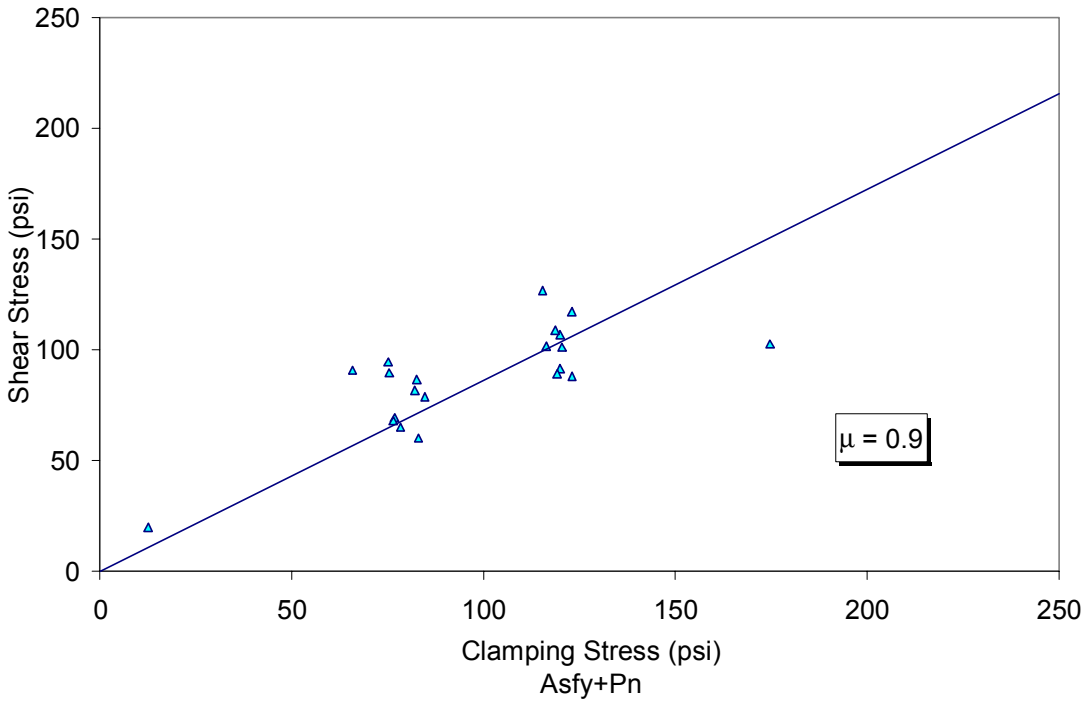

Figure 4.12: Reinforcing Bar Stirrups and No Connectors at Sustained Load

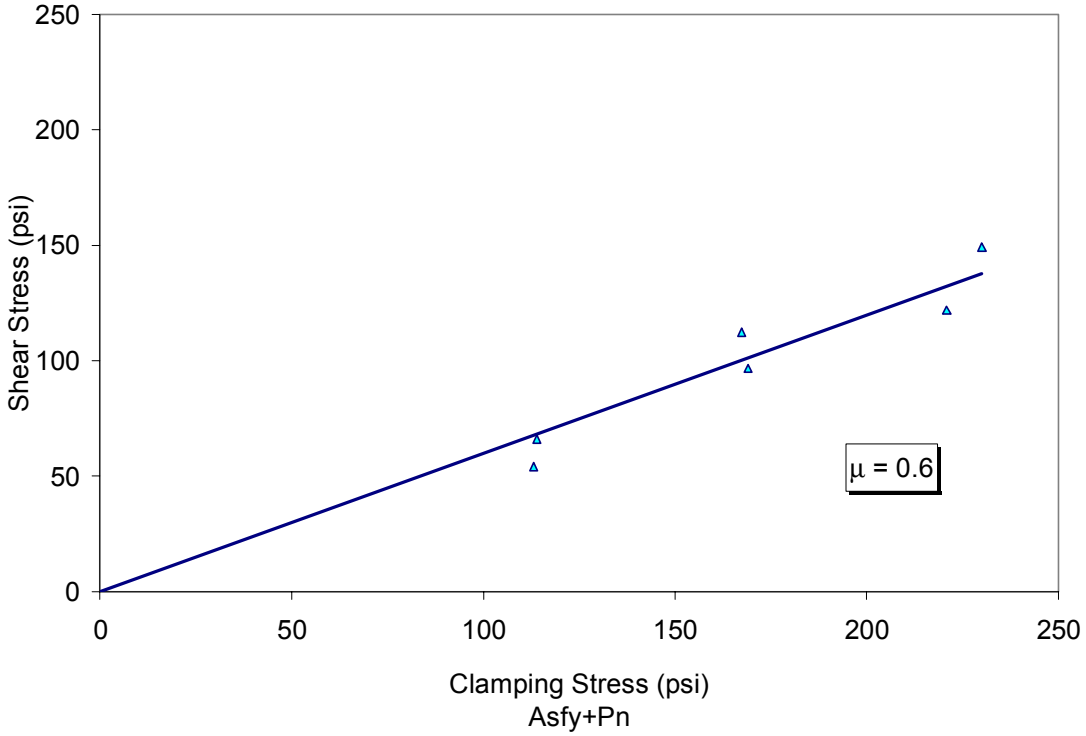

Figure 4.13: Headed Shear Stud at Sustained Load

4.8 Comparison with Current Code Equations

Figure 4.14 is a plot of the peak shearing stresses versus clamping stress. Overlaid on this plot are the AASHTO LRFD (2004) equations. The different equations are for concrete placed against hardened concrete with a roughened surface, concrete placed against hardened concrete but not with a roughened and concrete placed against a steel surface.

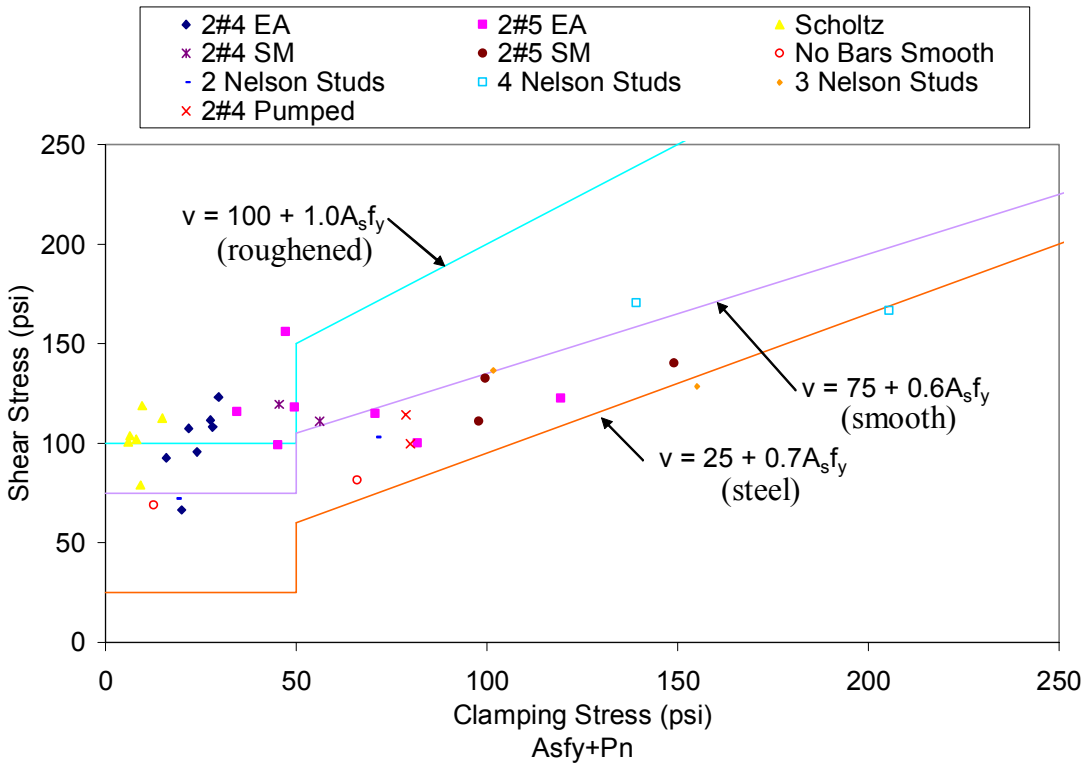

Figure 4.14: Peak Shear Stress vs. Clamping Stress

CHAPTER 5: SUMMARY, RECOMENDATIONS AND CONCLUSIONS

5.1 Summary

A full-depth precast deck panel system remains a viable option for rehabilitation of dilapidated decks. Construction delays to the motoring public can be minimized through the use of precast deck panel systems and special details. As opposed to cast-in-place construction a precast deck is produced in the controlled environment of a prestressing plant ensuring a higher quality concrete product.

In order to design a full-depth precast bridge, designers need some guidance on the horizontal shear transfer. Up to this point all design equations have been based on research for cast-in-place decks and it is necessary to incorporate the small nuances of the precast deck panel system that can affect the horizontal shear strength of the system. The designer must be able to ensure that adequate cohesion and or resistance from shear connectors crossing the interface will be sufficient to provide full composite action of the girder slab system.

A total of 29 push-off test were performed in this research. In these tests different parameters were investigated. The first parameter investigated was that of a prepared surface treatment at the bottom of the slab or a smooth surface. It was necessary to determine whether the cost of preparing an exposed aggregate slab was justified with a significant increase in strength. Second a trial series employing headed shear studs was investigated. The purpose of this detail was to address construction issues and to simplify the construction process. Lastly a trial detail of a hidden pocket was attempted. This detail required that the shear connector pocket not extend to the top of the slab. The

idea was to improve the rideability and aesthetics of the riding surface. This detail also requires pressure grouting of the haunch and pockets through a side port at the haunch.

5.2 Conclusions

The results do not indicate any significant increase in strength when the bottom of the slab is prepared with an exposed aggregate surface. When the headed shear stud system is used an exposed aggregate surface treatment is not required since the failure plane is then at the beam to haunch interface.

The headed shear stud system which utilized welded stud connectors on a plate that was embedded in the top flange of the beam had successful results. The specimens performed very similarly to the test specimens that utilized the typical reinforcement bar stirrups. Headed shear studs do have a lower yield stress though so an increased number of studs may be required.

The inverted cone hidden pocket system also performed comparably with the normal pocket detail. The downside to the system is that it can be cumbersome to form and remove the forms for the pocket. An inverted cone such as the one used in this research is likely not necessary. A simple cylinder or truncated cone with the wider side down would be easier to form and likely produce the same results.

The tests performed in this research indicated three different types of behavior based on the amount of steel crossing the interface. If the amount of steel crossing the interface had shear resistances lower than cohesion a sudden slip occurred when the crack between the interfaces formed. When the amount of resistance provided by the connector was roughly equal to the cohesion a sudden slip was still noted but the sustained load was approximately equal to the peak load. When the amount of resistance from the shear

connectors was much greater than the cohesion as the crack formed, the steel began to progressively take the load until the steel yielded. No sudden slips were noted for these tests. For those tests with low amounts of steel the stress in the shear connector was not near yield. For those with higher amounts of steel the stress in the reinforcing bars was closer to the yield stress. Beyond the peak load the yielding of the connectors was obtained generally within a slip of 0.15 in. to 0.30 in.

For low clamping stresses the AASHTO equations were mostly successful at predicting the horizontal shear strengths. Values for cohesion based on a non roughed surface provided the closest representation of the data.

5.3 Design Recommendations

Based on the results of this research, the current shear friction design philosophy needs to be revised. Currently the AASHTO LRFD manual allows the designer to take the horizontal shear strength as the combination of the chemical cohesion at the interface plus coulomb friction with the clamping force being provided by steel crossing the interface plus any normal force provided by the deck and appurtenances. In actuality resistance provided by friction does not occur until a crack is formed. A crack is formed when the cohesion bond is broken. The proposed modification to the AASHTO equation would be as follows if the two components are separated. This is consistent with the results seen as the amount of steel is increased.

$$v_n = \max \begin{vmatrix} cA_{cv} \\ \mu(A_s f_y + P_n) \end{vmatrix}$$

where

c = cohesion = 75 psi

A_{cv} = Interface area

μ = 0.9 for a grout on concrete interface
0.6 for a grout on steel interface

A_s = Area of shear connector crossing interface

f_y = Connector yield stress

P_n = Additional normal force

The coefficient of friction in the shear strength equation also accounts for the contribution of shear resistance provided by dowel action of the shear connectors. When the shear portion of the equation controls it is acceptable to use the yield stress since in these cases the peak load is occurring near the point when the reinforcement yields. It is recommended that a minimum area of steel criteria be established. However, based on this research there is insufficient data to establish a minimum area of steel. Figure 5.1 shows the proposed equation plotted against the results from this research. As one would expect the peak load results plot just above the cohesion or friction line and the post peak results plot along the friction line as seen in Figure 5.2.

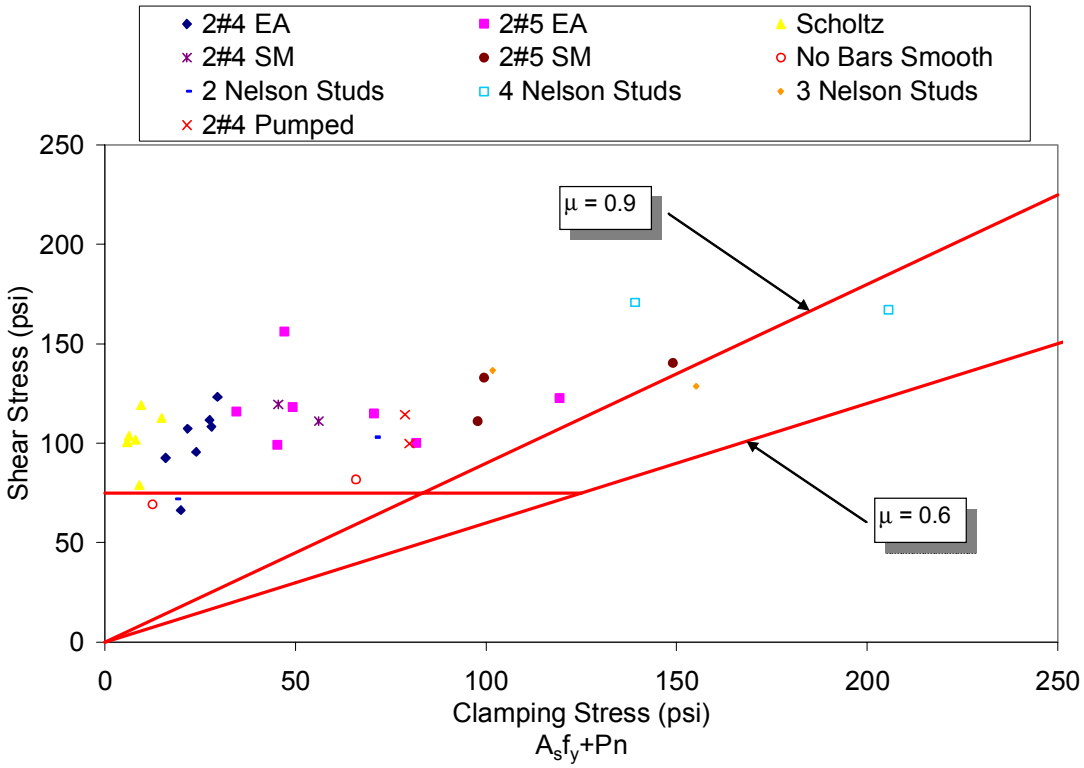

Figure 5.1: Peak Shear Stress Results with Proposed Equations

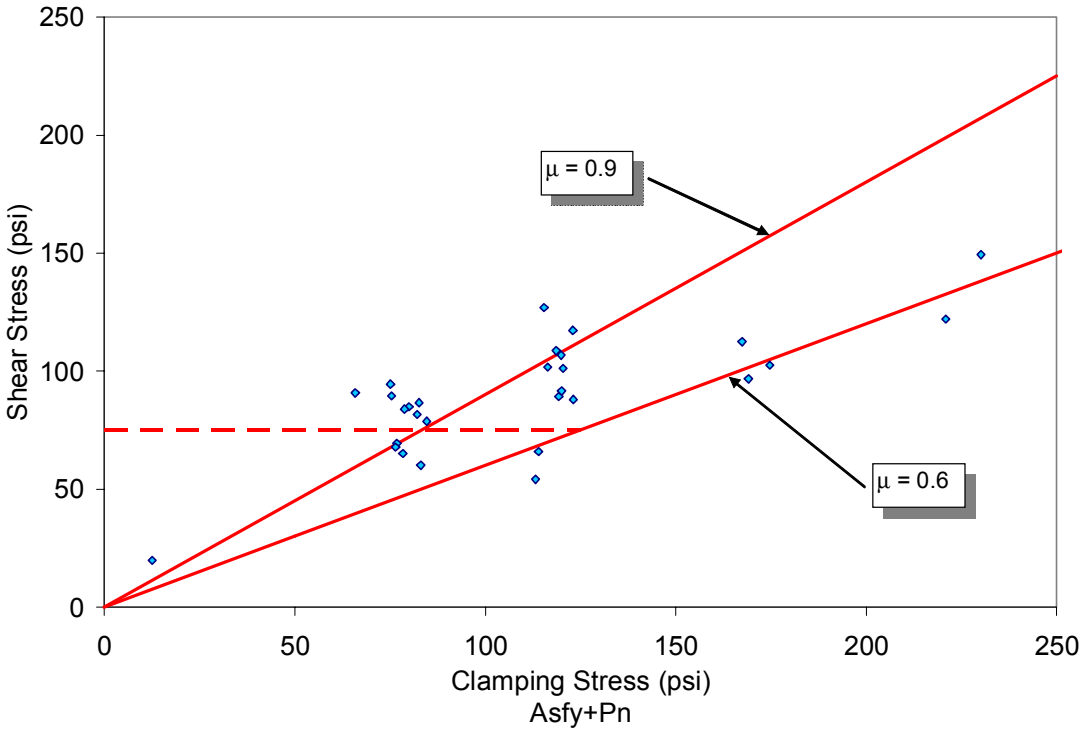

Figure 5.2: Post Peak Results with Proposed Equations

5.4 Construction Recommendations

From the experiences of this research it is important to make sure that the quality of the formwork used for grouting operations is good. In order to have good flow with the grout it is recommended that the maximum amount of water be used. With this high degree of flow it is imperative that the formwork be tight against the concrete and small crevices filled with a weather stripping materials or caulk. Care must also be given that enough time is available to finish grouting operations. Grouts have very fast set times. It is important to determine that the grout can be batched and placed before the grout begins to set as the grout can set in a matter of minutes. Both the Set 45® Hot Weather Grout and the Five Star® Highway Patch grouts performed well with good flow characteristics and compressive strength. The Set 45® Hot Weather extended with pea gravel also performed well and it is recommended that all the manufacturer's instructions be carefully followed when batching grout.

Based on this research no significant increases in strength were found by exposing the aggregate on the bottom slab surface. It is the researcher's opinion that an exposed aggregate surface on the bottom of the slab does not provide a sufficient increase in horizontal shear resistance to justify the additional cost of exposing the aggregate.

A hidden pocket detail was found to perform comparably to the normal pocket detail and feasible to construct. Having an inverted cone type pocket was not found to provide additional performance of the system. The disadvantage of the hidden pocket detail is that the haunch and pocket must be pressure grouted. The hidden pocket detail

provides promise for those that desire a more uniform riding surface when a wearing surface overlay is not provided.

REFERENCES

AASHTO (2003). *Standard Specifications for Highway Bridges, 17th Edition*, American Association of State Highway and Transportation Officials, Washington, D.C.

AASHTO (2004). *AASHTO LRFD Bridge Design Specifications, 3rd Edition with 2005 and 2006Iinterims*, American Association of State Highway and Transportation Officials, Washington D.C.

AISC (1999), LRFD *Specification for Structural Steel Buildings*, American Institute of Steel Construction, Chicago, Illinois.

AISC (2005), LRFD *Specification for Structural Steel Buildings*, American Institute of Steel Construction, Chicago, Illinois.

ACI (1963). *Building Code Requirements for Reinforced Concrete, ACI 318-63*, American Concrete Institute, Farmington Hills, Michigan.

ACI (2002). *Building Code Requirements for Structural Concrete and Commentary, ACI 318-02*, American Concrete Institute, Farmington Hills, Michigan.

ACI (2004). *Building Code Requirements for Structural Concrete and Commentary, ACI 318-05*, American Concrete Institute, Farmington Hills, Michigan.

ACI-ASCE Committee 333 (1960), "Tentative Recommendations for Design of Composite Beams and Girders for Building." *ACI Journal*, 57(12), 609-628

ASTM C 39 (2001). "Standard Test Method for Compressive Strength of Cylindrical Concrete Specimens," *Annual Book of ASTM Standards*, ASTM International, Vol. 04.02, West Conshohocken, PA, 2003.

ASTM C 109 (2002). "Standard Test Method for Compressive Strength of Hydraulic Cement Mortars (Using 2-in. Cube Specimens)," *Annual Book of ASTM Standards*, ASTM International, Vol. 04.01, West Conshohocken, PA, 2003.

Banta, T. E. (2005). "Horizontal Shear Transfer Between Ultra High Performance Concrete and Lightweight Concrete," Virginia Tech, Blacksburg.

Birkeland, P. W., and Birkeland, H. W. (1966). "Connections in Pre-Cast Concrete Construction." *ACI Journal*, 63(3), 345-367.

Biswas, M. (1986). "Precast Bridge Deck Design Systems." *PCI Journal*, 41-94.

Comite Euro-International du Beton (CEB)-Federation Internationale de la Precontrainte (FIP) (1990). *Model Code for Concrete* Structures, (MC-90), CEB, Thomas Telford, London.

Hanson, N. W. (1960). "Precast-Prestressted Concrete Bridges Horizontal Shear Connections." *Journal PCA Research and Development Laboratories*, 2(2), 38-58

Hsu, T. T. C., Mau, S. T., and Chean, B. (1987). "Theory of Shear Transfer Strength of Reinforced Concrete." *ACI Journal*, 84(2), 149-160.

Hwang, S.-J., Yu, H.-W., and Lee, H.-J. (200). "Theory of Interface Shear Capacity of Reinforced Concrete." *Journal of Structural Engineering*, 126(6), 700-707.

Hwang, S.-J., Yu, H.-W., and Lee, H.-J. (2000). "Theory of Interface Shear Capacity of Reinforced Concrete." *Journal of Structural Engineering*, 126(6), 700-707.

Issa, M. A., Yousif, A. A., Issa, M. A., Kaspar I. I., Khayyat S. Y. (1995). "Field Performance of Full Depth Precast Concrete Panels in Bridge Deck Reconstruction." *PCI Journal*, 40(3), 82-108.

Issa, M. A., Idriss, A., Kaspar, I. I., and Khayyat, S. Y. (1995). "Full Depth Precast and Precast, Prestressed Concrete Bridge Deck Panels." *PCI Journal*, 40(1), 59-80.

Issa, M. A., Yousif, A. A., Issa, M. A., Kaspar, I. I., and Khayyat, S. Y. (1998). "Analysis of Full Depth Precast Concrete Bridge Deck Panels." *PCI Journal*, 74-85.

Köksal, H. O., Karakoç, C., and Yildirim, H. (2005). "Compression Behavior and Failure Mechanisms of Concrete Masonry Prisms." *Journal of Materials in Civil Engineering*, 17(1), 107-115.

Lam, D., El-Lobody, E. (2005). "Behavior of Headed Stud Shear Connectors in Composite Beam." *ASCE Journal of Structural Engineering*, 131(1), 96-107

Loov, R. E., (1978). "Design of Precast Connections." *Paper presented at a seminar organized by Compa International Pte, Ltd.*

Loov, R. E., and Patnaik, A. K. (1994). "Horizontal Shear Strength of Composite Concrete Beams With a Rough Interface." *PCI Journal*, 39(1), 48-66.

Mast, R.F. (1968). "Auxiliary Reinforcement in Concrete Connections." *ASCE Journal*, 94(ST6), 1485-1504

Mattock, A. H. (1969). "Shear Transfer in Reinforced Concrete." *ACI Journal*, 119-128.

Mattock, A. H., and Hawkins, N. M. (1972). "Shear Transfer in Reinforced Concrete - Recent Research." *PCI Journal*, 17(2), 55-75.

Mattock, A. H., Johal, L., and Chow, H. C. (1975). "Shear Transfer in Reinforced Concrete with Moment or Tension Acting Across the Shear Plane." *PCI Journal*, 20(4), 76-93.

Mattock, A. H., Li, W. K., and Wang, T. C. (1976). "Shear Transfer in Lightweight Reinforced Concrete." *PCI Journal*, 21(1), 20-39.

Menkulasi, F. (2002). "Horizontal Shear Connectors for Precast Prestressed Bridge Deck Panels," Virginia Tech, Blacksburg.

Patnaik, A. K. (2001). "Behavior of Composite Beams with Smooth Interface." *Journal of Structural Engineering*, 127(4), 359-366.

PCI (2005). *Bridge Design Manual*, Precast/Prestressed Concrete Institute, Chicago, Illinois.

Powell, L. C., and Powell, D. W. (2000). "Precast Concrete Alternate Provides Unique Solution for Airport Terminal Bridge." *PCI Journal*, 18-25.

Roddenberry, M. R., Lyons, J. C., Easterling, W. S. and Murray, T. M. (2002). "Performance and Strength of Welded Shear Studs" *Composite Construction in Steel and Concrete IV,* Proceedings of an Engineering Foundation Conference, ASCE, New York, 458-469

Saemann, J. C., and Washa, G. W. (1964). "Horizontal Shear Connections Between Precast Beams and Cast-in-Place Slabs." *ACI Journal*, 61(11), 1383-1408.

Scholz, D. P. (2004). "Performance Criteria Recomendations for Mortars Used In Full Depth Precast Concrete Bridge Deck Panel Systems," Virginia Tech, Blacksburg.

Shaikh, A. F. (1978). "Proposed Revisions to Shear-Friction Provisions." *PCI Journal*, 23(2), 12-21.

Shim, C. S., Kim, J. H., Chang, S. P., and Chung, C. H. "The Behavior of Shear Connections in a Composite Beam with a Full-Depth Precast Slab." *Proceedings of the Institution of Civil Engineers*, 101-110.

Topkaya, C., Yura, J. A. And Williamson, E. B. (2004) "Composite Shear Stud Strength at Early Concrete Ages" *ASCE Journal of Structural Engineering*, 130(6). 952-960

Walraven, J., Frenay, J., and Pruijssers, A. (1987). "Influence of Concrete Strength and Load History on the Shear Friction Capacity of Concrete Members." *PCI Journal*, 32(1), 66-84

Yamane, T. (1998). "Full Depth Precast, Prestressed Concrete Bridge Deck System." *PCI Journal*, 50-66.

APPENDIX A

Load versus Slip Diagrams
&
Load versus Strain Diagrams

Test Series 1

Shear Connectors: 2 Legs - No. 4 Bar Stirrup
Grout Type: Five Star Highway Patch
Slab Surface Treatment: Exposed Aggregate
No. Replications: 2

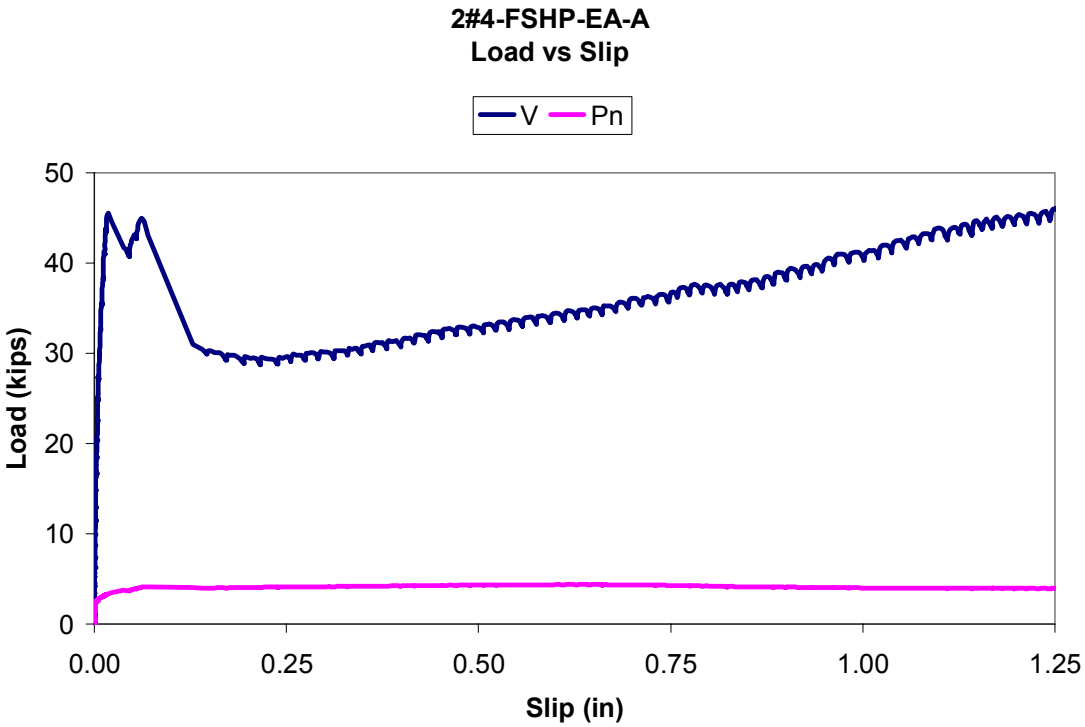

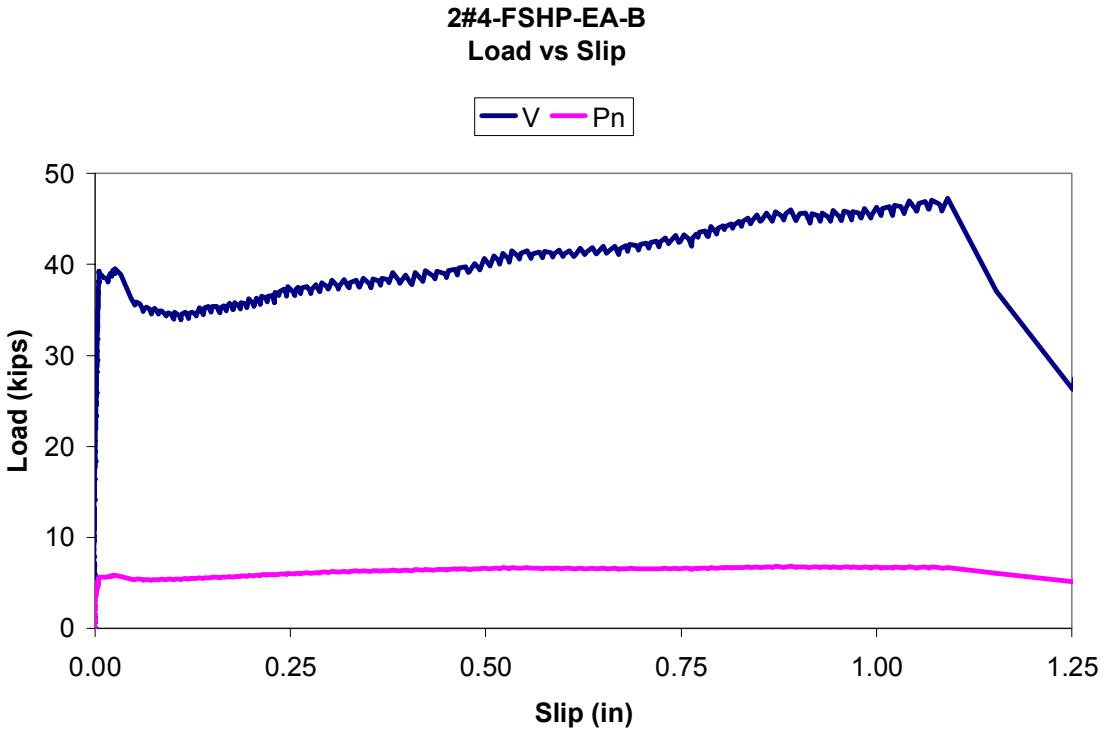
2#4-FSHP-EA-B
Load vs Slip
V
Pn
50
40
30
20
10
0
Load (kips)
0.00
0.25
0.50
0.75
1.00
1.25
Slip (in)

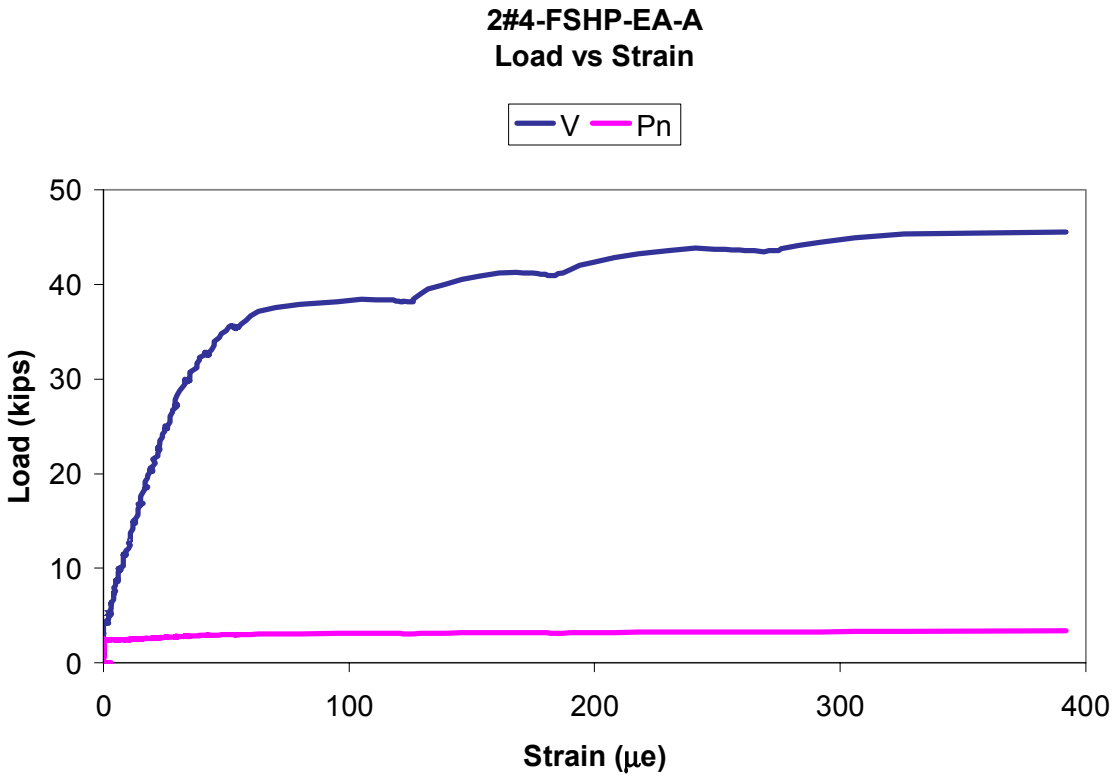
2#4-FSHP-EA-A
Load vs Strain
V
Pn
50
40
30
20
10
0
Load (kips)
0
100
200
300
400
Strain (με)

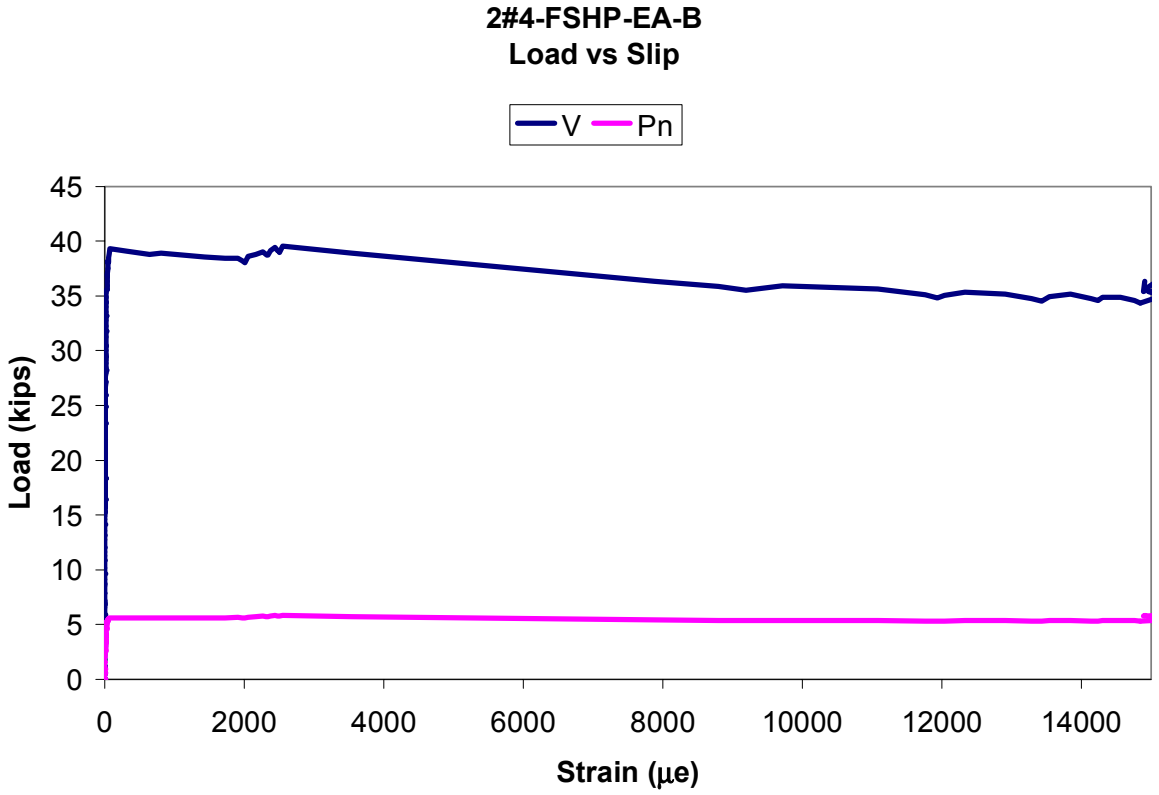
2#4-FSHP-EA-B
Load vs Slip
V
Pn
Load (kips)
45
40
35
30
25
20
15
10
5
0
0
2000
4000
6000
8000
10000
12000
14000
Strain (με)

Test Series 2

Shear Connectors: 2 Legs - No. 4 Bar Stirrup
Grout Type: Set 45 Hot Weather Extended
Slab Surface Treatment: Exposed Aggregate
No. Replications: 2

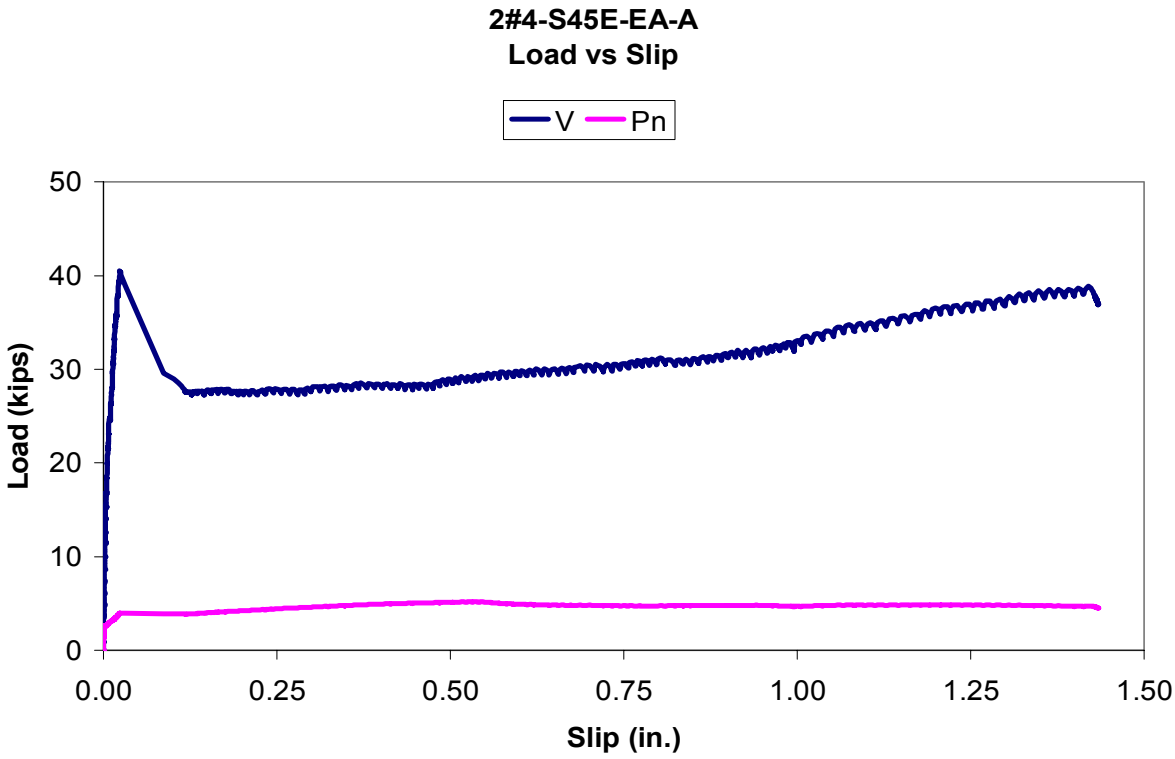

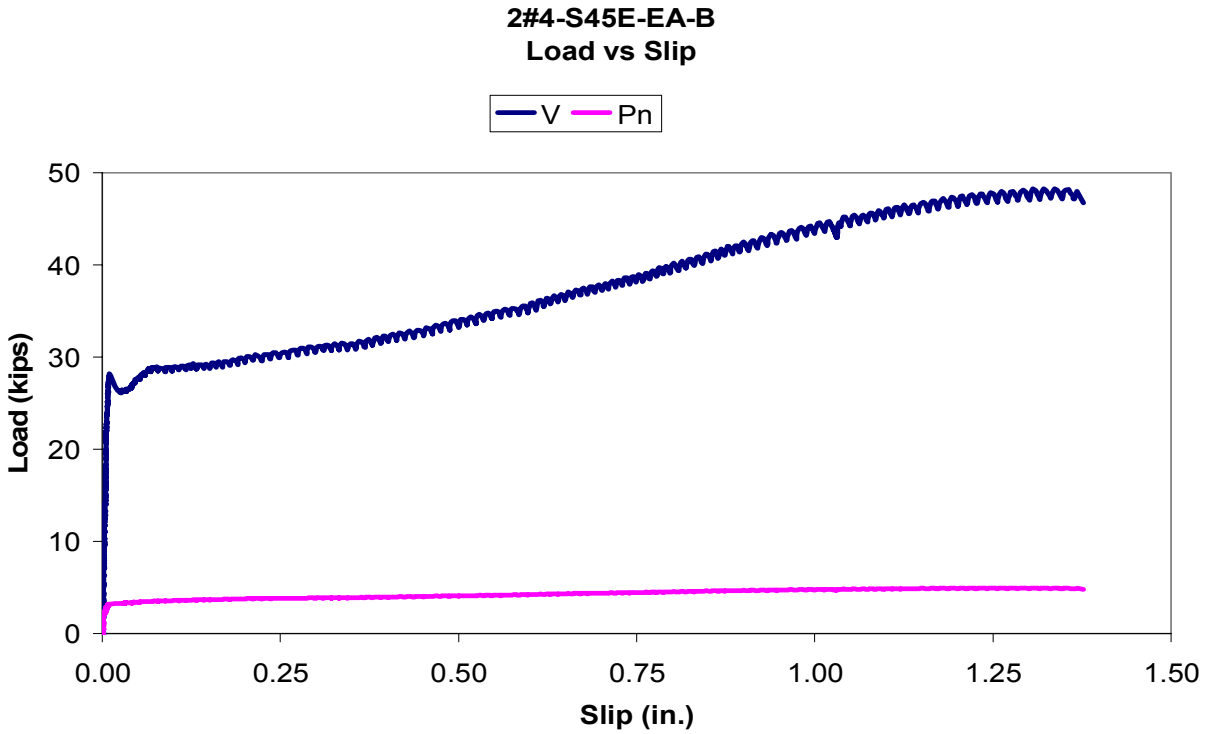
2#4-S45E-EA-B
Load vs Slip
V
Pn
Load (kips)
Slip (in.)
0
10
20
30
40
50
0.00
0.25
0.50
0.75
1.00
1.25
1.50

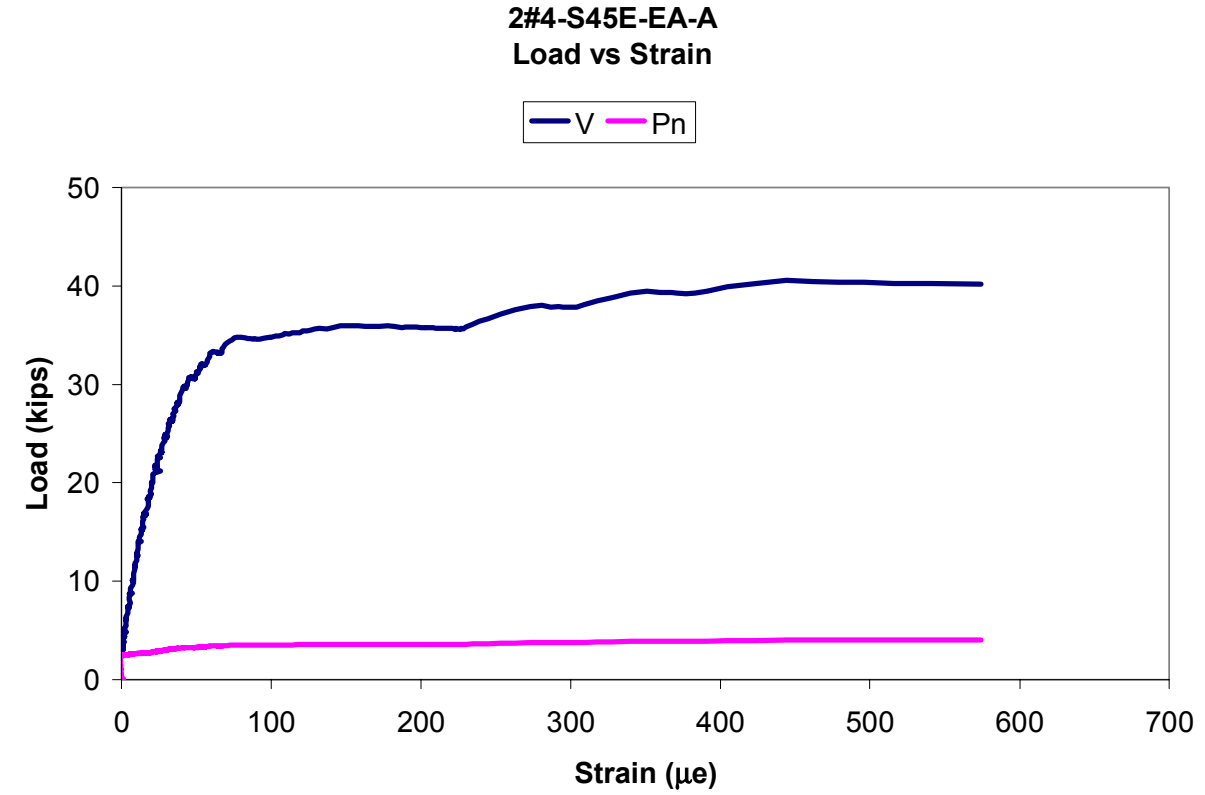
2#4-S45E-EA-A
Load vs Strain
V
Pn
Load (kips)
Strain (με)
0
10
20
30
40
50
0
100
200
300
400
500
600
700

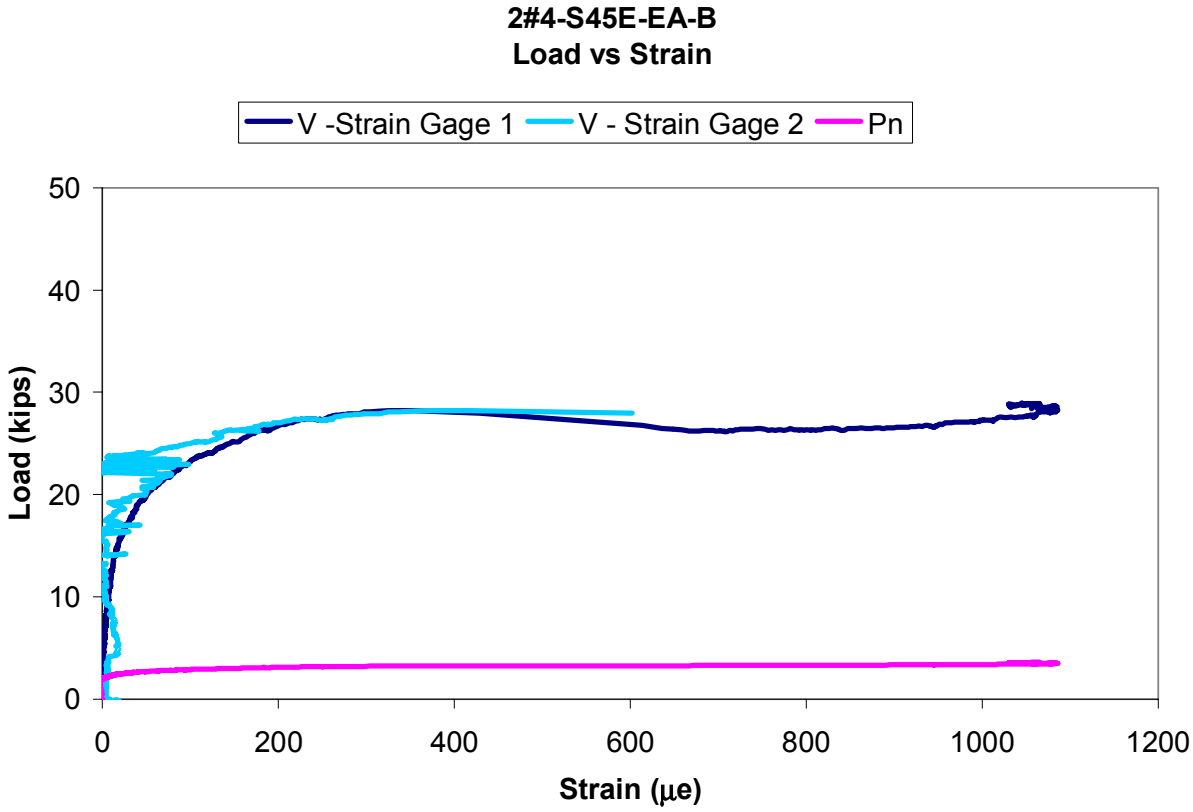
2#4-S45E-EA-B
Load vs Strain
V -Strain Gage 1
V - Strain Gage 2
Pn
Load (kips)
50
40
30
20
10
0
0
200
400
600
800
1000
1200
Strain (με)

Test Series 3

Shear Connectors: 2 Legs - No. 4 Bar Stirrup
Grout Type: Set 45 Hot Weather Neat
Slab Surface Treatment: Exposed Aggregate
No. Replications: 3

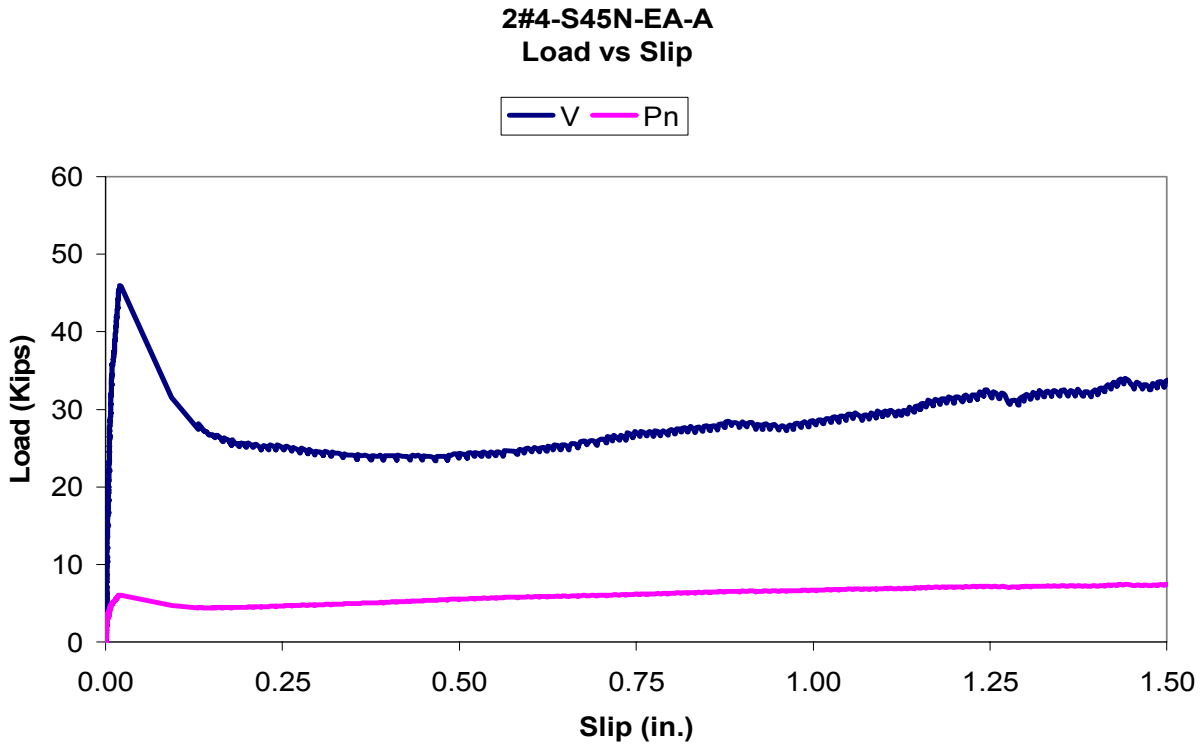

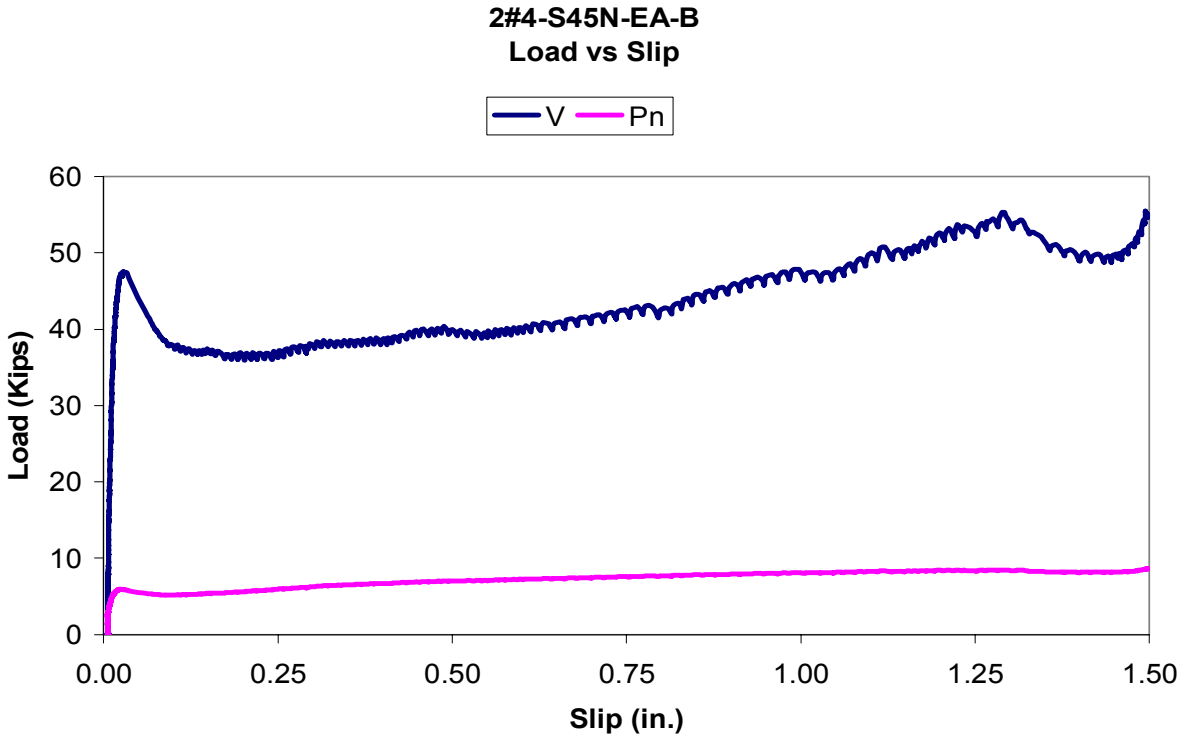
2#4-S45N-EA-B
Load vs Slip
V
Pn
60
50
40
30
20
10
0
Load (Kips)
0.00
0.25
0.50
0.75
1.00
1.25
1.50
Slip (in.)

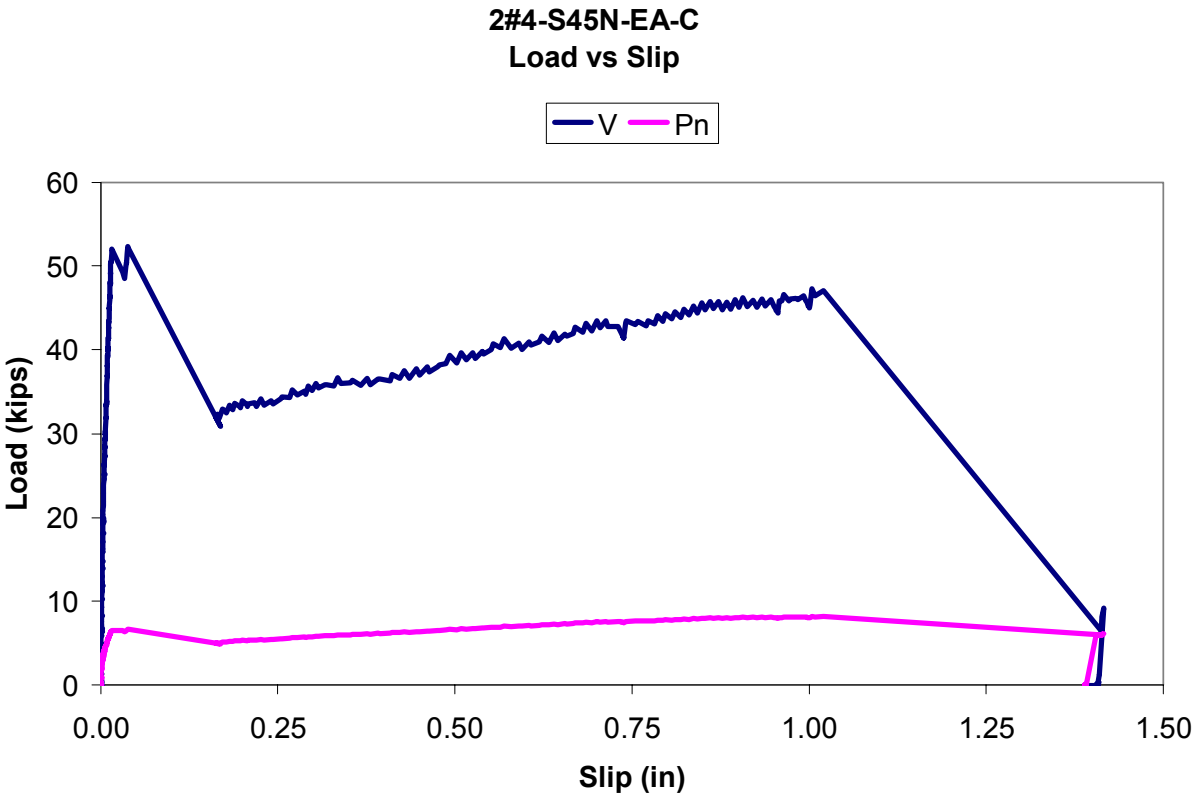
2#4-S45N-EA-C
Load vs Slip
V
Pn
60
50
40
30
20
10
0
Load (kips)
0.00
0.25
0.50
0.75
1.00
1.25
1.50
Slip (in)

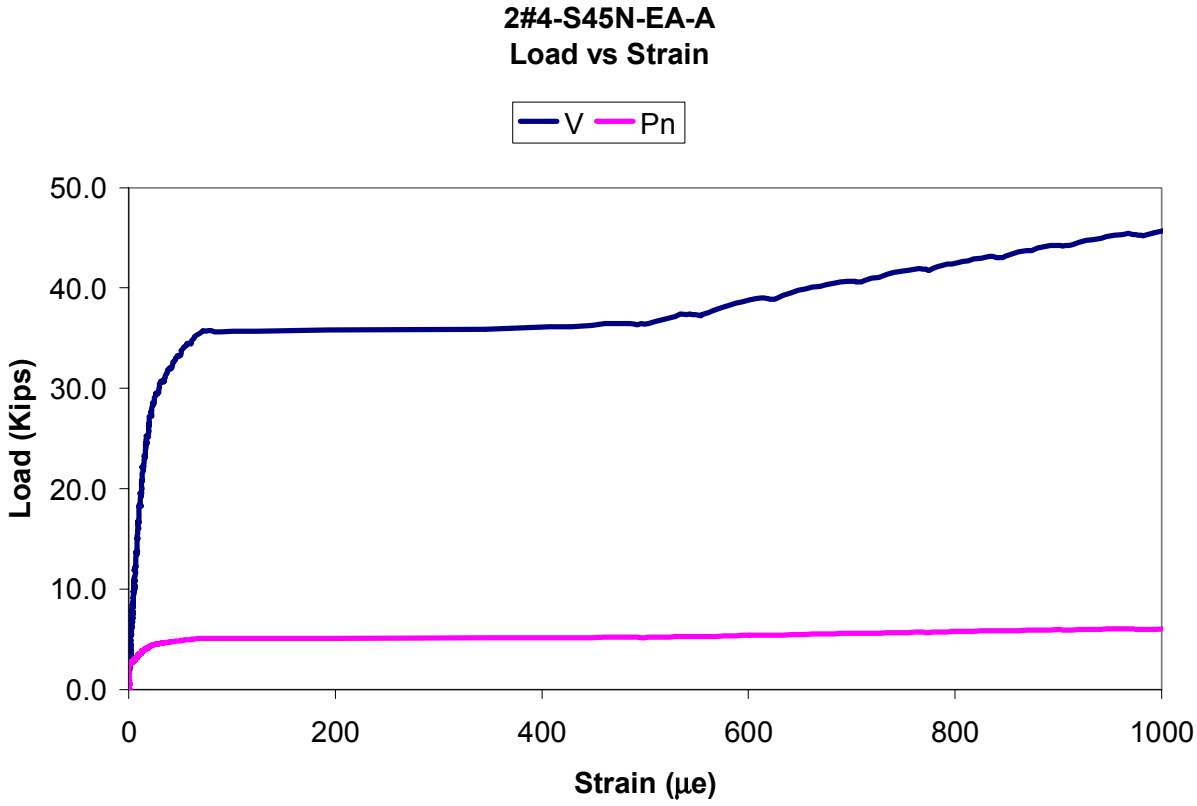
2#4-S45N-EA-A
Load vs Strain
V
Pn
50.0
40.0
30.0
20.0
10.0
0.0
Load (Kips)
0
200
400
600
800
1000
Strain (με)

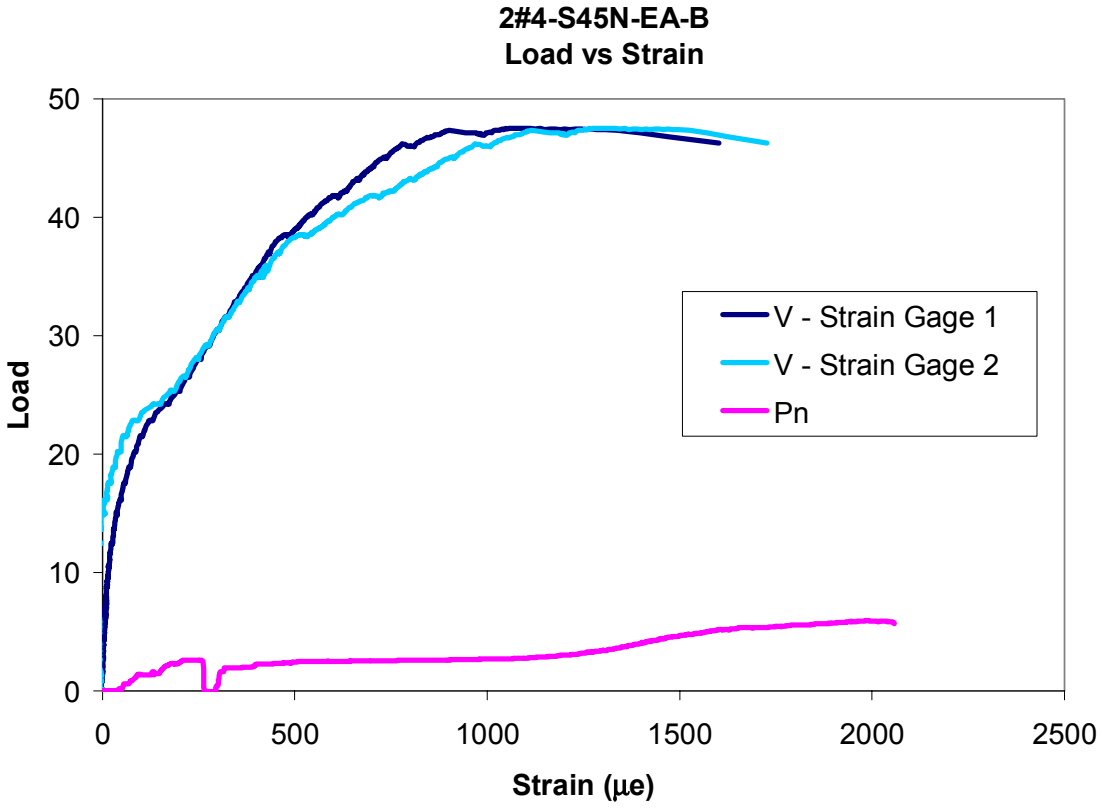
2#4-S45N-EA-B
Load vs Strain
Load
Strain (με)
0
10
20
30
40
50
0
500
1000
1500
2000
2500
V - Strain Gage 1
V - Strain Gage 2
Pn

Test Series 4

Shear Connectors: 2 Legs - No. 5 Bar Stirrup
Grout Type: Set 45 Hot Weather Extended
Slab Surface Treatment: Exposed Aggregate
No. Replications: 2

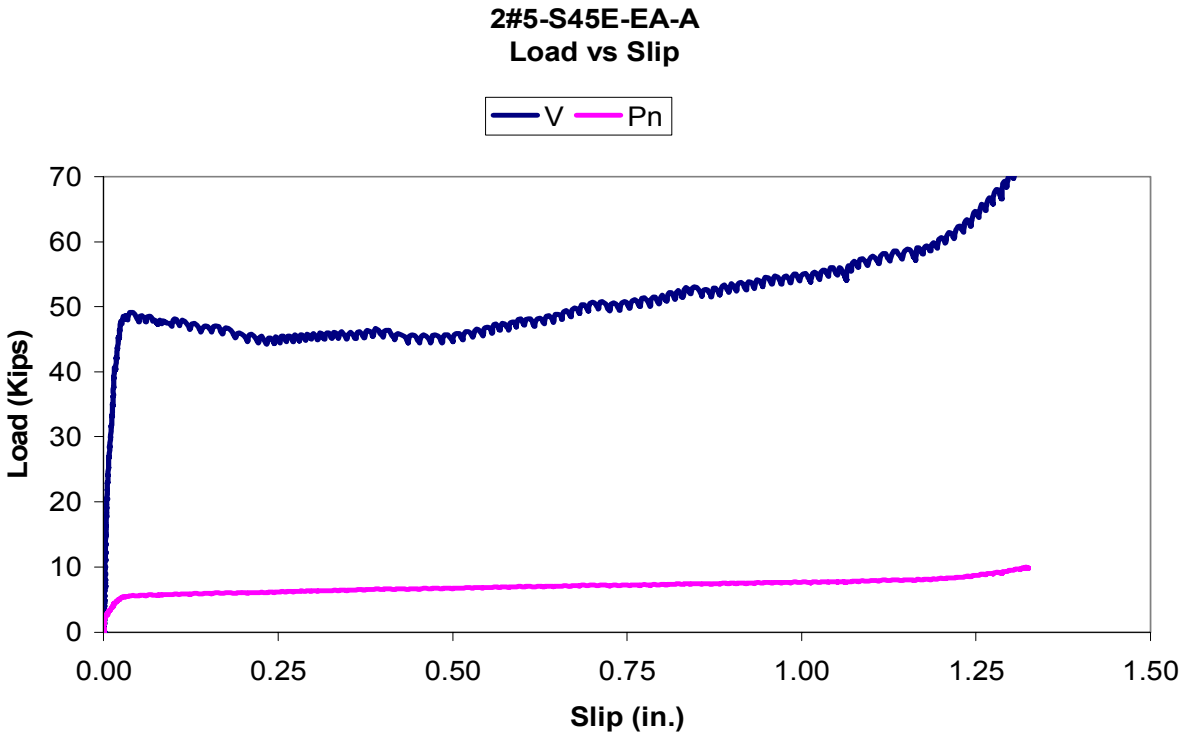

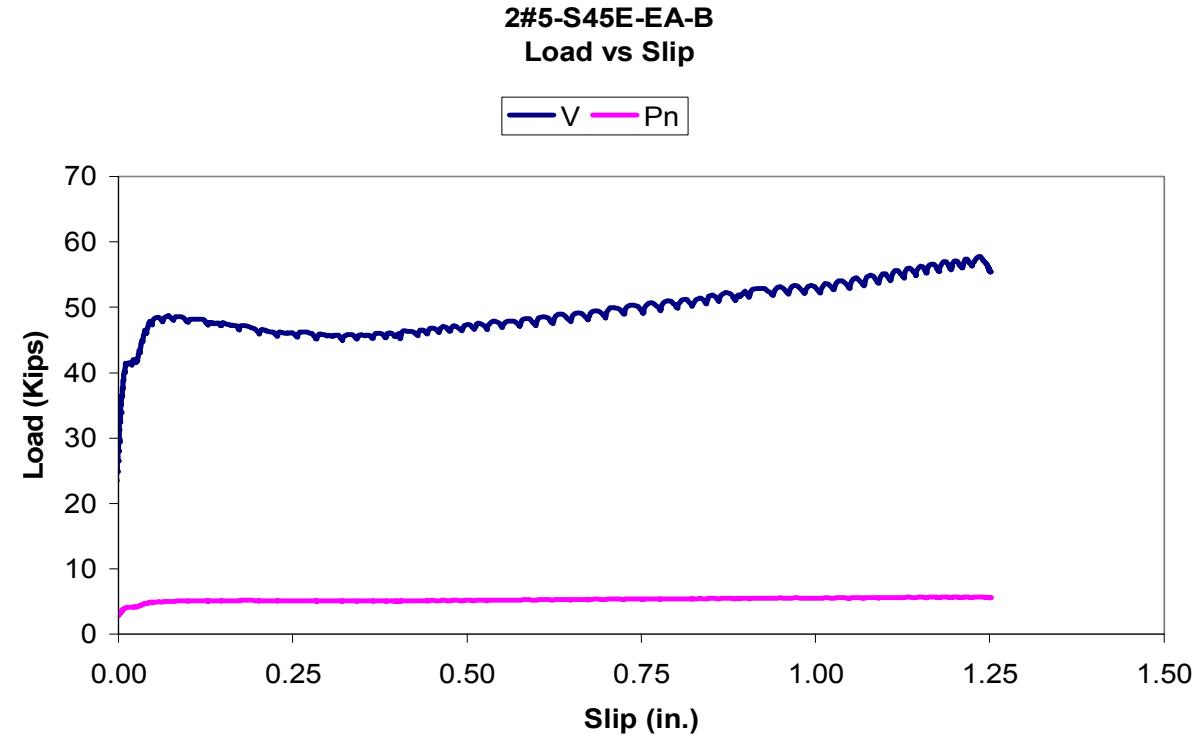
2#5-S45E-EA-B
Load vs Slip
V
Pn
Load (Kips)
70
60
50
40
30
20
10
0
0.00
0.25
0.50
0.75
1.00
1.25
1.50
Slip (in.)

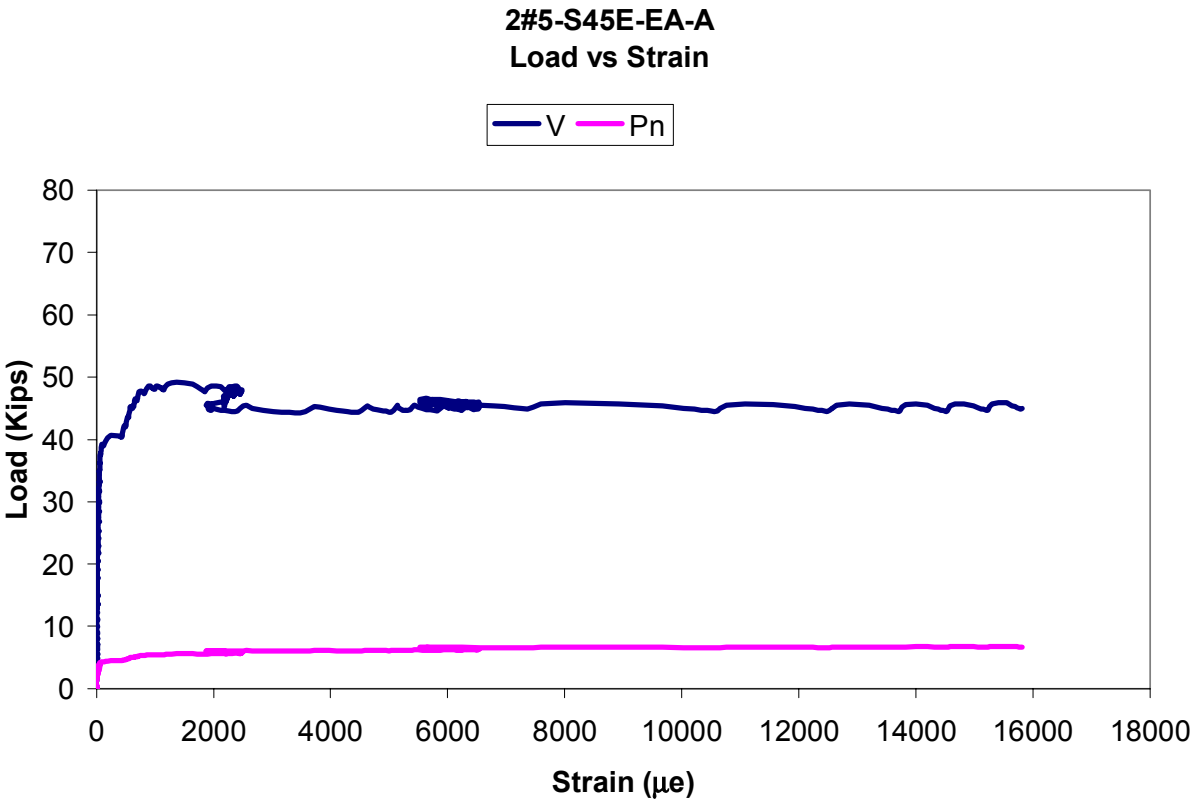
2#5-S45E-EA-A
Load vs Strain
V
Pn
Load (Kips)
80
70
60
50
40
30
20
10
0
0
2000
4000
6000
8000
10000
12000
14000
16000
18000
Strain (με)

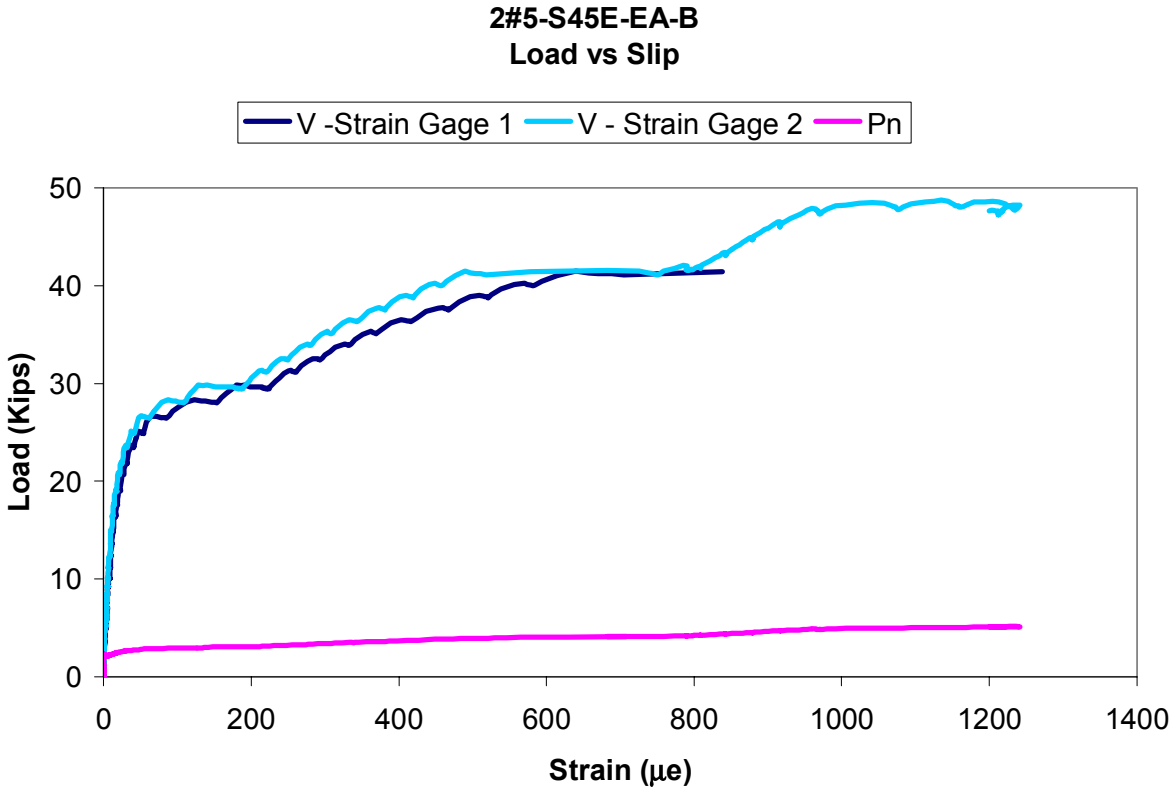
2#5-S45E-EA-B
Load vs Slip
V -Strain Gage 1
V - Strain Gage 2
Pn
Load (Kips)
50
40
30
20
10
0
0
200
400
600
800
1000
1200
1400
Strain (με)

Test Series 5

Shear Connectors: 2 Legs - No. 5 Bar Stirrup
Grout Type: Five Star Highway Patch
Slab Surface Treatment: Exposed Aggregate
No. Replications: 2

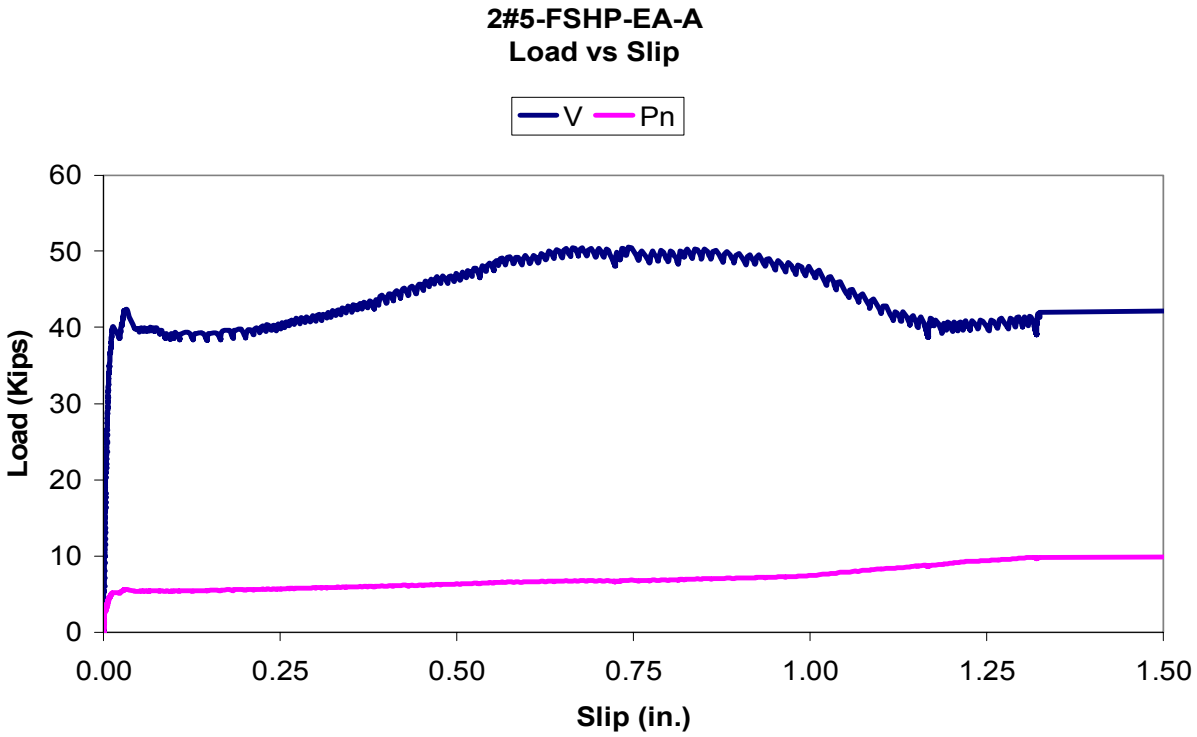

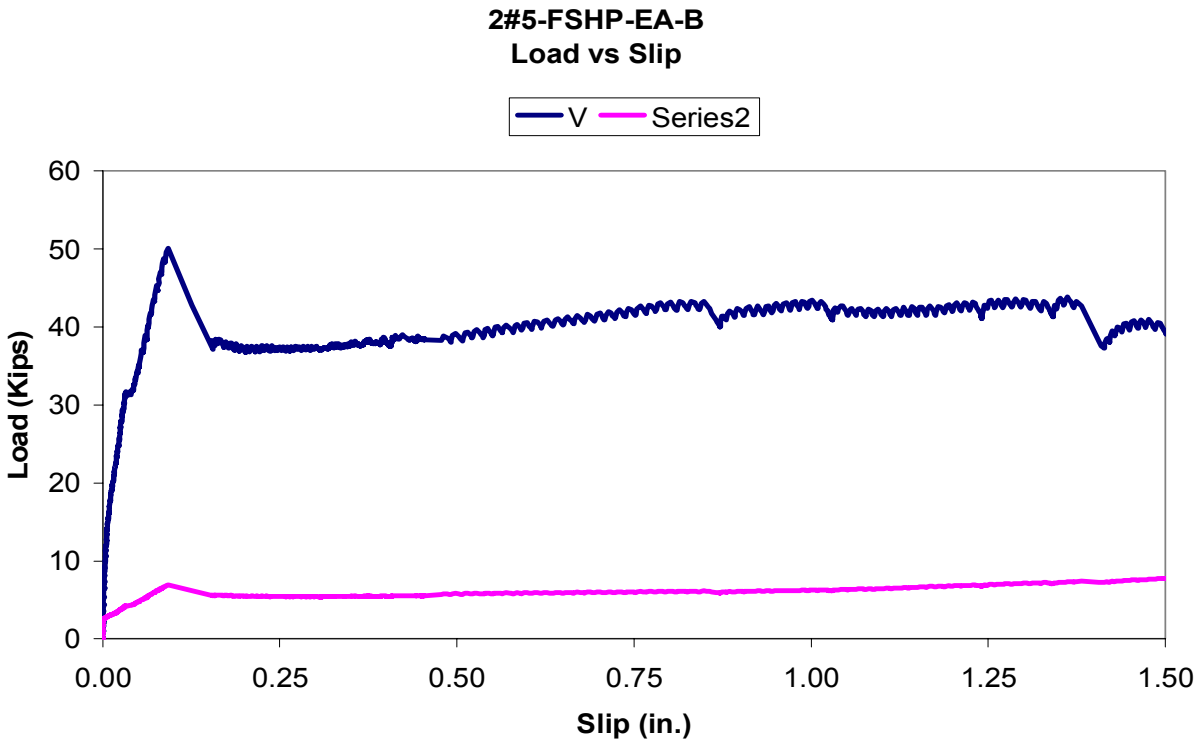
2#5-FSHP-EA-B
Load vs Slip
V
Series2
60
50
40
30
20
10
0
Load (Kips)
0.00
0.25
0.50
0.75
1.00
1.25
1.50
Slip (in.)

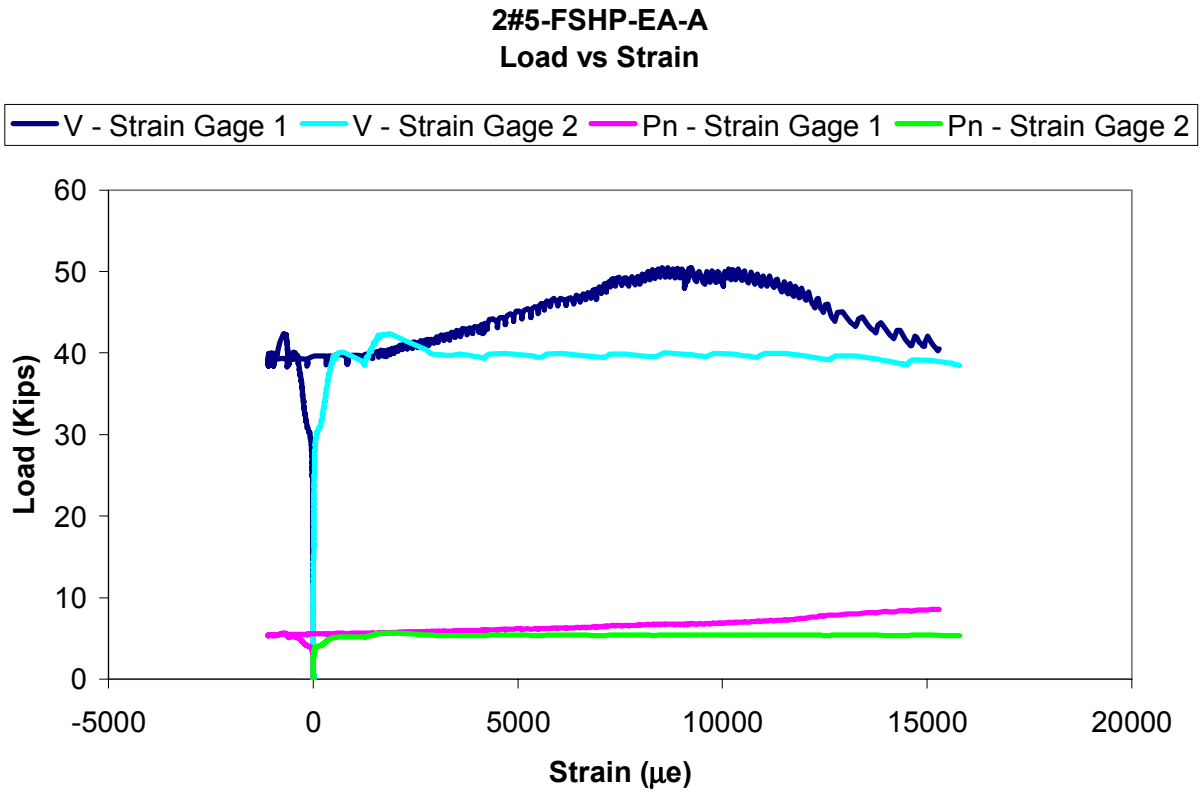
2#5-FSHP-EA-A
Load vs Strain
V - Strain Gage 1
V - Strain Gage 2
Pn - Strain Gage 1
Pn - Strain Gage 2
60
50
40
30
20
10
0
Load (Kips)
-5000
0
5000
10000
15000
20000
Strain (με)

2#5-FSHP-EA-B
Load vs Strain

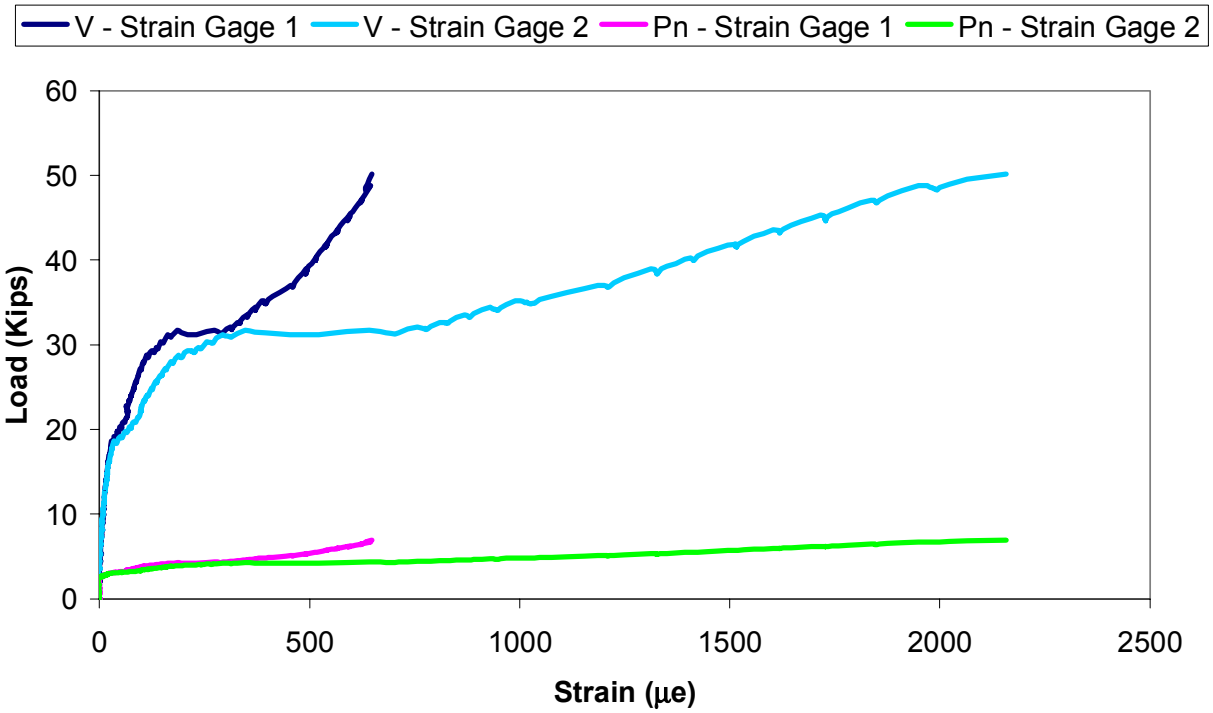

Test Series 6

Shear Connectors: 2 Legs - No. 5 Bar Stirrup
Grout Type: Set 45 Hot Weather Neat
Slab Surface Treatment: Exposed Aggregate
No. Replications: 3

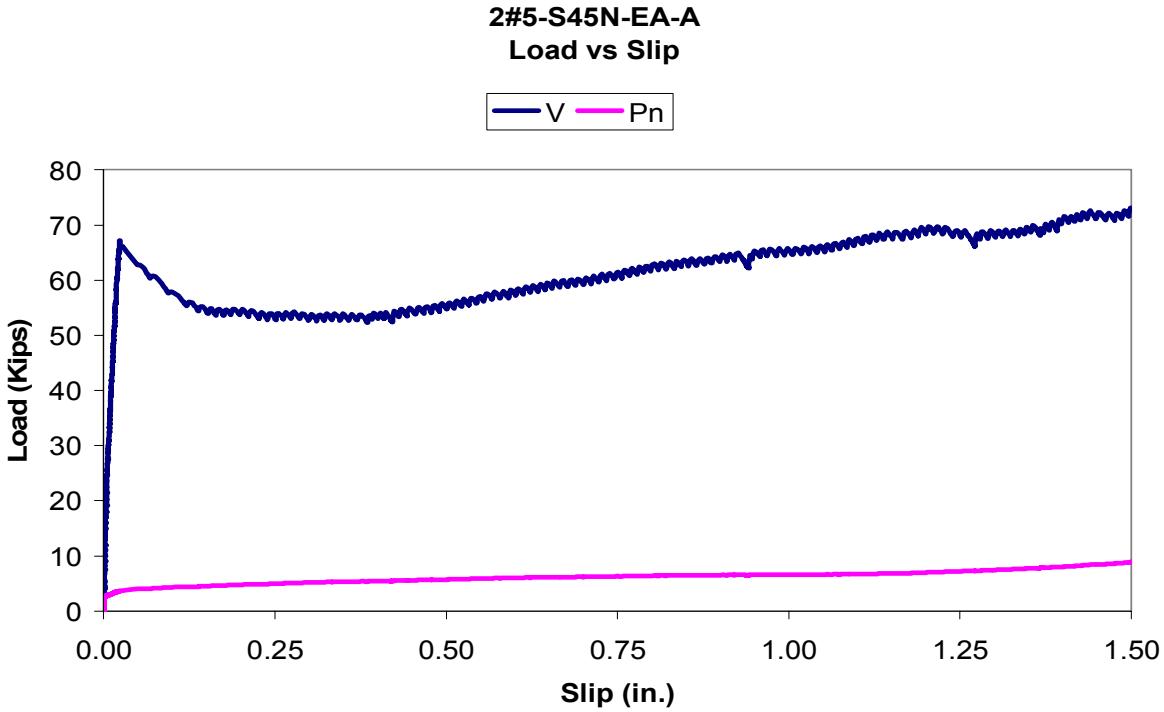

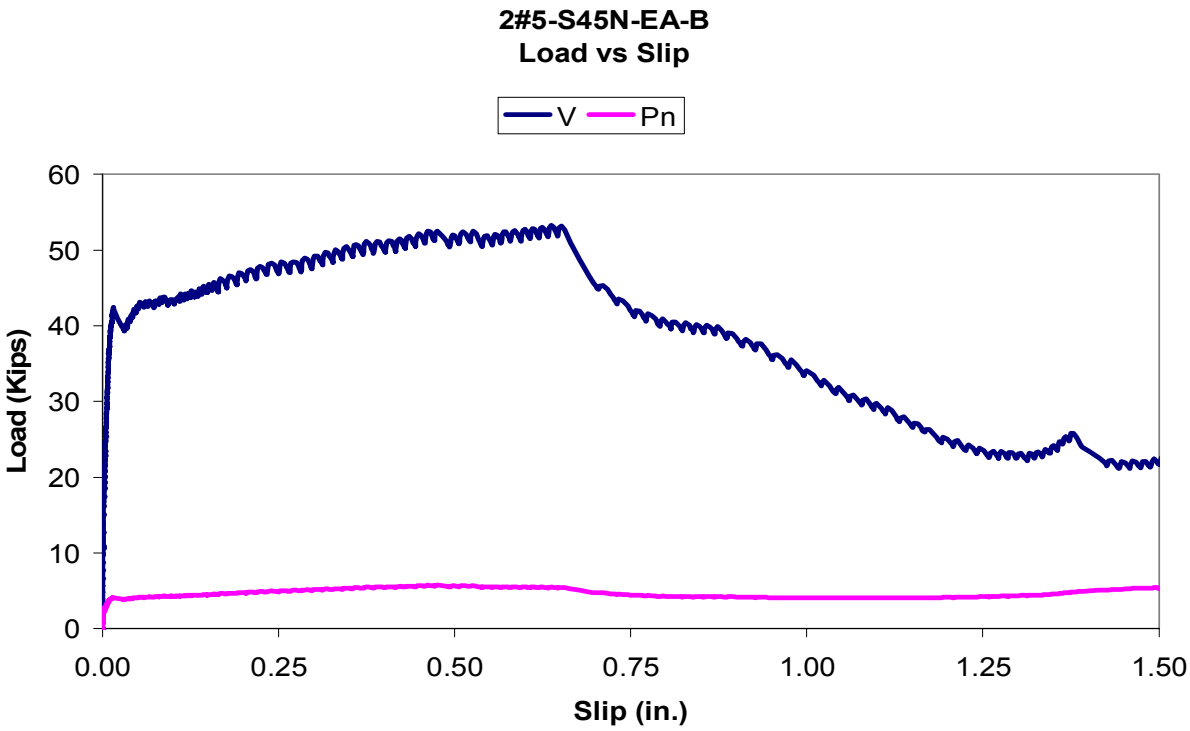
2#5-S45N-EA-B
Load vs Slip
V
Pn
Load (Kips)
60
50
40
30
20
10
0
0.00
0.25
0.50
0.75
1.00
1.25
1.50
Slip (in.)

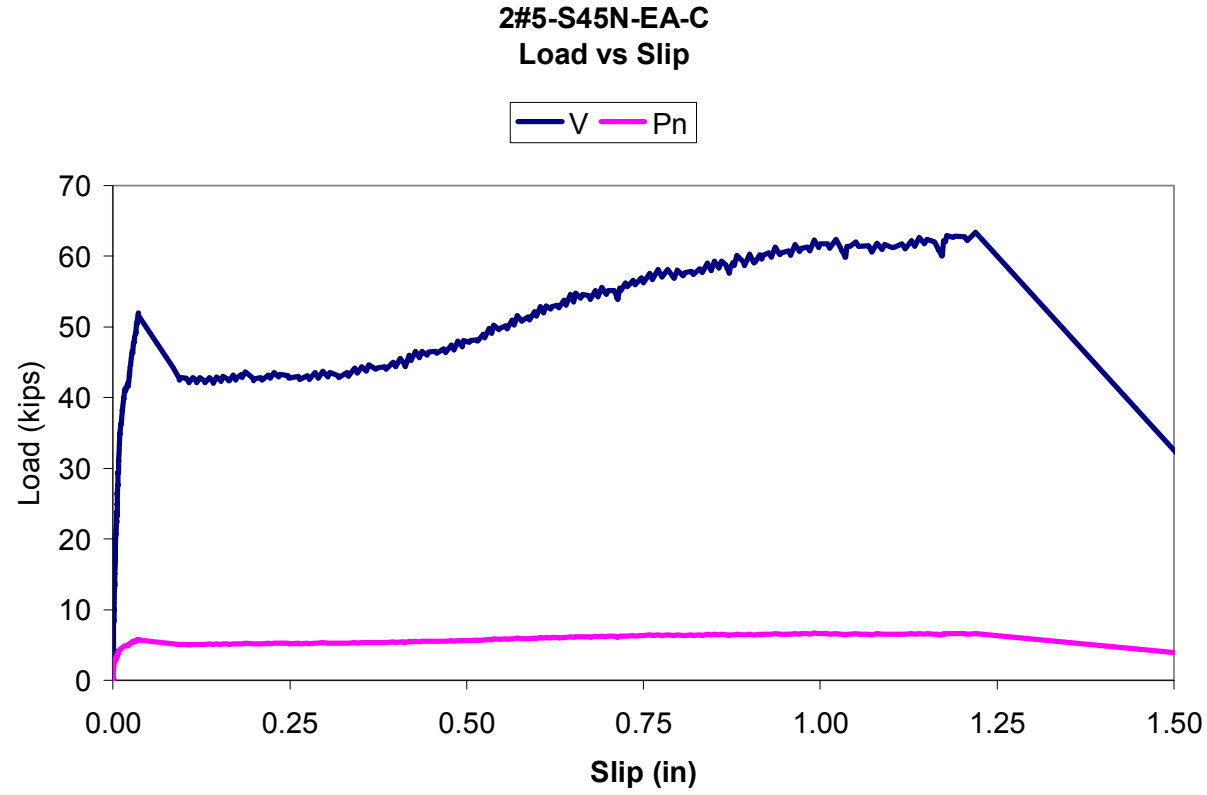
2#5-S45N-EA-C
Load vs Slip
V
Pn
Load (kips)
70
60
50
40
30
20
10
0
0.00
0.25
0.50
0.75
1.00
1.25
1.50
Slip (in)

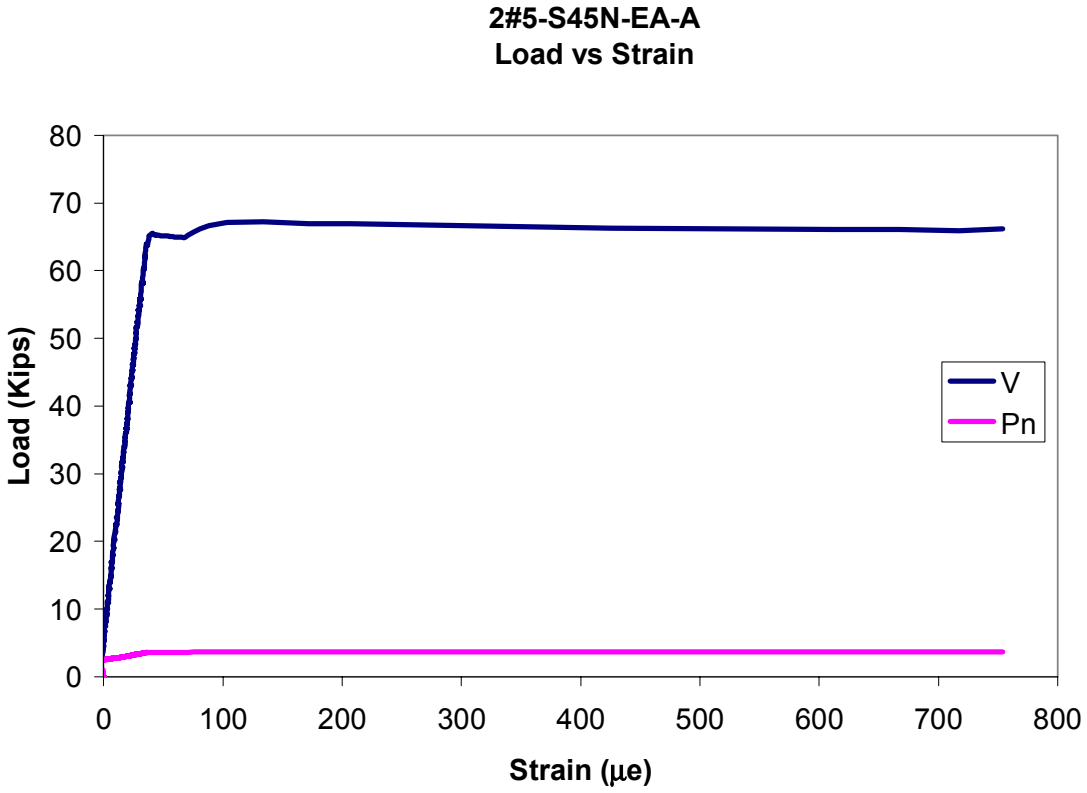
2#5-S45N-EA-A
Load vs Strain
Load (Kips)
80
70
60
50
40
30
20
10
0
0
100
200
300
400
500
600
700
800
Strain (με)
V
Pn

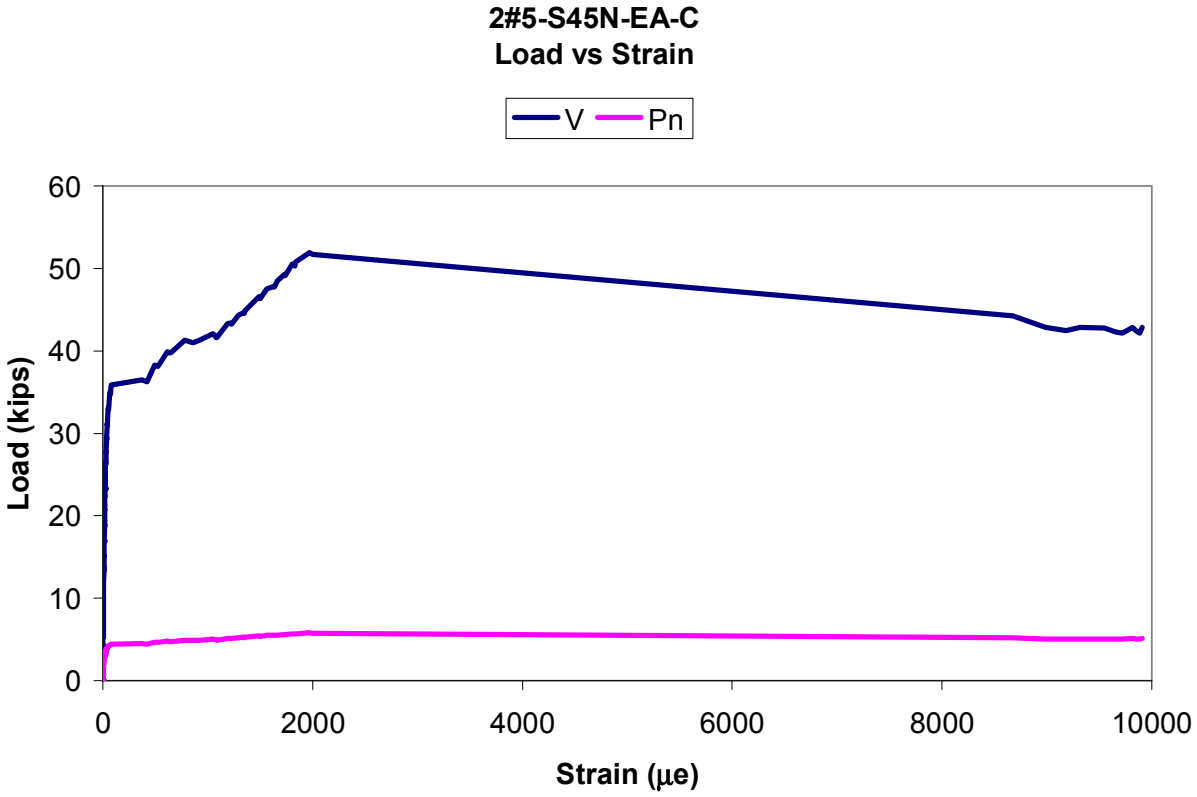
2#5-S45N-EA-C
Load vs Strain
V
Pn
Load (kips)
60
50
40
30
20
10
0
0
2000
4000
6000
8000
10000
Strain (με)

Test Series 7

Shear Connectors: 2 Legs - No. 4 Bar Stirrup
Grout Type: Five Star Highway Patch
Slab Surface Treatment: Smooth
No. Replications: 2

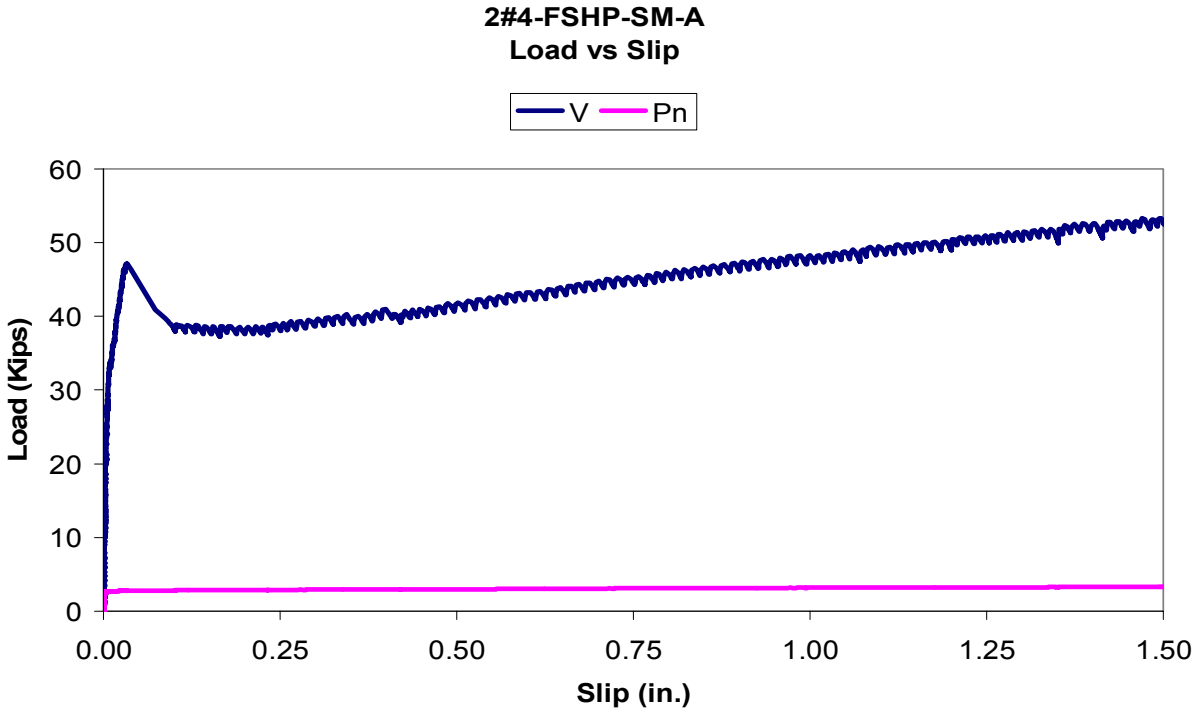

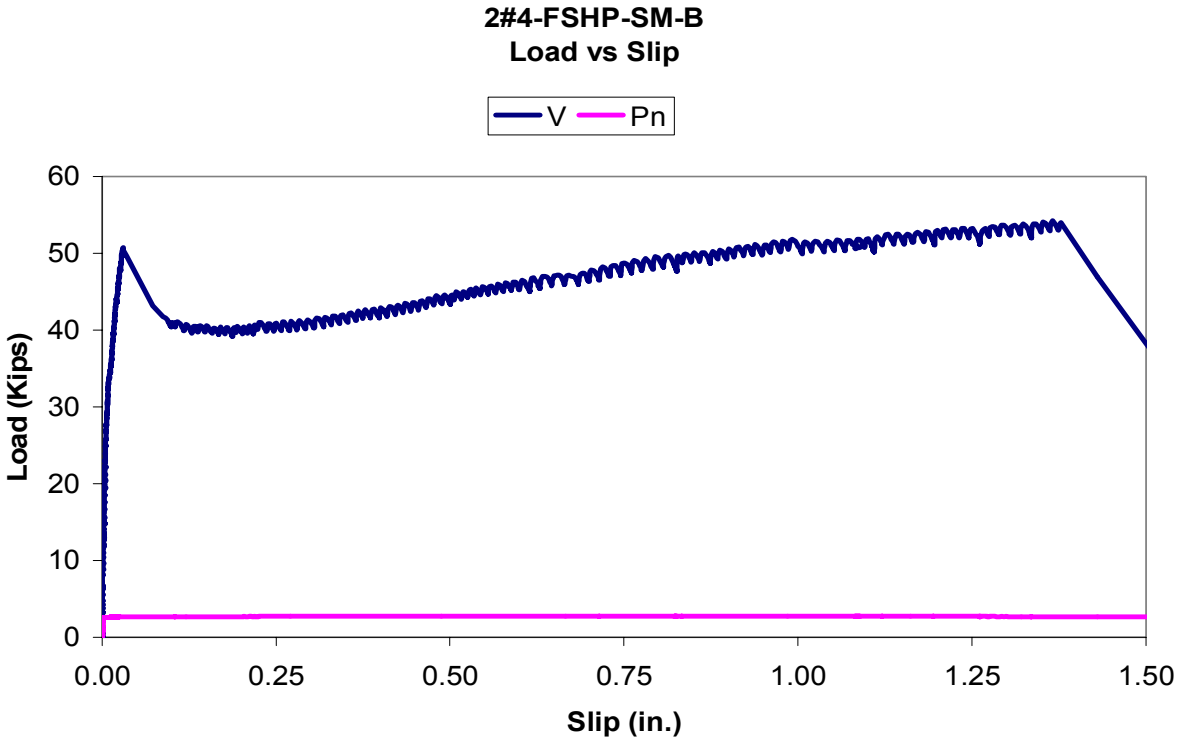
2#4-FSHP-SM-B
Load vs Slip
V
Pn
60
50
40
30
20
10
0
Load (Kips)
0.00
0.25
0.50
0.75
1.00
1.25
1.50
Slip (in.)

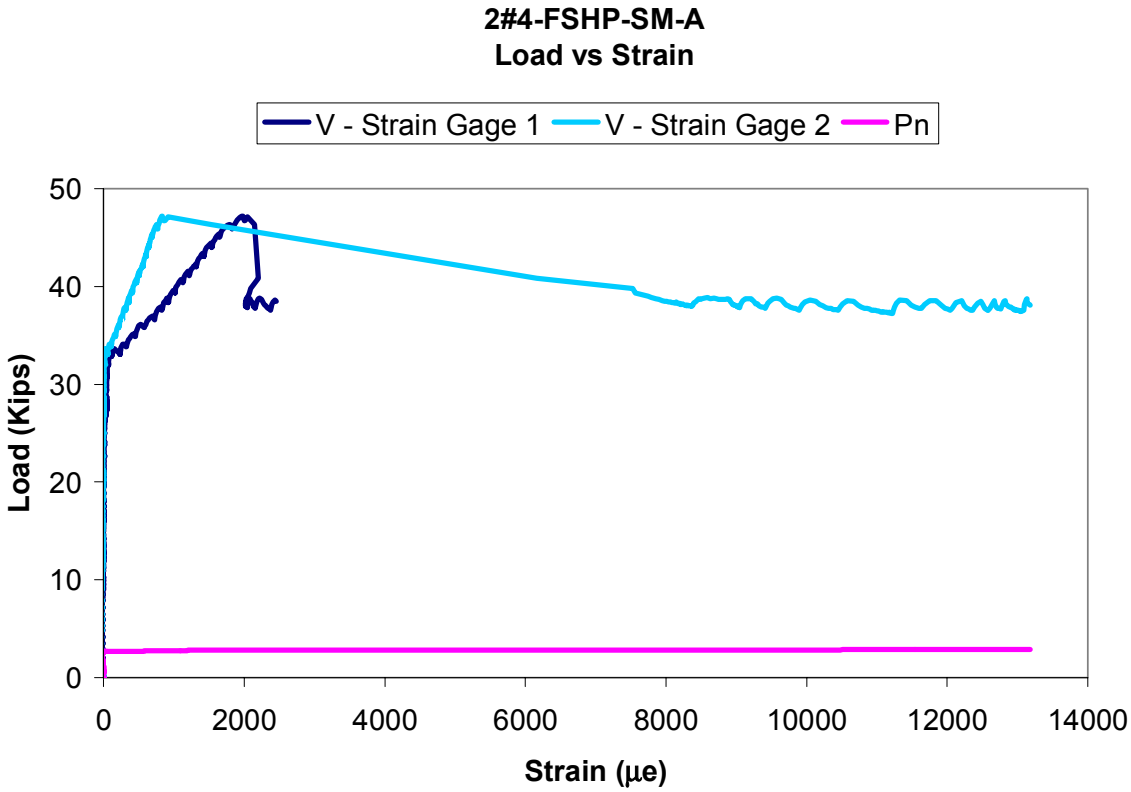
2#4-FSHP-SM-A
Load vs Strain
V - Strain Gage 1
V - Strain Gage 2
Pn
50
40
30
20
10
0
Load (Kips)
0
2000
4000
6000
8000
10000
12000
14000
Strain (με)

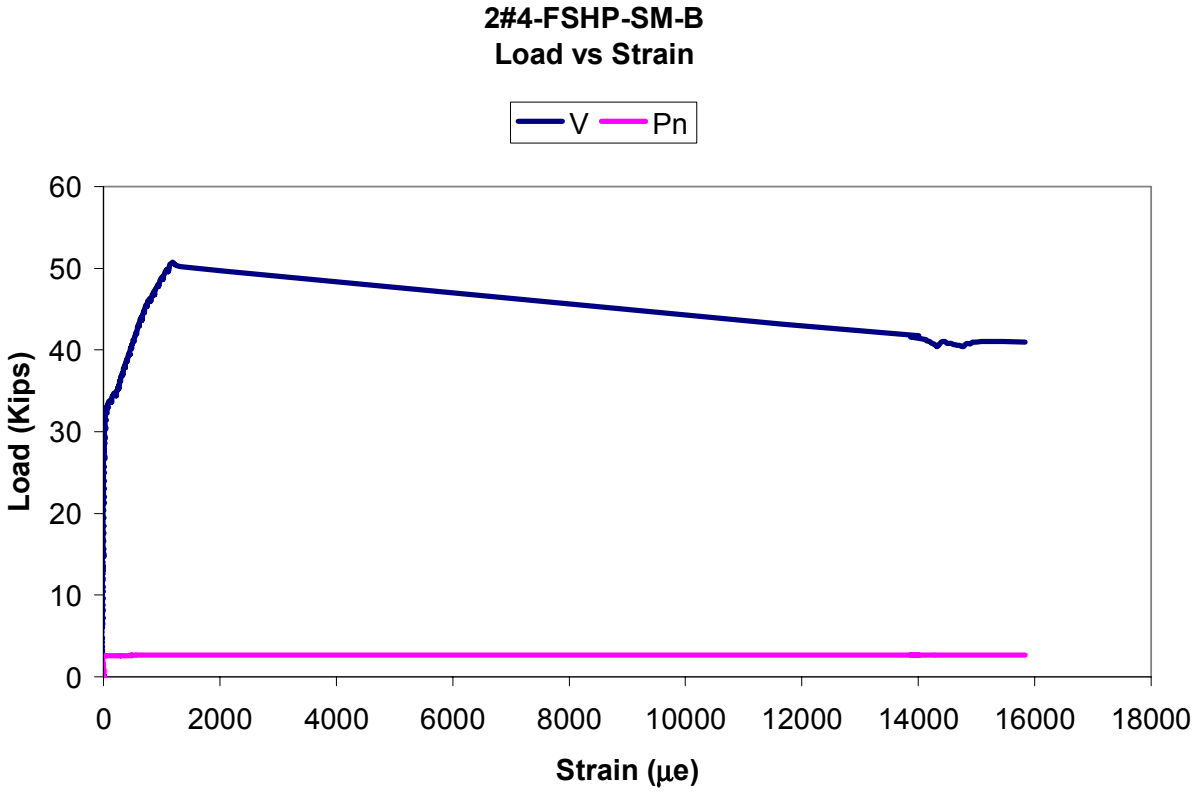
2#4-FSHP-SM-B
Load vs Strain
V
Pn
Load (Kips)
60
50
40
30
20
10
0
0
2000
4000
6000
8000
10000
12000
14000
16000
18000
Strain (με)

Test Series 8

Shear Connectors: 2 Legs - No. 5 Bar Stirrup
Grout Type: Five Star Highway Patch
Slab Surface Treatment: Smooth
No. Replications: 3

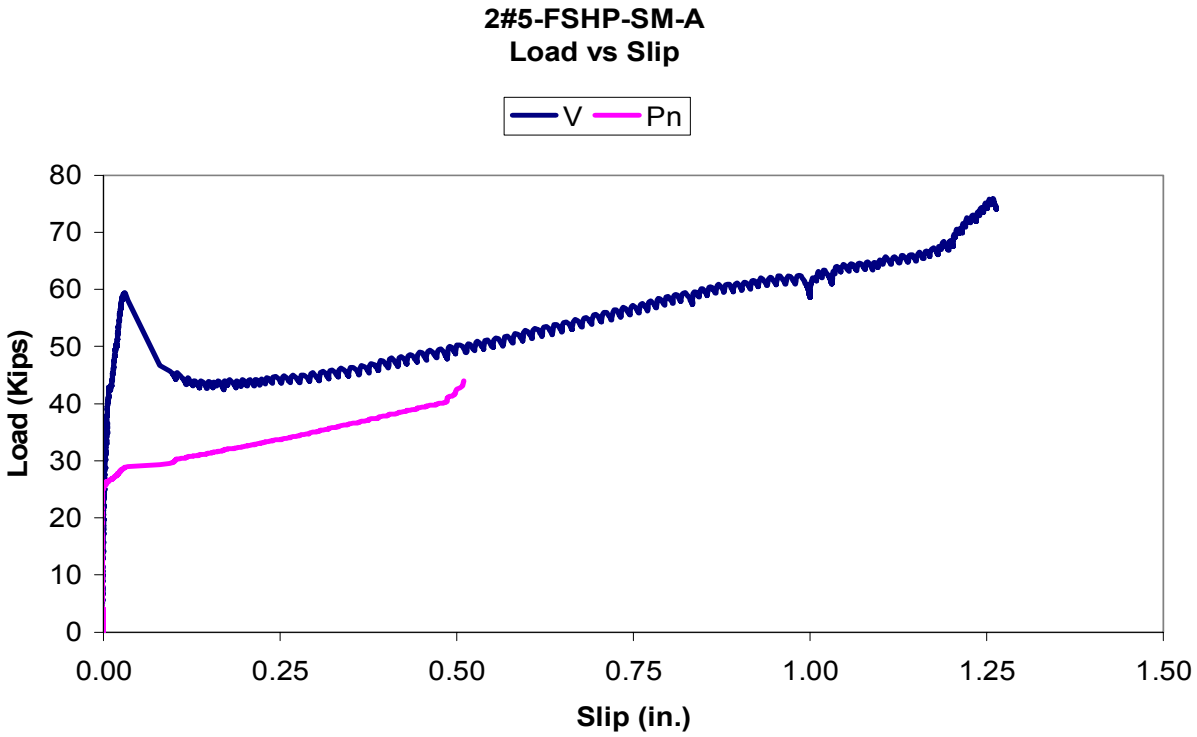

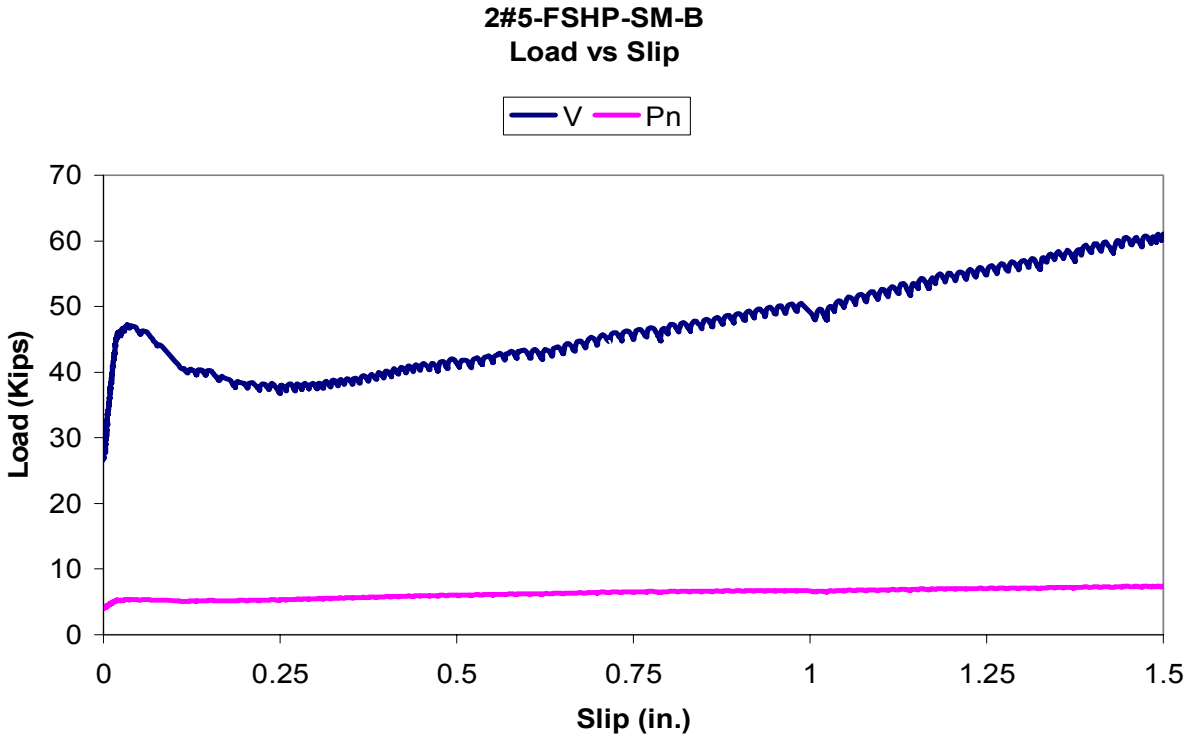
2#5-FSHP-SM-B
Load vs Slip
V
Pn
70
60
50
40
30
20
10
0
Load (Kips)
0
0.25
0.5
0.75
1
1.25
1.5
Slip (in.)

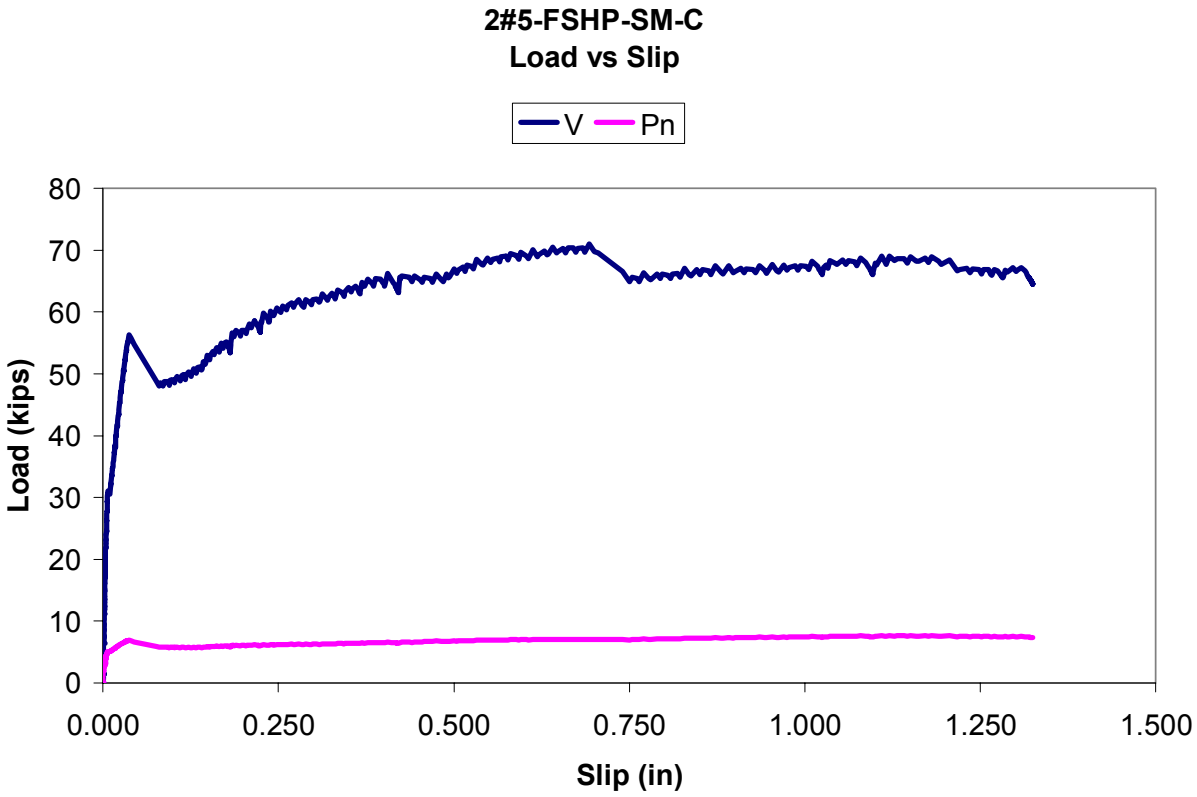
2#5-FSHP-SM-C
Load vs Slip
V
Pn
80
70
60
50
40
30
20
10
0
Load (kips)
0.000
0.250
0.500
0.750
1.000
1.250
1.500
Slip (in)

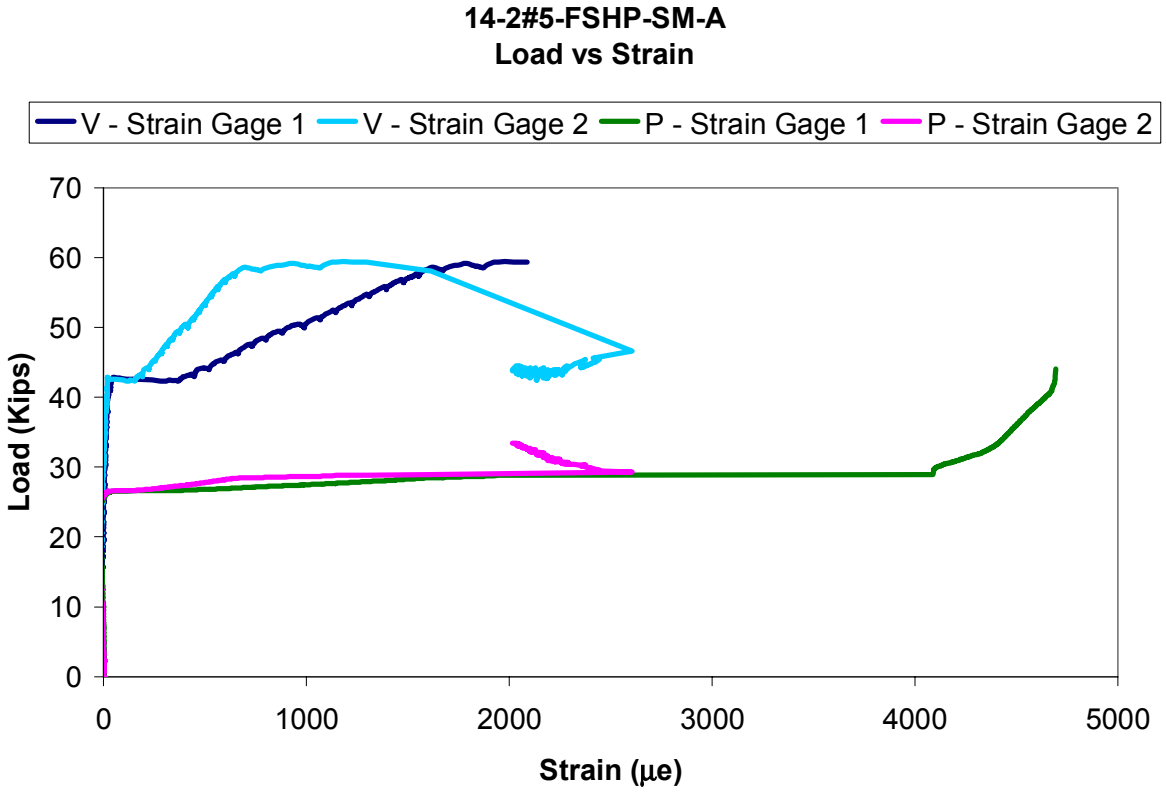
14-2#5-FSHP-SM-A
Load vs Strain
V - Strain Gage 1
V - Strain Gage 2
P - Strain Gage 1
P - Strain Gage 2
Load (Kips)
70
60
50
40
30
20
10
0
0
1000
2000
3000
4000
5000
Strain (με)

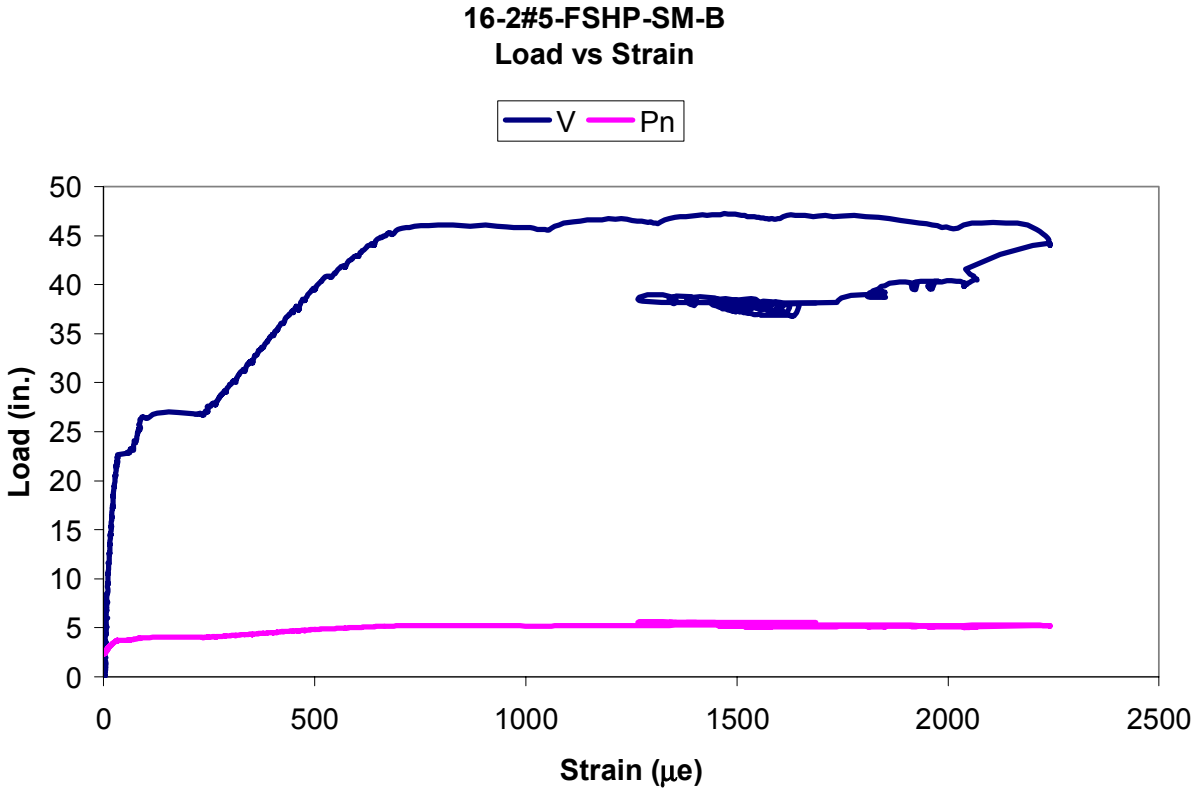
16-2#5-FSHP-SM-B
Load vs Strain
V
Pn
Load (in.)
Strain (με)
0
5
10
15
20
25
30
35
40
45
50
0
500
1000
1500
2000
2500

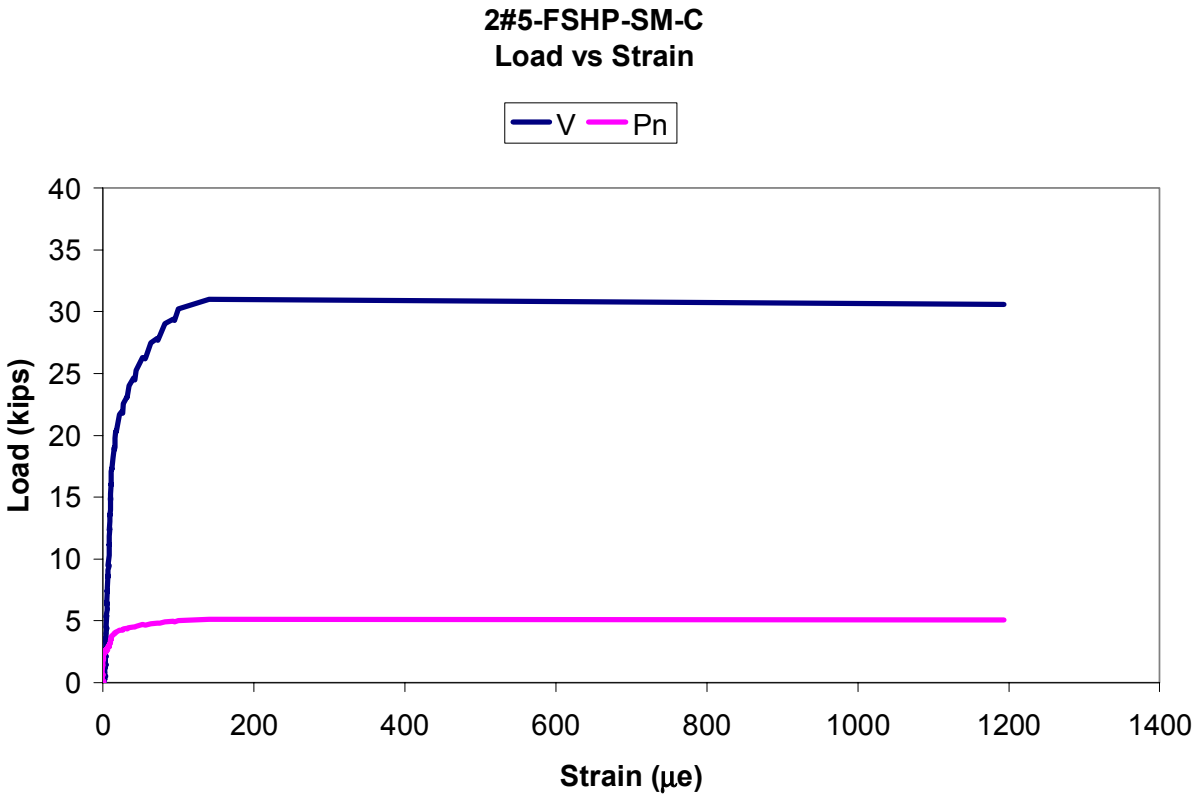
2#5-FSHP-SM-C
Load vs Strain
V
Pn
Load (kips)
0
5
10
15
20
25
30
35
40
0
200
400
600
800
1000
1200
1400
Strain (με)

Test Series 9

Shear Connectors: None
Grout Type: Five Star Highway Patch
Slab Surface Treatment: Smooth
No. Replications: 2

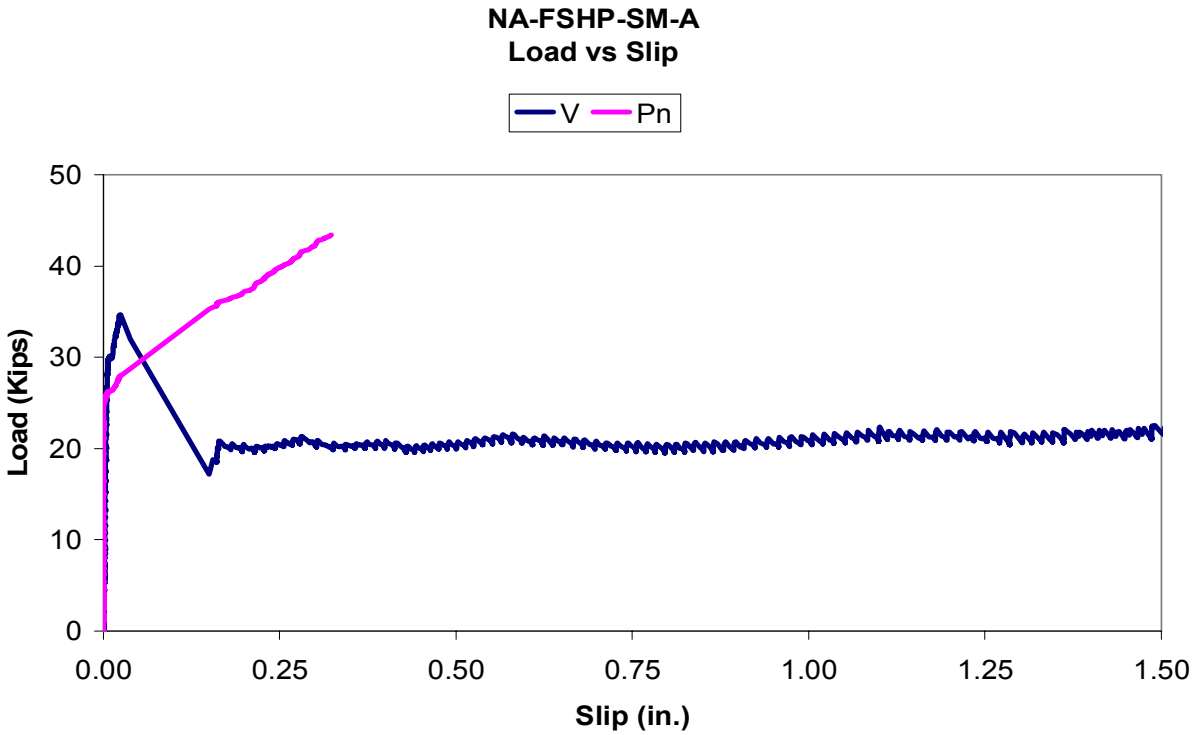

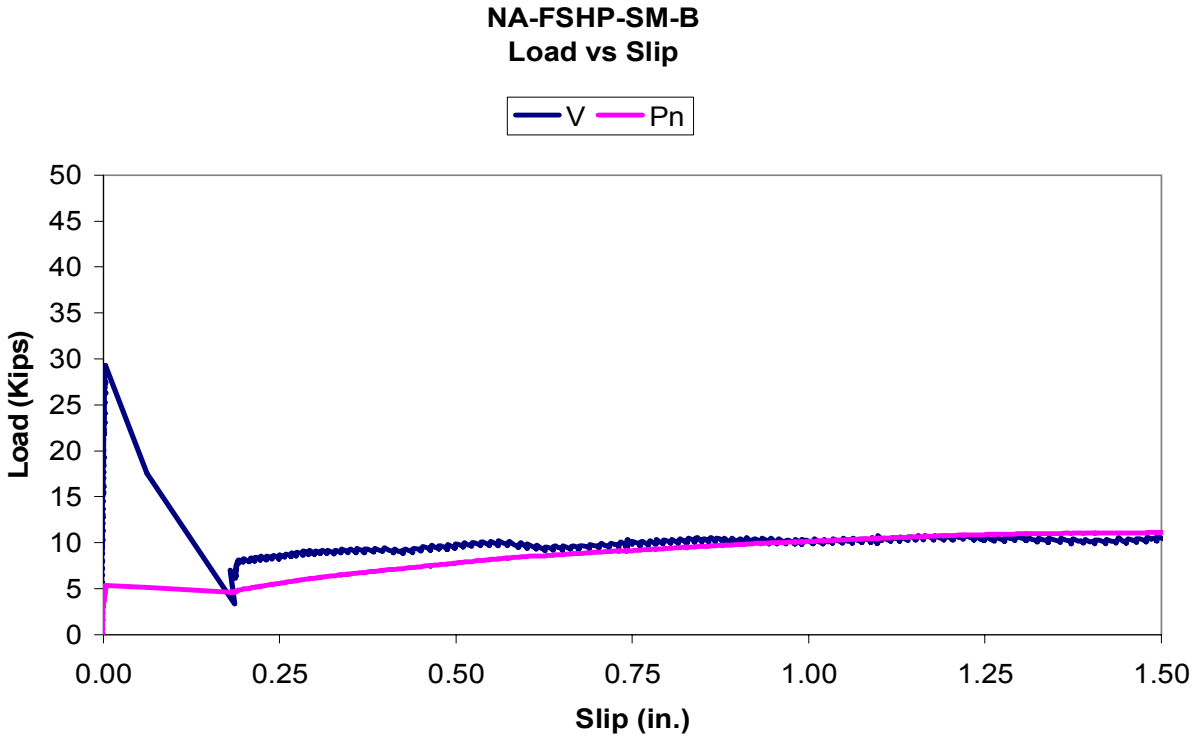
NA-FSHP-SM-B
Load vs Slip
V
Pn
Load (Kips)
50
45
40
35
30
25
20
15
10
5
0
0.00
0.25
0.50
0.75
1.00
1.25
1.50
Slip (in.)

Test Series 10

Shear Connectors: 2 Headed shear studs
Grout Type: Five Star Highway Patch
Slab Surface Treatment: Smooth
No. Replications: 2

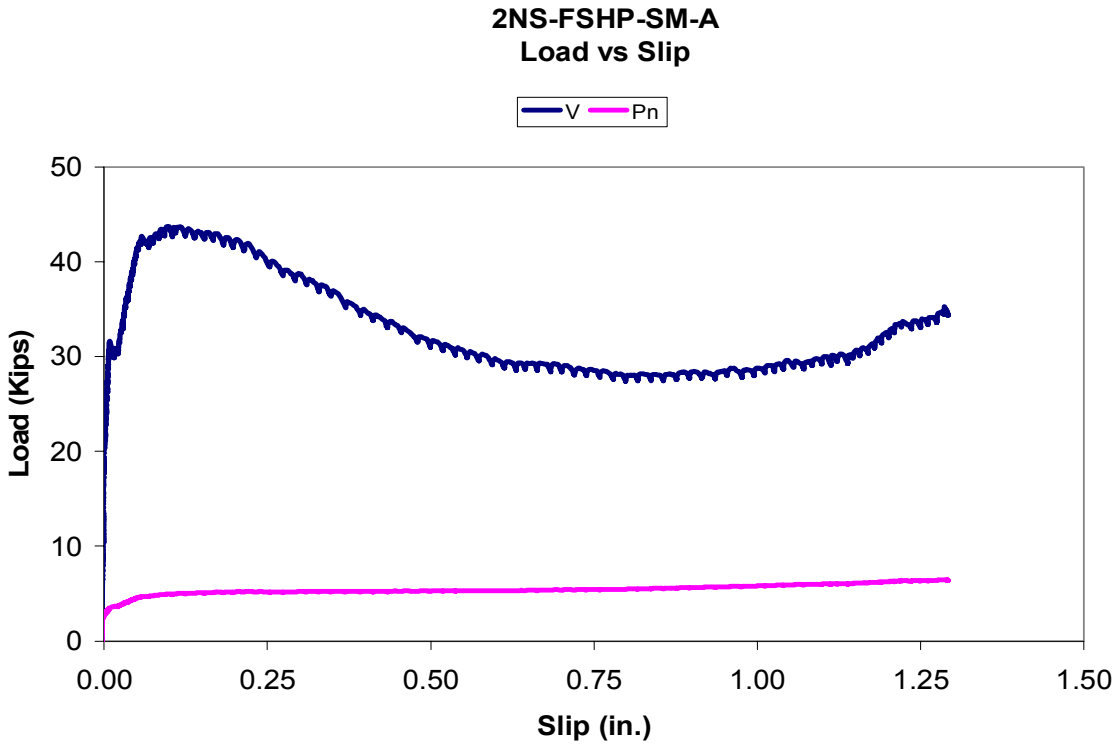

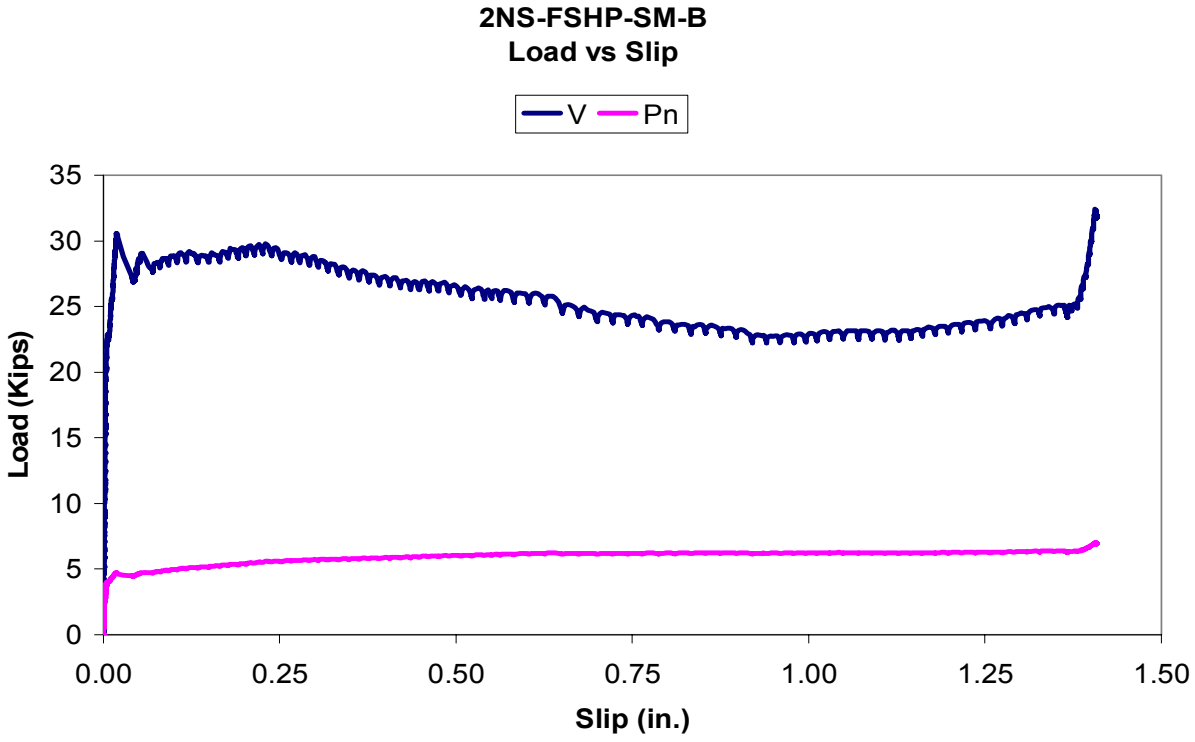
2NS-FSHP-SM-B
Load vs Slip
V
Pn
35
30
25
20
15
10
5
0
Load (Kips)
0.00
0.25
0.50
0.75
1.00
1.25
1.50
Slip (in.)

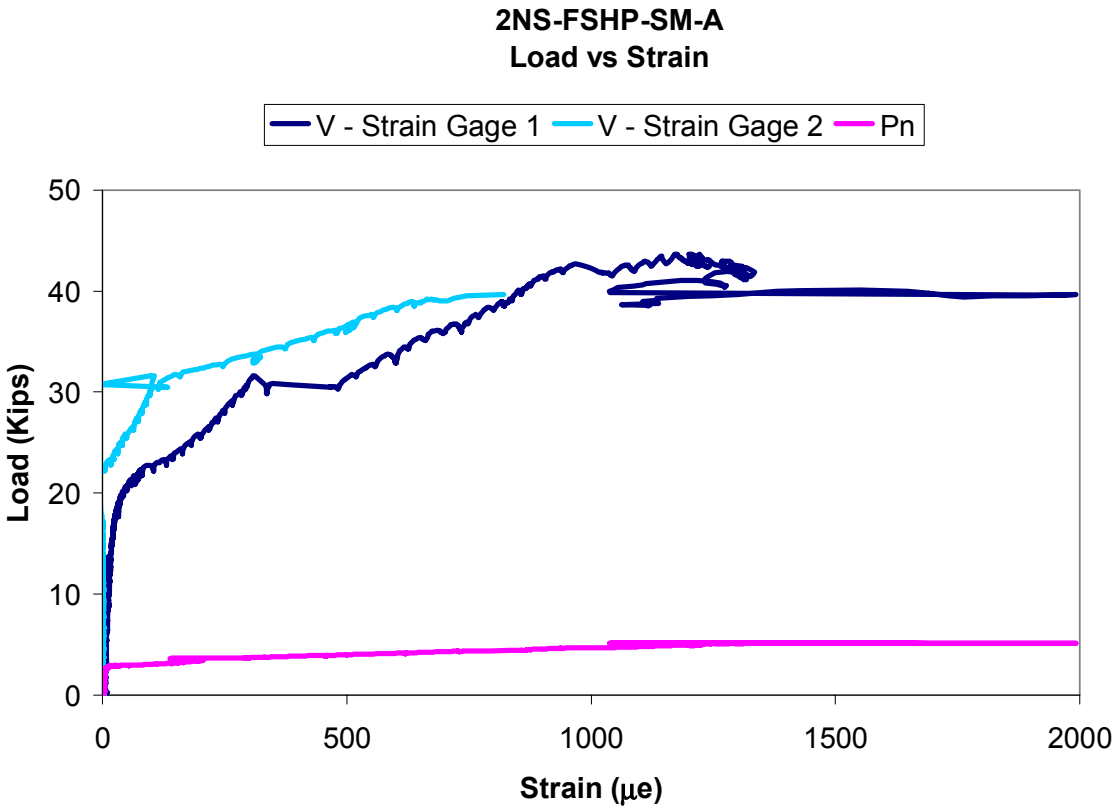
2NS-FSHP-SM-A
Load vs Strain
V - Strain Gage 1
V - Strain Gage 2
Pn
50
40
30
20
10
0
Load (Kips)
0
500
1000
1500
2000
Strain (με)

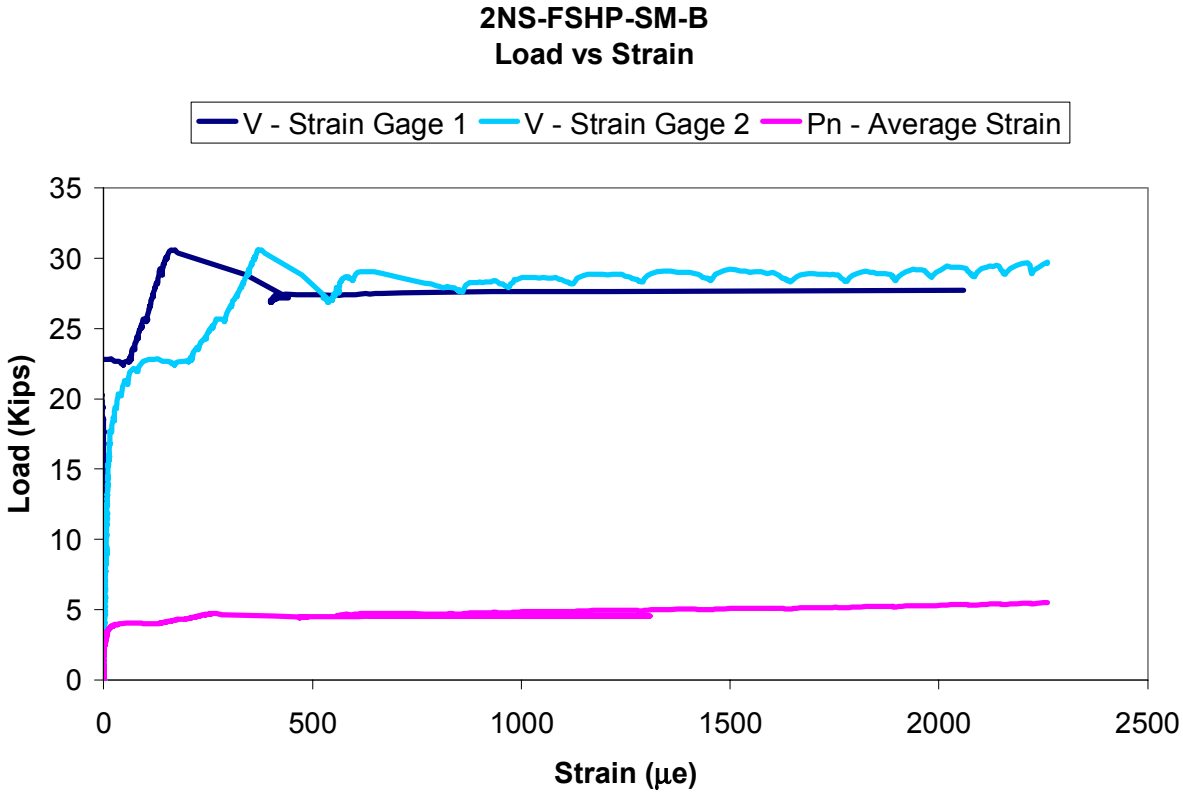
2NS-FSHP-SM-B
Load vs Strain
V - Strain Gage 1
V - Strain Gage 2
Pn - Average Strain
Load (Kips)
35
30
25
20
15
10
5
0
0
500
1000
1500
2000
2500
Strain (με)

Test Series 11

Shear Connectors: 4 Headed shear studs
Grout Type: Five Star Highway Patch
Slab Surface Treatment: Smooth
No. Replications: 2

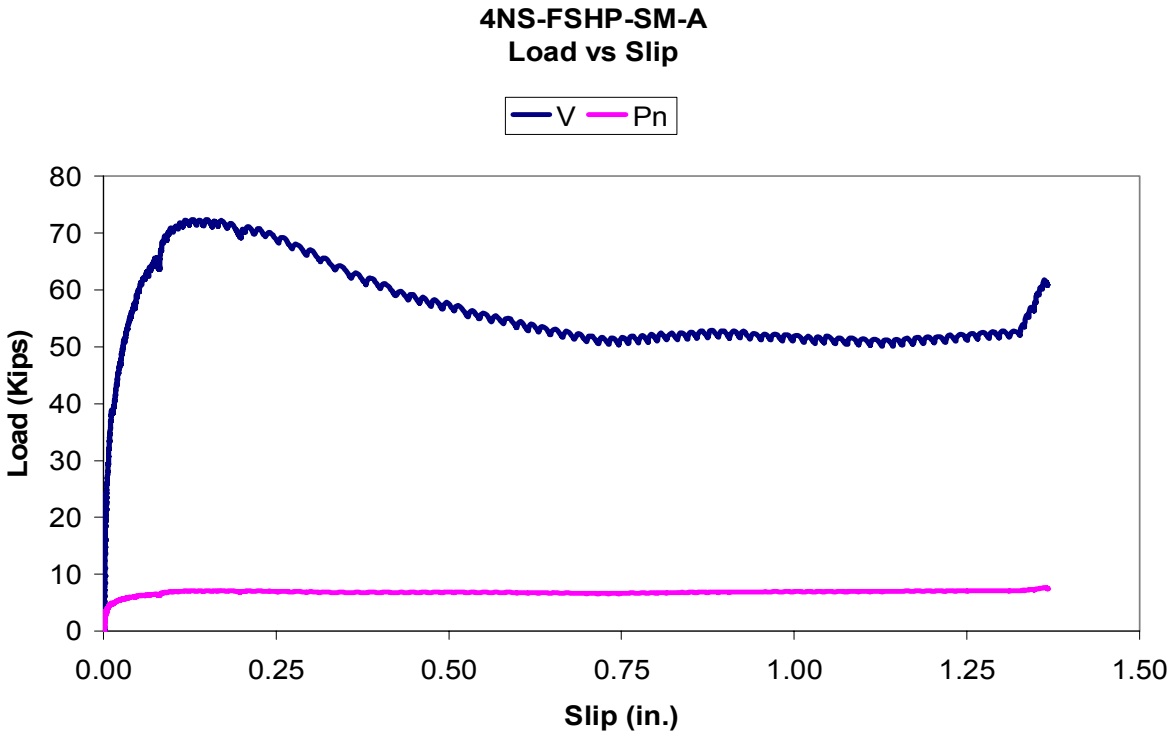

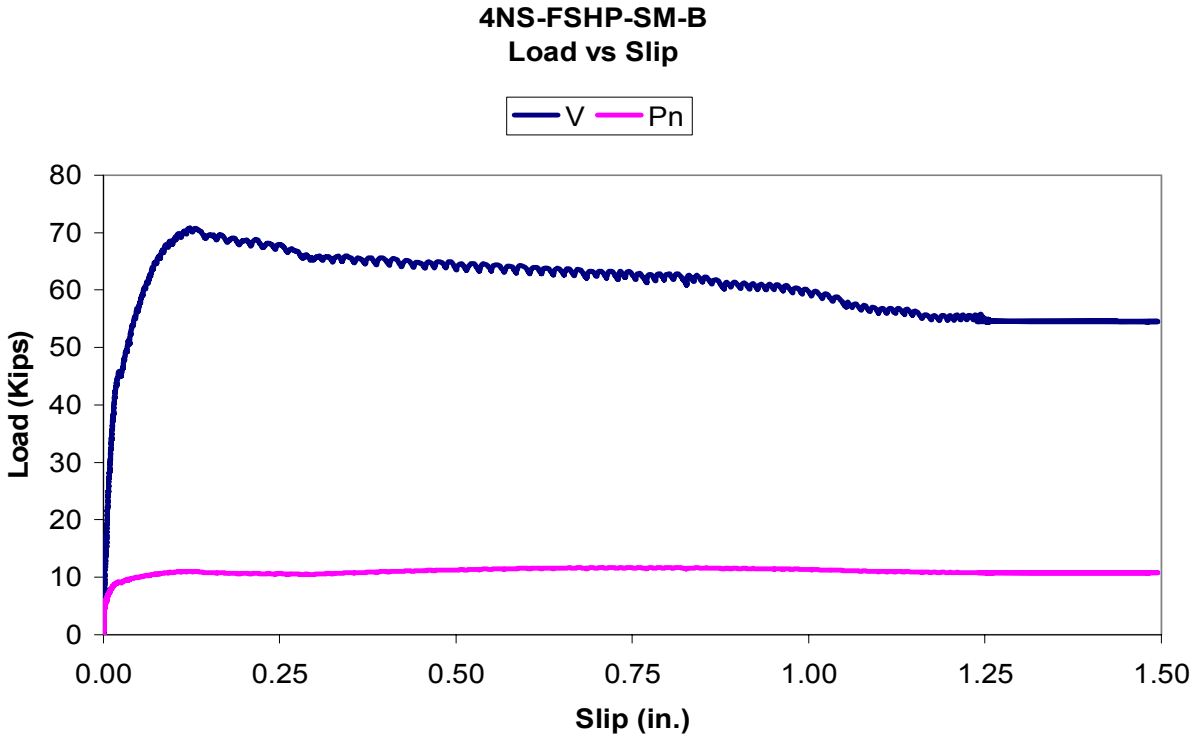
4NS-FSHP-SM-B
Load vs Slip
V
Pn
Load (Kips)
0
10
20
30
40
50
60
70
80
0.00
0.25
0.50
0.75
1.00
1.25
1.50
Slip (in.)

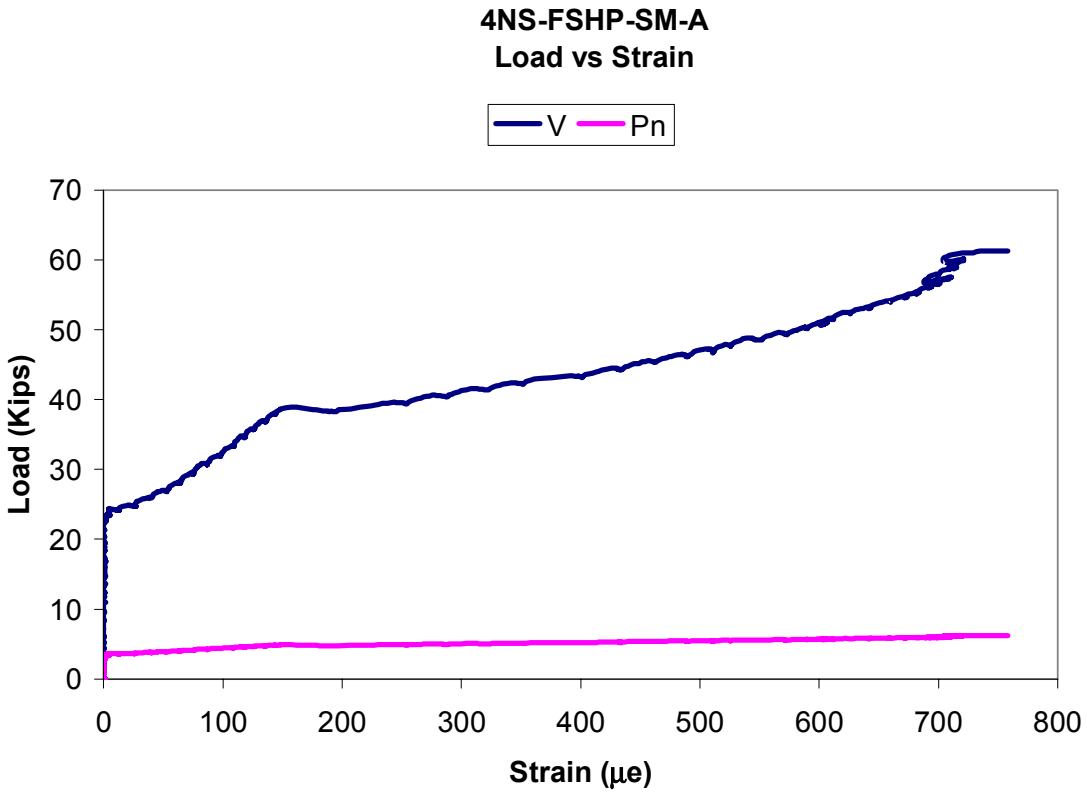
4NS-FSHP-SM-A
Load vs Strain
V
Pn
Load (Kips)
0
10
20
30
40
50
60
70
0
100
200
300
400
500
600
700
800
Strain (με)

4NS-FSHP-SM-B
Load vs Strain

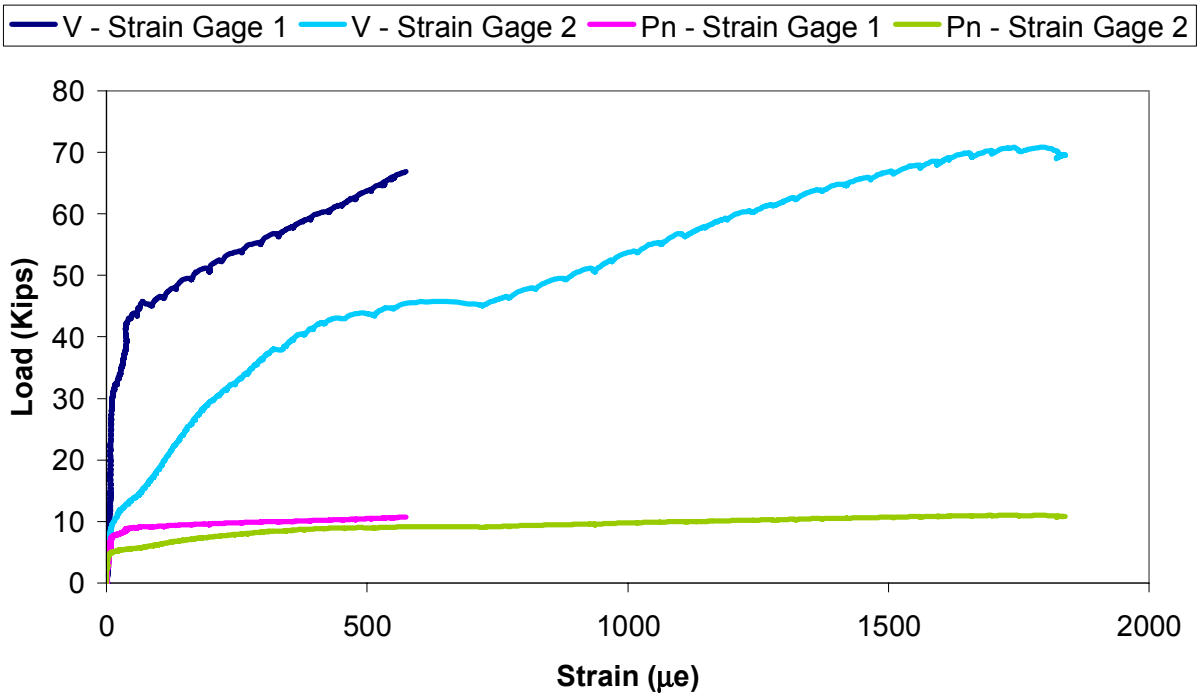

Test Series 12

Shear Connectors: 3 Headed shear studs
Grout Type: Five Star Highway Patch
Slab Surface Treatment: Smooth
No. Replications: 2

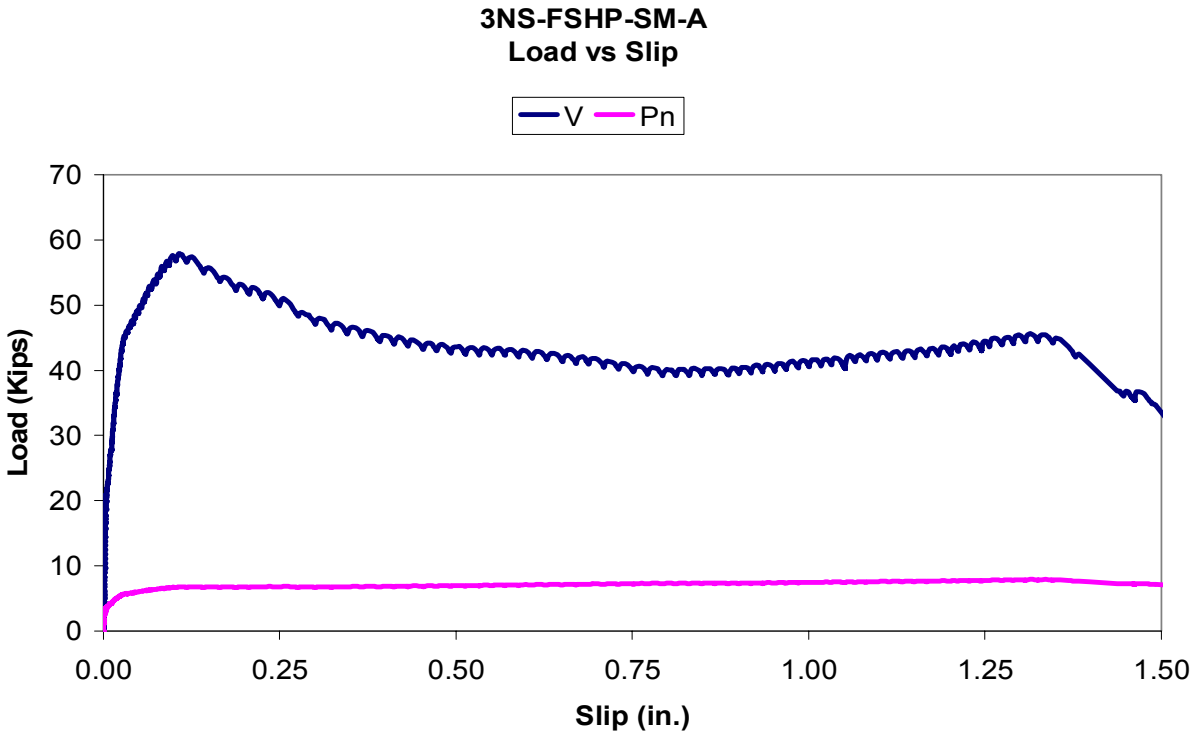

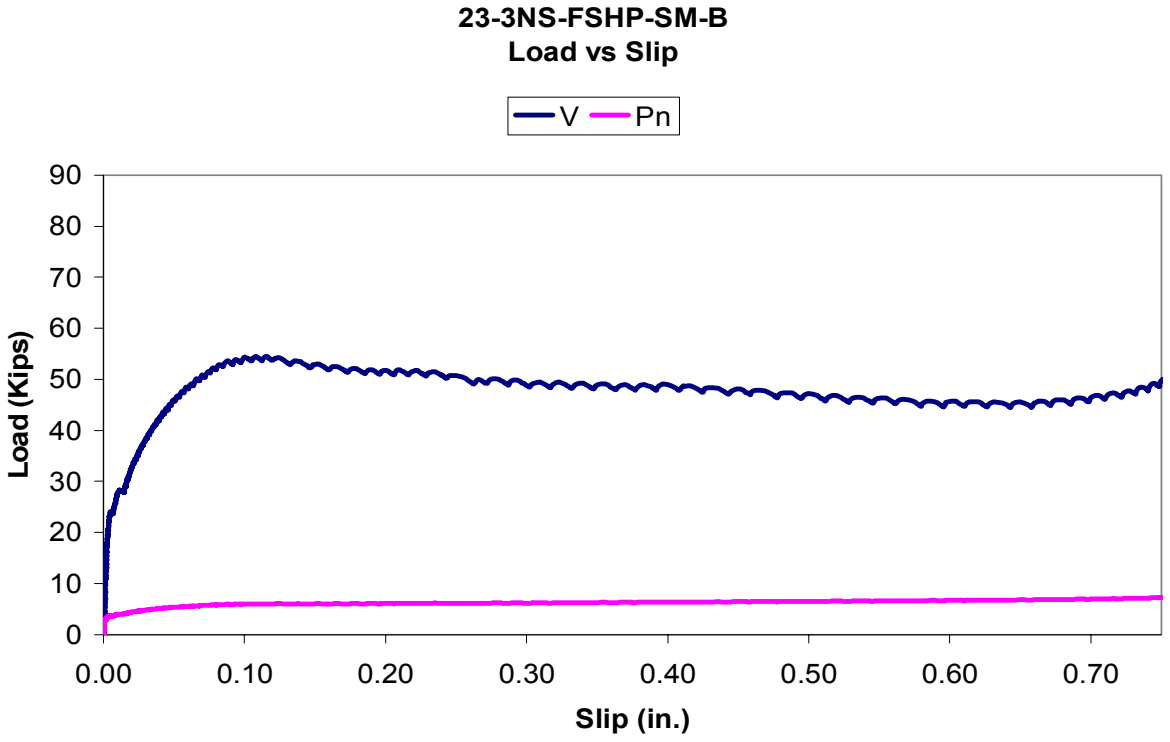
23-3NS-FSHP-SM-B
Load vs Slip
V
Pn
Load (Kips)
90
80
70
60
50
40
30
20
10
0
0.00
0.10
0.20
0.30
0.40
0.50
0.60
0.70
Slip (in.)

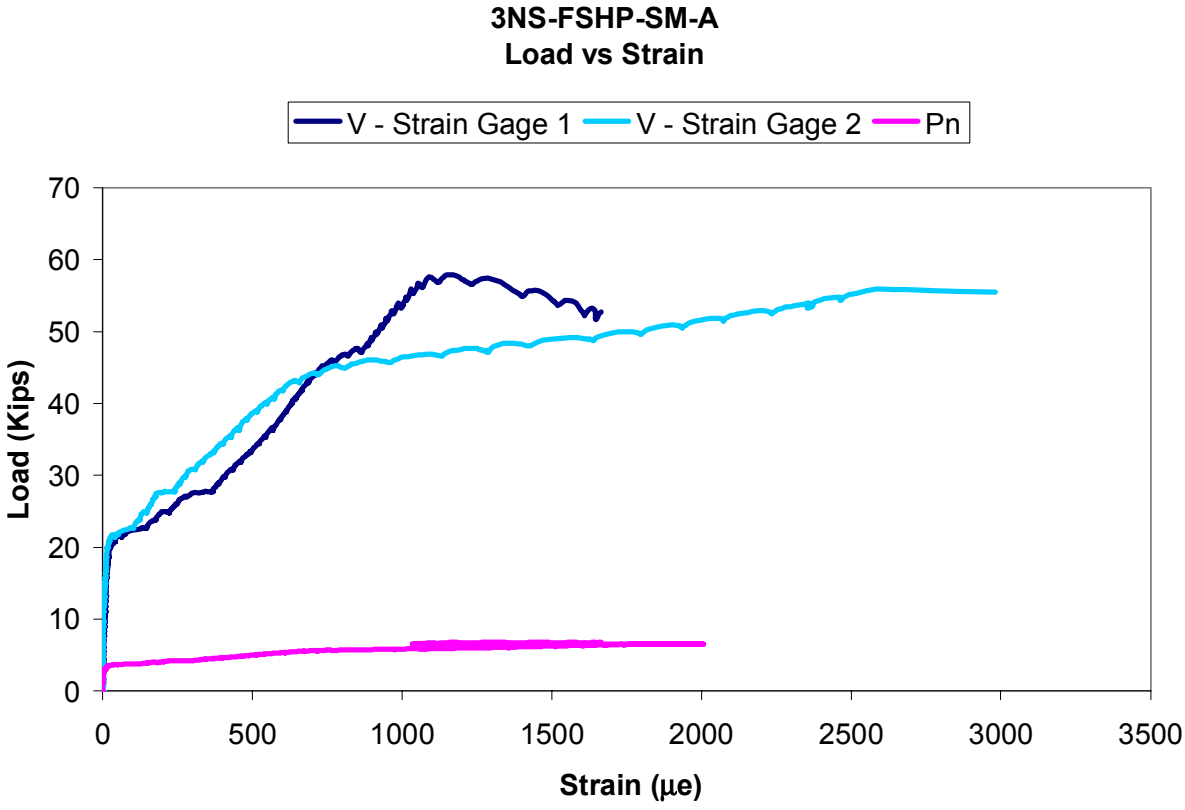
3NS-FSHP-SM-A
Load vs Strain
V - Strain Gage 1
V - Strain Gage 2
Pn
Load (Kips)
70
60
50
40
30
20
10
0
0
500
1000
1500
2000
2500
3000
3500
Strain (με)

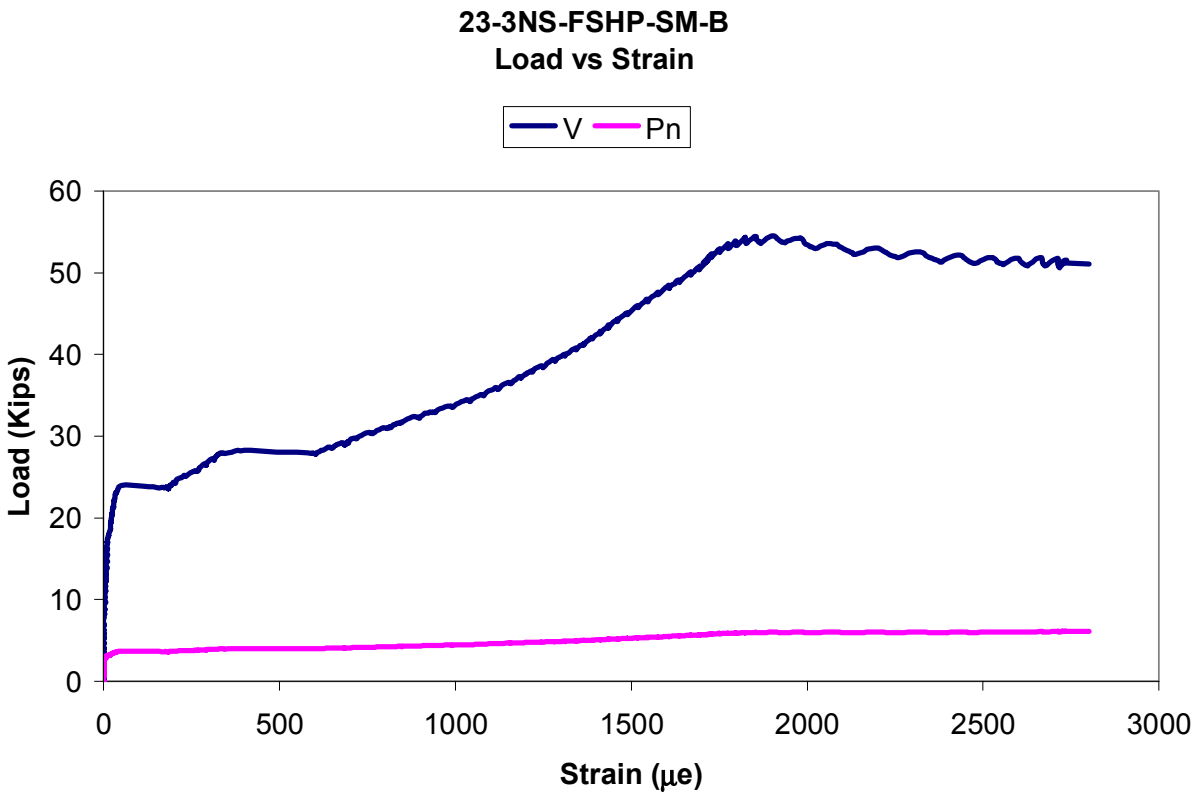
23-3NS-FSHP-SM-B
Load vs Strain
V
Pn
Load (Kips)
60
50
40
30
20
10
0
0
500
1000
1500
2000
2500
3000
Strain (με)

Test Series 13

Shear Connectors: 2 Legs – No. 4 Bars
Grout Type: Five Star Highway Patch
Slab Surface Treatment: Exposed Aggregate
No. Replications: 2

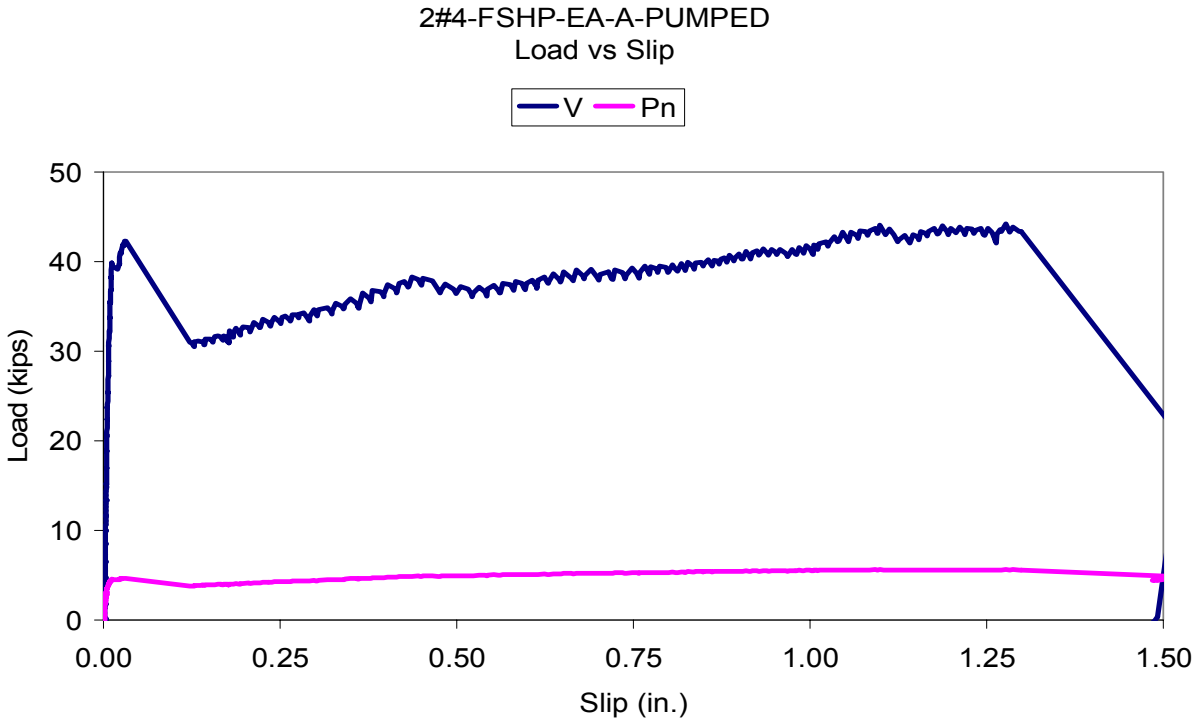

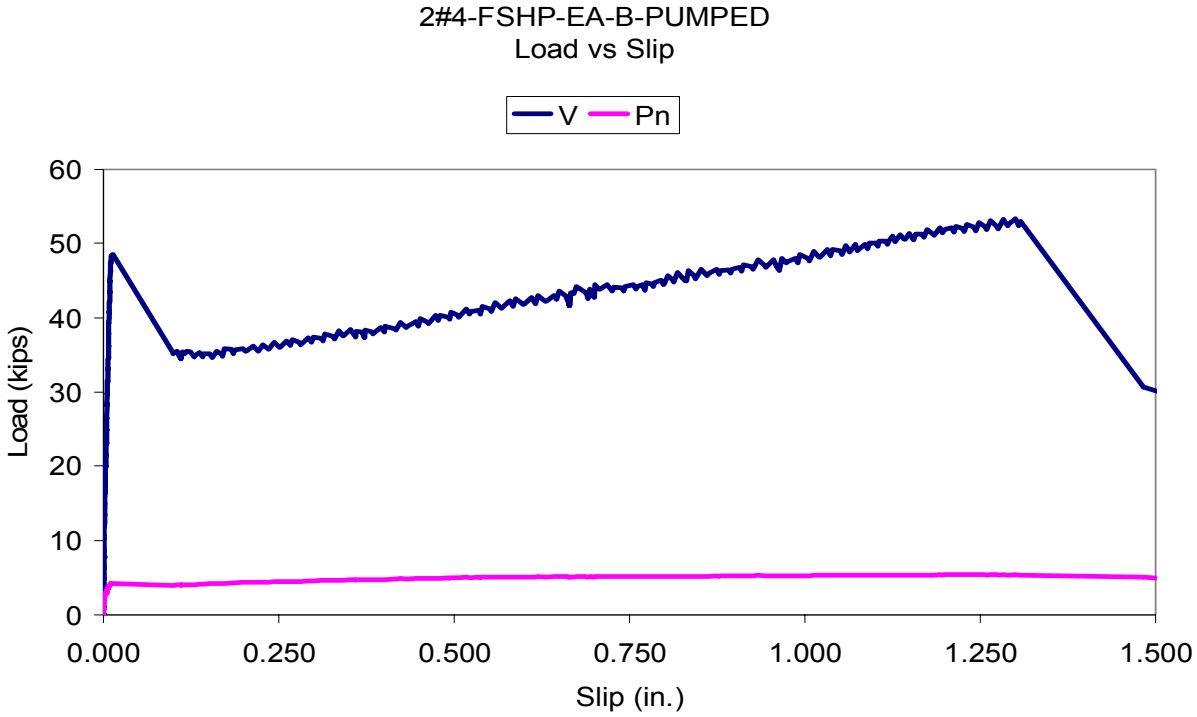
2#4-FSHP-EA-B-PUMPED
Load vs Slip
V
Pn
60
50
40
30
20
10
0
Load (kips)
0.000
0.250
0.500
0.750
1.000
1.250
1.500
Slip (in.)

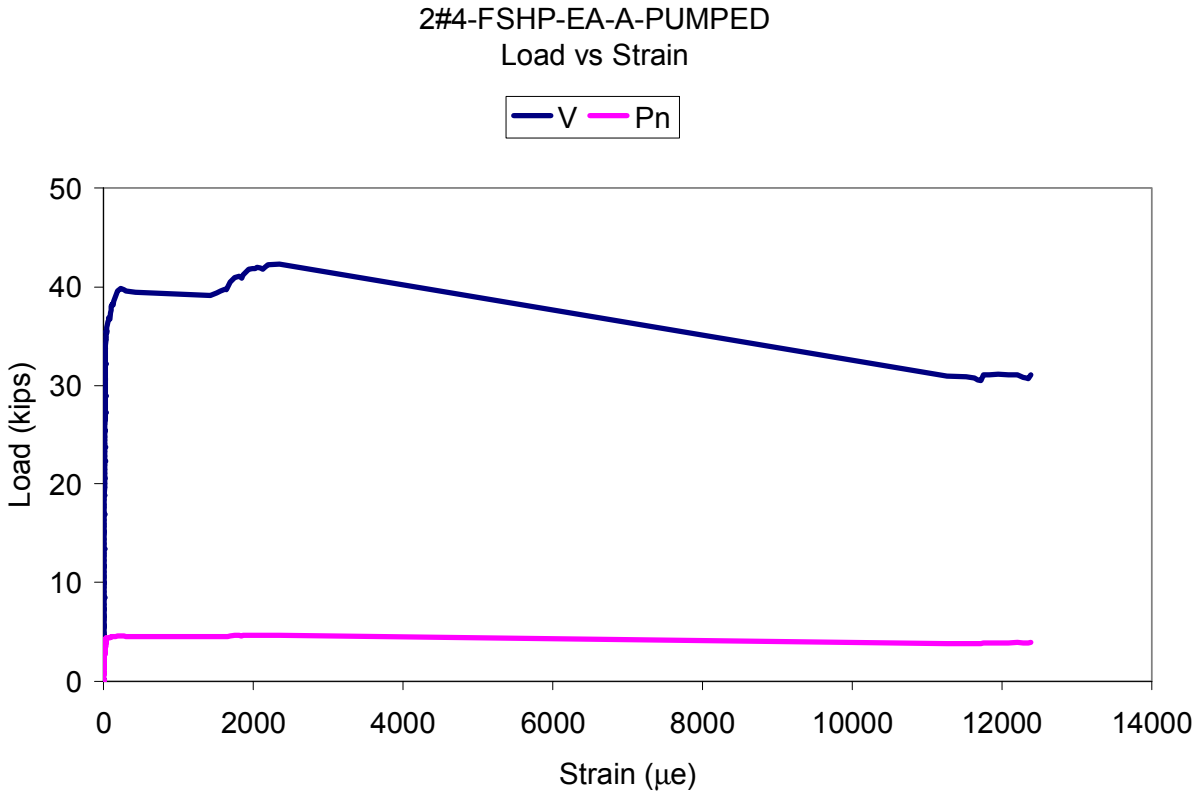
2#4-FSHP-EA-A-PUMPED
Load vs Strain
V
Pn
Load (kips)
50
40
30
20
10
0
0
2000
4000
6000
8000
10000
12000
14000
Strain (με)

APPENDIX B

Reinforcing Bar Tensile Tests

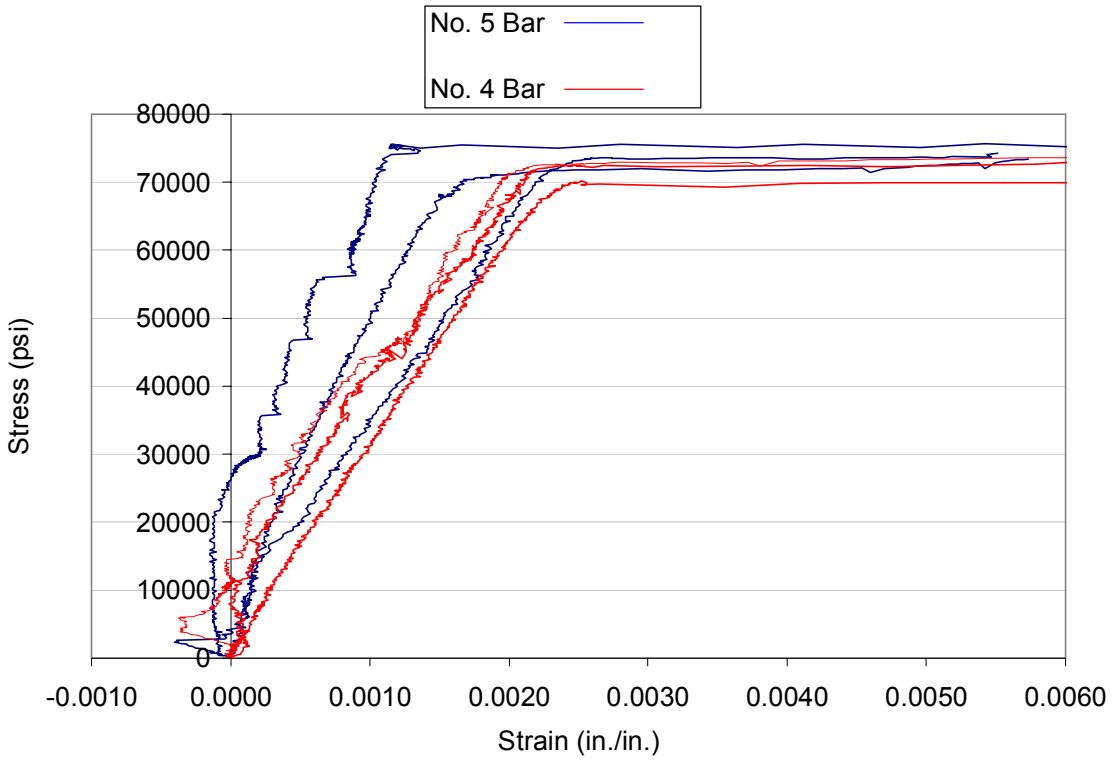
No. 5 Bar
No. 4 Bar
80000
70000
60000
50000
40000
30000
20000
10000
0
Stress (psi)
-0.0010
0.0000
0.0010
0.0020
0.0030
0.0040
0.0050
0.0060
Strain (in./in.)